

CENTRAL RESEARCH LIBRARY 5
DOCUMENT COLLECTION



3 4456 0022212 2

ORNL-3001
UC-37 - Instruments

INSTRUMENTATION AND CONTROLS DIVISION
ANNUAL PROGRESS REPORT
FOR PERIOD ENDING JULY 1, 1960

CENTRAL RESEARCH LIBRARY
DOCUMENT COLLECTION
LIBRARY LOAN COPY

DO NOT TRANSFER TO ANOTHER PERSON

If you wish someone else to see this
document, send in name with document
and the library will arrange a loan.



OAK RIDGE NATIONAL LABORATORY

operated by

UNION CARBIDE CORPORATION

for the

U.S. ATOMIC ENERGY COMMISSION

Printed in USA. Price **\$2.50**. Available from the
Office of Technical Services
Department of Commerce
Washington 25, D. C.

LEGAL NOTICE

This report was prepared as an account of Government sponsored work. Neither the United States, nor the Commission, nor any person acting on behalf of the Commission:

- A. Makes any warranty or representation, expressed or implied, with respect to the accuracy, completeness, or usefulness of the information contained in this report, or that the use of any information, apparatus, method, or process disclosed in this report may not infringe privately owned rights; or
- B. Assumes any liabilities with respect to the use of, or for damages resulting from the use of any information, apparatus, method, or process disclosed in this report.

As used in the above, "person acting on behalf of the Commission" includes any employee or contractor of the Commission, or employee of such contractor, to the extent that such employee or contractor of the Commission, or employee of such contractor prepares, disseminates, or provides access to, any information pursuant to his employment or contract with the Commission, or his employment with such contractor.

ORNL-3001
ERRATA

INSTRUMENTATION AND CONTROLS DIVISION ANNUAL PROGRESS REPORT
FOR PERIOD ENDING JULY 1, 1960

Page	Errata
24	Add caption to Photo 50357 to read: Fig. 7.2. Personal Radiation Monitor, Disassembled.
38	Add caption to Photo 50354 to read: Fig. 7.13. Internal Construction.

ORNL-3001
Instruments
TID-4500 (15th ed.)

Contract No. W-7405-eng-26

INSTRUMENTATION AND CONTROLS DIVISION

ANNUAL PROGRESS REPORT

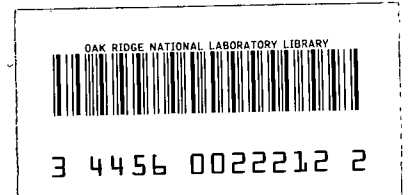
For Period Ending July 1, 1960

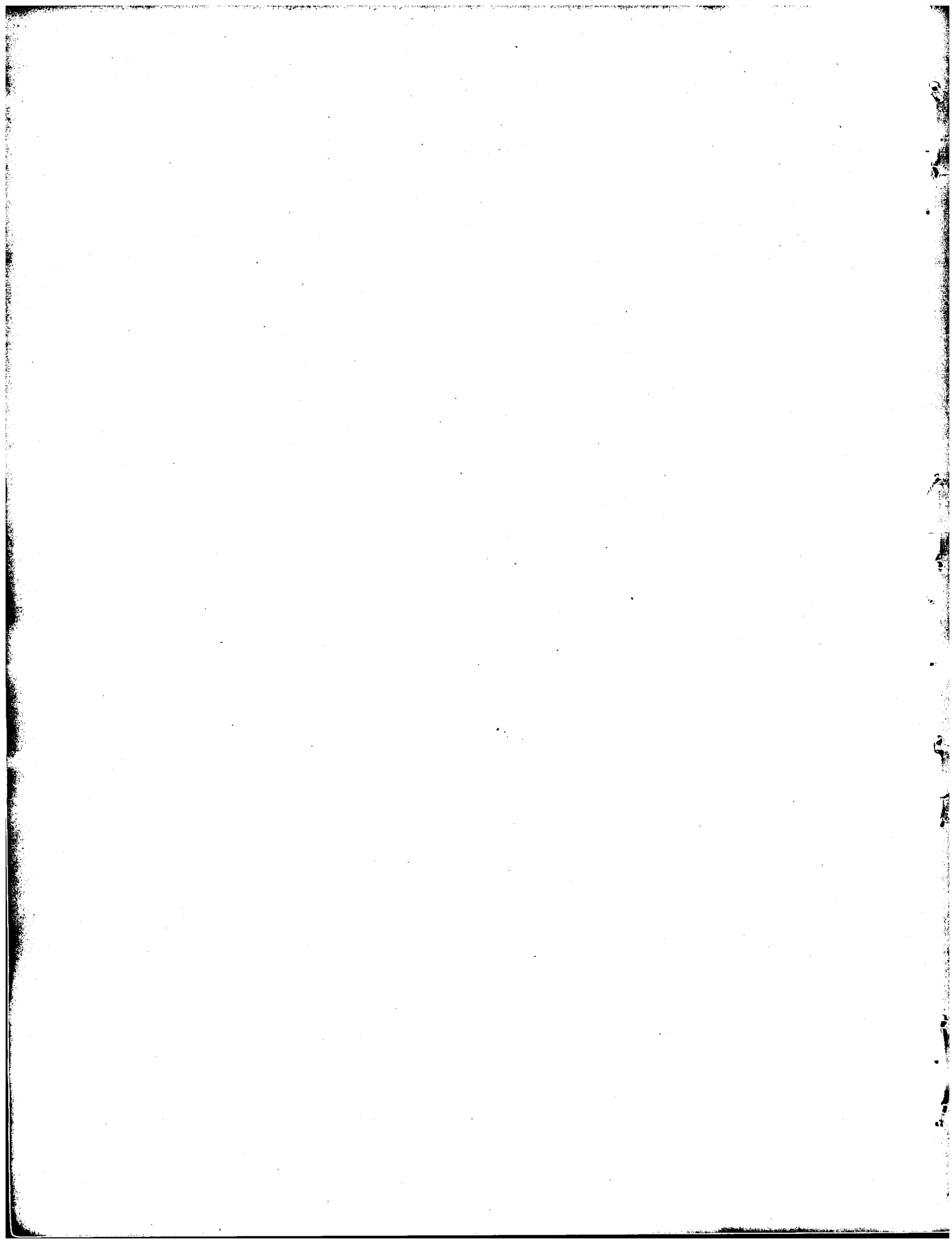
C. J. Borkowski, Director
C. S. Harrill, Associate Director

DATE ISSUED

JAN 27 1961

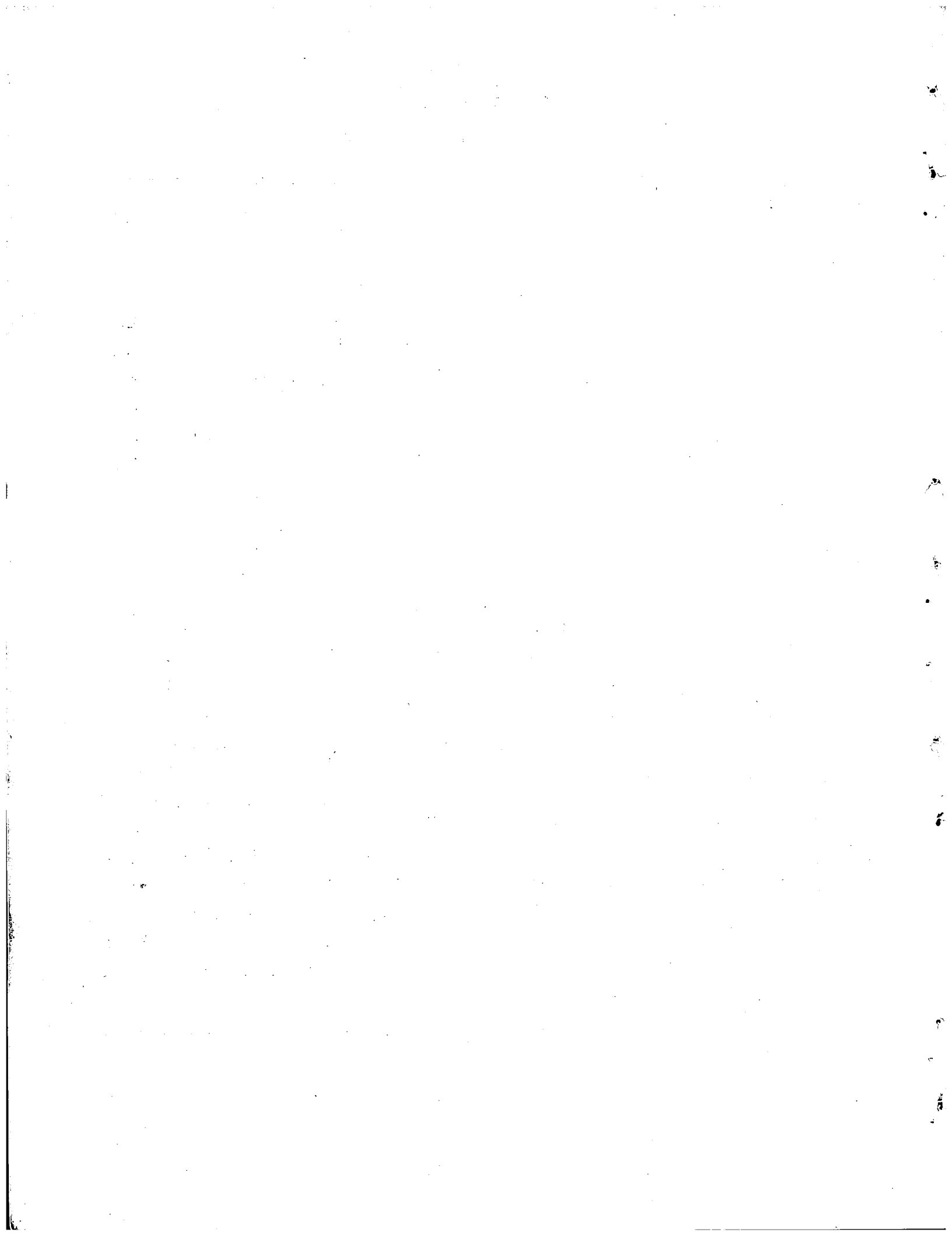
OAK RIDGE NATIONAL LABORATORY
Oak Ridge, Tennessee
operated by
UNION CARBIDE CORPORATION
for the
U.S. ATOMIC ENERGY COMMISSION





CONTENTS

1.	Q-2110 Remote Electrometer Head.....	1
2.	Linear-to-Logarithmic Electrometer.....	4
3.	Portable Alpha Counter Q-1975A.....	8
4.	Metal-Identification Meter Q-2076.....	10
5.	Transistorized, Portable, Gamma Single-Channel Analyzer for Airborne Monitoring.....	14
6.	A High-Gain, Low-Noise, Linear Pulse Amplifier (Q-2069A).....	18
7.	Personal Radiation Monitor.....	22
8.	Silicon Surface-Barrier Nuclear-Particle Spectrometer.....	42
9.	Alpha-Survey Probe.....	55
10.	Zener-Diode Regulated Power Supplies for Minneapolis- Honeywell and Leeds & Northrup Recorders.....	58
11.	Temperature Control of the 30-Mw Cooling System for the ORR.....	62
12.	Modification of a Bausch & Lomb Spectronic 20 Colorimeter- Spectrophotometer for In-Line Applications.....	69
13.	Instrumentation for Salt Field Experiment.....	73
14.	Status Report on Automatic Experimental Data Handling and Computation at ORNL.....	76
15.	Homogeneous Reactor Project Instrumentation and Controls.....	80
16.	Performance Tests of ORNL Fast Safety System for Pool-Type Reactors.....	102



1. Q-2110 REMOTE ELECTROMETER HEAD

F. M. Glass

It is very often desirable to use remote electrometer heads where long cable runs are necessary. Especially is this true in applications requiring very low current measurements and where noise would be a problem if high-gain feed-back amplifiers were used to degenerate the cable capacity for fast response. However, remote heads have not always been used in every application where they are desirable because of two main difficulties: (1) the range-switching mechanism is always expensive and quite bulky, and (2) the necessary size of the enclosure presents the problem of unwanted ion collection in a volume of undefinable geometry. The Q-2110 remote head employs VX10 thermal relays as a means of switching ranges. It is designed to be used with an ion chamber, described by Instrumentation and Controls drawing Q-2045A, and is housed in the extended shell of the chamber (see Fig. 1.1). The active volume of the chamber is 100 cc, with a pressure of 10 atmospheres giving it an effective geometry of 1000 cc. This means that the maximum error due to ion collection in the remote head will be 3%.

Any one of four input resistors plus a grounding contact may be selected remotely by means of a selector switch on the control panel. This is accomplished by supplying 1.25 v at 10 ma to any one of the five VX10 relays (see Fig. 1.2). Since the leakage resistances of all the relays, the 5886 electrometer tube, and any supporting insulators are in parallel, the total leakage may be as high as 10^{14} ohms under best environmental conditions. Therefore, the use of input resistors having a value greater than 10^{11} ohms is not recommended. It will be noted that one heater connection (H1) and the return contact (H1) on the VX10's are tied together. This is permissible only because the heater power supply is floating, and the signal return lead does not carry heater power. Therefore, no IR drop as a result of heater current appears on the signal return. The signal return lead may be terminated at ground or to the feedback bus if feedback is employed.

This head was designed to be used only with electrometers having the necessary d-c heater supply and switching arrangement.

UNCLASSIFIED
PHOTO 50322

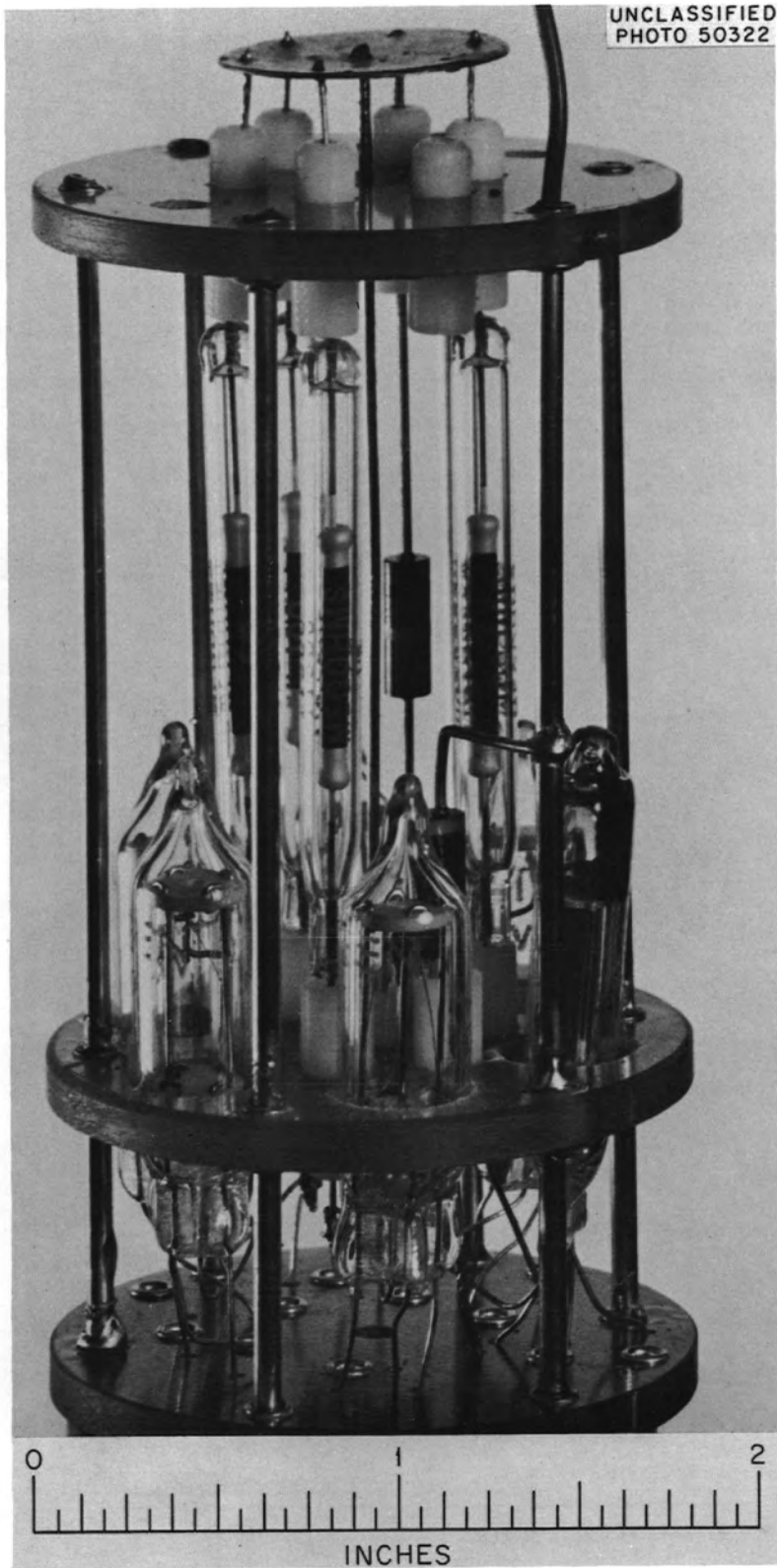


Fig. 1.1. Preamplifier.

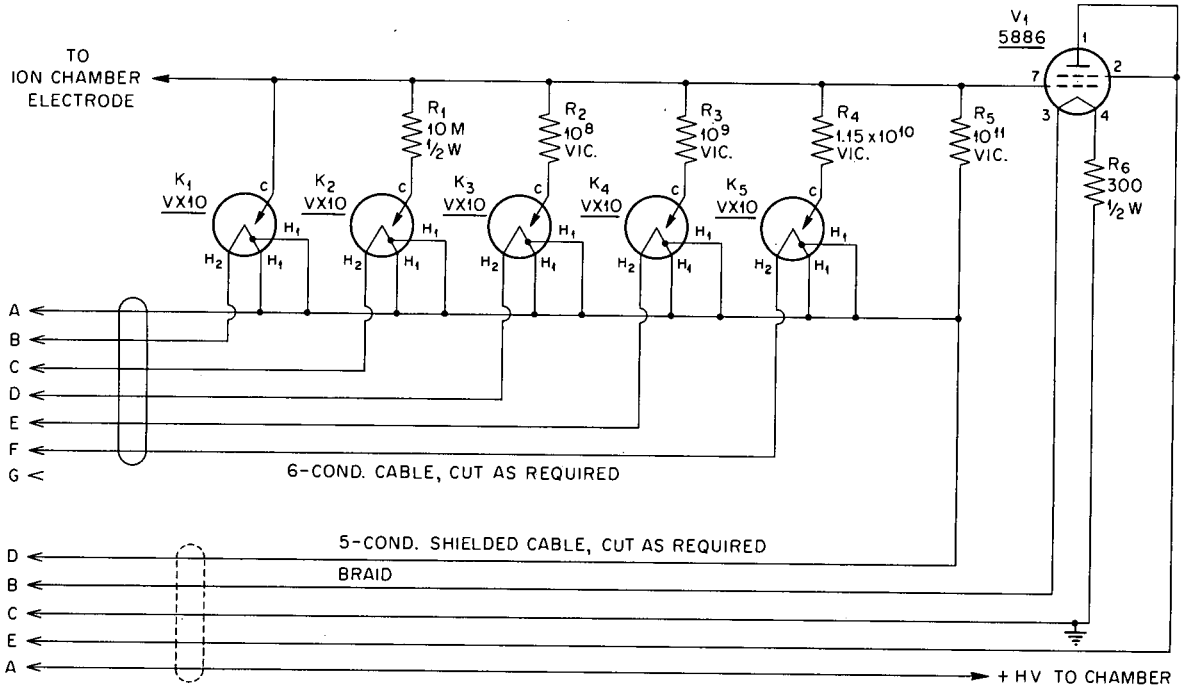


Fig. 1.2. Electrometer with Remote Input and Integral Ion Chamber Remote Head Circuit.

2. LINEAR-TO-LOGARITHMIC ELECTROMETER

F. M. Glass

There has been a pressing need for a radiation-background monitor that will give an alarm or control signal at a predetermined level with the accuracy that can be achieved only with a stable linear-type instrument. In addition it should have a continuous range without switching of several decades above this alarm level so that a strip-chart record of any high excursions could be made.

To meet this need the Q-2114 electrometer has been designed. It has a linear response up to 5×10^{-12} amp. Starting at 5×10^{-12} amp the response goes through a transition from linear to logarithmic and remains logarithmic for three more decades. Two test currents are provided for a two-point calibration check on the log scale. This instrument, when used with an ion chamber of the proper volume, can be set to alarm at the desired radiation level within its expanded linear range.

The linear-to-logarithmic response transition is accomplished by placing a 5799 diode in the grid circuit of a 5886 electrometer tube which serves as a voltage amplifier (see Fig. 2.1). Normally this diode is biased out of conduction, and the electrometer tube amplifies linearly the IR drop across the 10^{11} -ohm resistor which parallels the diode in the electrometer grid circuit. When this IR drop equals 0.5 v or greater, the diode starts conducting, and the voltage across the diode-resistor combination becomes a logarithmic function of current. The output of the voltage amplifier is fed from the remote head through a cable to two vacuum tube voltmeters (VTVM's) on the main chassis. The two input grids of the VTVM's are fed in parallel, and both are biased for linear operation. However, the grid of the second triode in the log channel meter is so biased that, with the transistor clamp absent from the cathode circuits, the 50- μ a meter reading is off scale below zero. With the transistor clamp disabled, the bias setting is correct when a current of 5×10^{-12} amp in the electrometer input causes the log-range meter to come on scale at zero. This is the input current required for a full-scale reading on

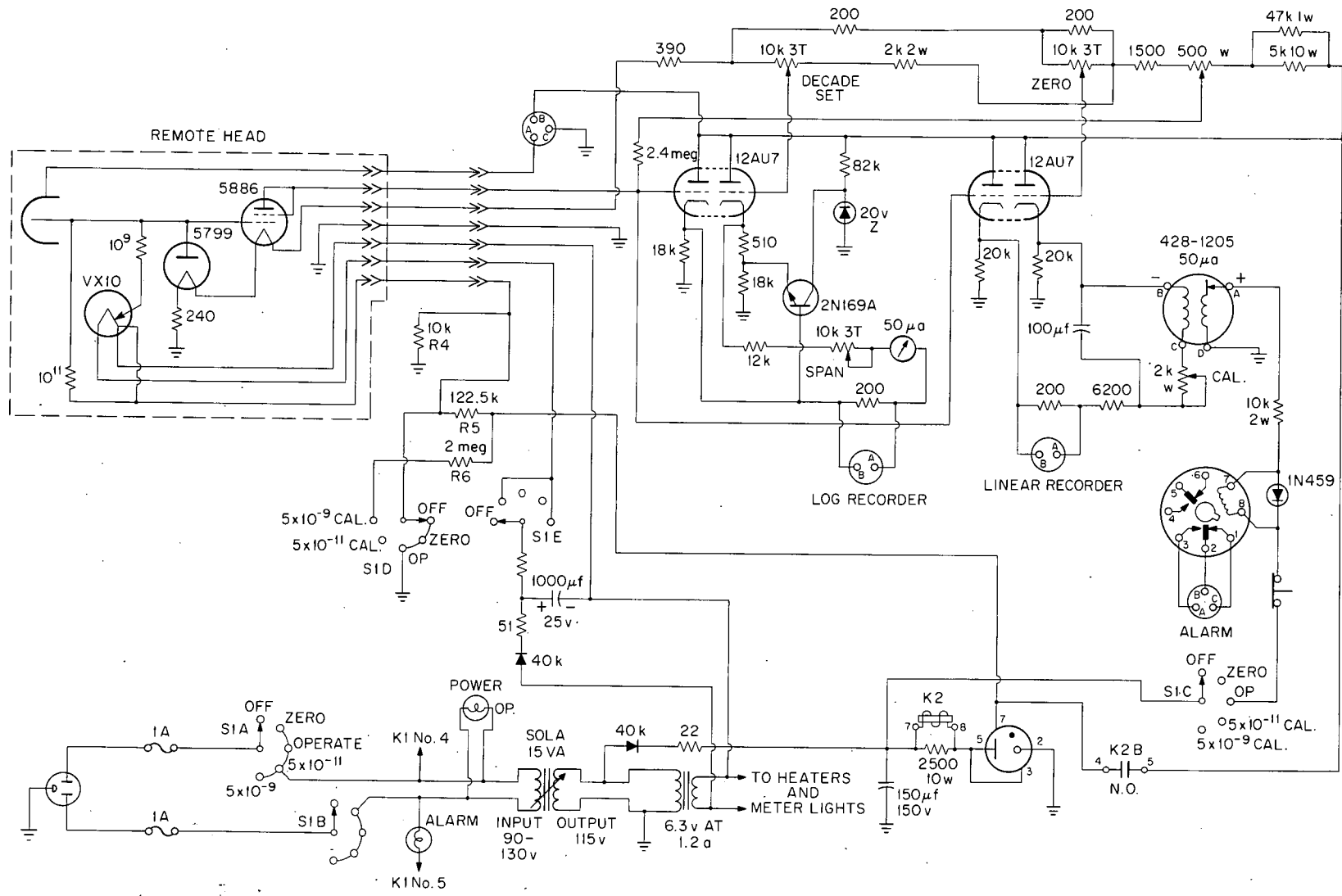


Fig. 2.1. Linear-to-Logarithmic Electrometer.

the linear meter that does not have its zero suppressed. The above-mentioned bias adjustment is made with the 10-kilohm potentiometer designated "DECADE SET." A 10-kilohm potentiometer in the meter circuit serves as the span adjustment. The 2N169A transistor is added in the cathode circuits to serve the double function of clamping the log meter just on scale so as to prevent wear on the strip-chart log recorder and to produce a clean, sharp transition from linear to logarithmic response. The latter is accomplished by taking advantage of the fact that the collector current as a function of base-to-emitter voltage is very nonlinear. The logarithmic response over the first half decade is due almost entirely to the current-release characteristics of this clamp, while the second half-decade response is almost entirely due to the logarithmic response of the 5799 diode. The 2N169A clamp has completely released before the top of the first decade has been reached.

Although both meter circuits are fed in parallel, they can be independently calibrated. Both circuits have recorder output, but only the linear meter provides an alarm-and-control signal. The alarm relay is energized by a contact-making meter. Manual reset is necessary once the circuit is energized. The switching circuitry is so arranged that the alarm-and-control power relay cannot be energized during startup or when making calibration checks with the built-in current test signals.

A novel and very desirable feature of this electrometer is that remote zero and two current calibration checks are provided by a single-contact high-impedance thermal relay. When the control switch "S1" is in the zero position, the thermal relay (VX10) is energized, shorting the electrometer grid circuit to ground through a 10^9 resistor (see S1D, S1E in Fig. 2.1). This zero is valid in any background if the linear meter reads less than full scale when the switch is turned to the "operate" position. When in the "operate" position, the relay is not energized, and the 10^{11} -ohm resistor is the only resistive grid return to ground. In the 5×10^{-11} -amp "calibrate" position, the 10^{11} -ohm resistor is returned to a potential of 5.65 v above ground by removing the shunt across R4. In the 5×10^{-11} -amp "calibration" position, the VX10 relay is again energized, allowing current to flow through the 10^9 -ohm resistor which is now in parallel with the 10^{11} -ohm resistor. To compensate for the rise

in potential of the electrometer grid circuit, R6 is switched in parallel with R5 to raise the potential from 5.65 to 6 v.

This instrument is in the developmental stage, and complete production drawings are not yet available. However, as indicated by the following specifications, it looks quite promising:

Range	5×10^{-12} amp full scale, linear 5×10^{-12} to 5×10^{-9} amp, logarithmic
Linearity	-2%, linear
Stability	Drift < 2% of full scale after 10 min

3. PORTABLE ALPHA COUNTER Q-1975A

F. M. Glass

A portable, transistorized, alpha scintillation counter has been designed for the purpose of detecting low-level alpha contamination on hands, clothing, lunch counters, and other places where contamination could be a health hazard. This instrument features compactness, light weight, a permanent-type battery, and a built-in charger. The scintillation probe, designed by M. M. Chiles, has a large sensitive area (approximately 100 cm², with 75% effective area) which reduces surveying time by a factor of ten under the time required by our previous models.

The circuitry (see Fig. 3.1) consists of a feedback amplifier pair, a trigger pair, a register driver, a 900-v regulated supply for the photo-multiplier tube, and a battery charger. The amplifier employs both negative voltage feedback and positive current feedback to increase the input impedance. The negative voltage feedback stabilizes the gain to the extent that gain is independent of supply voltage, temperature and h_{FE} (base current gain) of the two transistors. The potentiometer in the collector circuit of Q2 serves as a gain control providing variable gain from 1 to 11. The input impedance is 220 kilohms when working into the 2.2-kilohm load, which is the input impedance of the discriminator. The discriminator delivers a 17-msec pulse which drives the normally biased-off 2N270 to

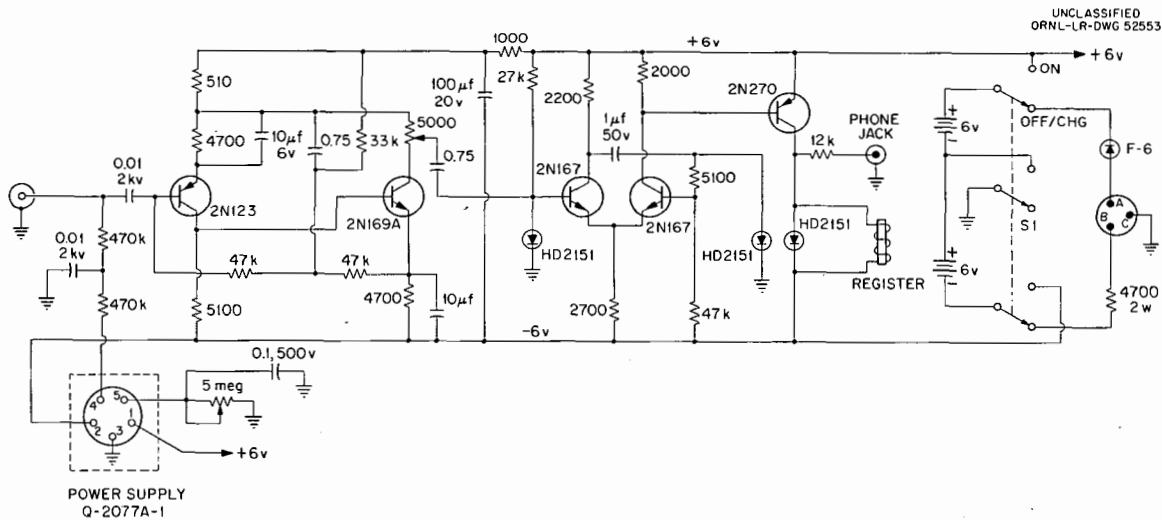


Fig. 3.1. Portable-Alpha-Counter Circuit.

saturation. The 2N270 drives the mechanical register and supplies audio power to a phone jack for head-phone operation, if so desired.

The instrument is powered by two 6-v, 500 ma-hr, rechargeable batteries. The built-in charger which operates from the 115-v, 60-cycle line limits the charging current to a value that will not allow the gassing potential of the cells to be reached (1.49 v). This prevents damage to the cells even if left on charge for months. The transistorized power supply that supplies power to the photomultiplier tube delivers a regulated 900 v at 20 μ a.

The specifications are shown below:

Size	7-1/2 \times 3-3/4 \times 3-1/4 in.
Weight	3 lb 9 oz
Battery drain	12 ma
Resolution	0.06 sec
Stability	Count rate increases 0.14% per $^{\circ}$ C for Pu ²³⁹ , within the temperature limits of 0 to 60 $^{\circ}$ C

4. METAL-IDENTIFICATION METER Q-2076

F. M. Glass

The design of the Metal-Identification Meter, model Q-2076, is the result of the joint efforts of the Metallurgy and Instrument Development Groups. It features compactness, low battery drain, and simplicity in construction and operation (see Fig. 4.1). It is useful in the nondestructive identification of metals. It operates on the principle that positive identification of most metals is possible on the basis of conductivity measurements. The Q-2076 has sufficient sensitivity to give full-scale deflection on the meter for a change in conductivity ratio of 1 to 1.2. The meter serves as an indicator only. The position of a ten-turn dial at maximum meter reading is a measure of conductivity. This instrument is most useful in identifying metals by comparing them with known samples.

Principle of Operation

A small r-f coil which serves as the tank coil of a self-excited oscillator is located in a probe. Eddy currents are induced in the metal under test when the probe is placed on the metal. The induced eddy currents are proportional to the conductivity of the metal, and their phase relation is such that they oppose the magnetic lines of force inducing them. Therefore, the inductance of the oscillator coil is reduced by a factor that is proportional to the magnitude of the eddy currents. This results in an increase in the frequency of the self-excited oscillator. A method by which a measure of conductivity can be obtained is now at hand.

Ferromagnetic action may override the above effects and result in lowering the oscillator frequency, which is also a usable and reproducible phenomena.

Circuitry

The circuit consists of a self-excited oscillator, two limiter stages, a variable band-pass filter, and a meter circuit (see Fig. 4.2).

UNCLASSIFIED
PHOTO 49216



Fig. 4.1. Assembly View of Metal-Identification Meter.

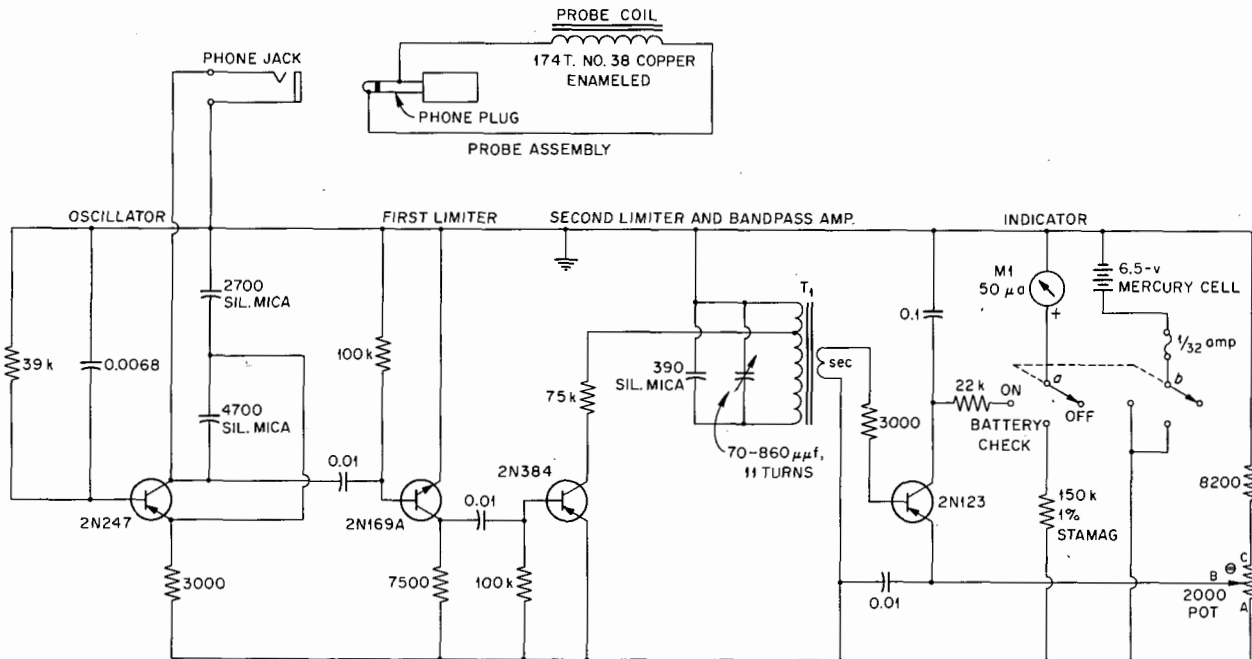


Fig. 4.2. Metal-Identification-Meter Circuit.

The oscillator is a grounded-base circuit employing shunt feedback to the emitter. The tank has low inductance and high capacity which swamps out capacity changes in the probe cable and the transistor. The Q of the tiny coil in the probe is so low that it greatly affects the amplitude of the output signal. Therefore, the amplitude of the signal is reduced appreciably by high-loss materials under test. The frequency of the oscillator, when testing various metals, ranges from 222 kc with carbon steel to 272 kc for silver.

Since the output of the oscillator is not constant, a double-stage limiter is used to normalize the signal amplitude. These stages are self-biased and operate class C. As self-biased limiters they are not affected by temperature changes within nondestructive limits. Limiter action is such that its output is normalized within 2%. To supplement this action, the value of R6 has been chosen to give a compensating attenuation on the high-frequency end of the range, where the signals would normally have about 2% greater amplitude. This same resistor (R6) serves as decoupling between the 2N384 collector and the band-pass filter, thereby providing higher Q . The loaded Q of this tuned circuit

is 300 at 250 kc. Although "skirt" selectivity is unimportant it is very good since the LC ratio is low. However, the 830-cycle band width resulting from the Q of 300 is not sufficiently narrow to give the necessary selectivity. By biasing the 2N123 in the meter circuit so that it conducts over only a few degrees of each cycle, the selectivity is improved to the extent that a 400-cycle change in frequency will give full-scale deflection on the meter. This technique lowers the requirements for "skirt" selectivity but makes extremely good limiting essential.

The specifications are shown below:

Size	6-7/8 × 3 × 2-1/2 in.
Power requirements	6 v at 2.3 ma

5. TRANSISTORIZED, PORTABLE, GAMMA SINGLE-CHANNEL ANALYZER FOR AIRBORNE MONITORING

J. T. DeLorenzo

Introduction

The instrument described below was designed as an airborne field-survey instrument for use by the Health Physics Division. ^(A) Major design objectives were: (1) capability of analyzing 0.25- to 1.0-Mev gamma fields of low intensity; (2) portability and compactness; (3) simplicity of circuit design for easy adjustment and servicing; (4) capability of driving a portable Curtiss-Wright milliamp recorder; (5) capability of operation in temperatures ranging from 0 to 45°C.

Circuit Description

Figure 5.1 is a schematic of the circuit. The instrument uses a 14-stage photomultiplier tube (6810A) with a 2-in.-dia by 3-in. NaI crystal. The 14-stage tube was selected to eliminate the need for a pulse amplifier. A corona-regulated, transistorized supply, described by Instrumentation and Controls drawing Q-2077, is used to regulate the first ten stages. A modified version of this design is used to supply the last four stages. This second supply is adjustable, permitting some control of photomultiplier gain.

An emitter follower couples the phototube output to a biased-diode (CR-1) discriminator stage. The diode bias determines the "E" level of the instrument.

A second emitter follower couples the output of the biased-diode discriminator to the upper and lower discriminators. The triggering level of the upper discriminator is adjustable with reference to the lower discriminator with the " ΔE " control potentiometer. The difference between the trigger levels of the two discriminators is the desired slit or window.

The inverted output pulse from the lower discriminator and the output pulse from the upper discriminator are fed into an anticoincidence circuit consisting essentially of two 1N67A diodes (CR-2, CR-3). A pulse is delivered out of the anticoincidence circuit when diode CR-2 is turned

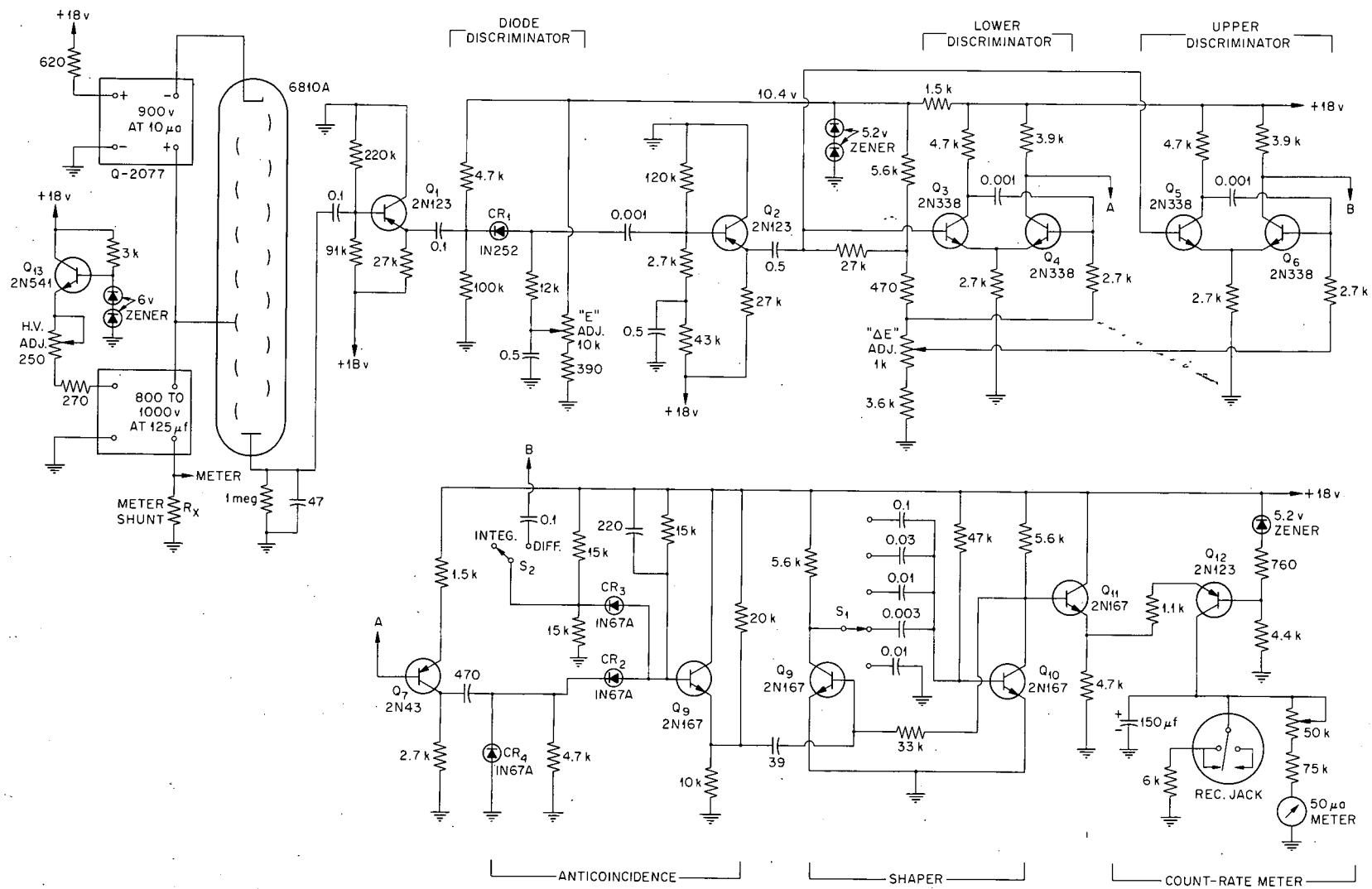


Fig. 5.1. Circuit Schematic of Portable Gamma Single-Channel Analyzer.

off by the lower discriminator with CR-3 held off by the upper discriminator. The presence of an output from the upper discriminator will turn on CR-3, thereby inhibiting the release of the anticoincidence output stage, Q8. The 220-picofarad capacitor across the 15-kilohm resistor in the base of Q8 serves to delay the pulse from the lower discriminator, thereby preventing false operation due to pulse rise-time delays.

The output pulse from the anticoincidence circuit is shaped by Q9 and Q10 operating as a single-shot multivibrator. The pulse width of the multivibrator can be varied with the range switch, S1. Four time constants can be selected with the switch and a fifth position permits the mechanical zero adjustment of the output meter in the count-rate meter.

The count-rate meter output circuit consists essentially of Q12 which is connected in the common-base mode. This serves to provide an ideal current source capable of generating as much as 6 v across the integrating tank in a linear fashion. An emitter follower, Q11, is used to drive Q12. A Zener diode in the base of Q12 serves to adjust the bias on Q12 in a manner to offset any variations in the B+ supply.

The entire instrument is powered by rechargeable nickel-cadmium batteries. Six 6-v cells are used in a series-parallel combination giving a +18-v supply with a 1 amp-hr capacity.

Performance

The high voltage for the photomultiplier tube was selected to produce photo-peak pulses equal to 1 v for 0.1 Mev.

The discriminator circuits are capable of accepting pulses whose amplitudes lie between 0.15 and 10 v. The window width is adjustable from 0 to 1 v.

Energy-axis shifts are expected to occur at differential counting rates in excess of 100,000 counts per minute (10-v pulses) because of voltage losses in the divider network for the last four stages of the photomultiplier tube.

The drift in count-rate output with temperatures ranging from 0 to 45°C is less than 4% of full scale. Most of this drift is developed in

the shaper and count-rate meter circuits and can be improved with small changes in the design.

A variation in power supply voltage of ± 2 v has almost no effect on the performance of the instrument other than a slight change in gain of the photomultiplier tube.

The instrument drain on the battery supply is approximately 50 ma. With the battery capacity provided, about 20 hr of continuous operation is possible before a recharge is necessary.

Physical Dimensions

The instrument is contained within a 14-1/2 in. \times 6 in. \times 6 in. aluminum case. The over-all weight is approximately 10 lb. A single handle mounted on the top of the case is provided to carry the instrument.

6. A HIGH-GAIN, LOW-NOISE, LINEAR PULSE AMPLIFIER
(Q-2069A)

N. W. Hill C. C. Courtney

Production designs have been completed on a linear pulse amplifier developed by E. Fairstein for use with Frisch-grid ionization chambers in alpha-particle spectrometers. This amplifier (Figs. 6.1 and 6.2) consists of a preamplifier having a cascode-connected input stage and two feedback groups having gains of 750 and 1.5, a main amplifier consisting of a single feedback group having a gain of 200, a biased-off postamplifier having a maximum gain of 16, and three White cathode followers - two of which are used as the output stages of the main and post amplifier, and the third as a driver for the gain control at the input of the last feedback group. Each of the three feedback groups in the amplifier employs a cathode follower to act as an output stage and to provide a bootstrap signal for the last amplifier in the loop.

The design goals for this amplifier were the highest possible signal-to-noise (S/N) ratio and a degree of gain stability which would permit full use of the S/N ratio. The input stage of the preamplifier is patterned after a circuit of Gatti's.¹ An E83F/6689 (V22) and an E88CC/6922 (V21) are connected as a cascode amplifier with the input grid of the E83F floating. The remainder of the circuit differs from Gatti's in that three equal-valued integrating-time constants are used to limit the high-frequency response.

The clipping and integrating times (which are equal for best S/N ratio) are adjustable over the range 1, 2.2, 4, 8, and 15 μ sec by a set of plug-in units. The pulse-shaping networks are all in the preamplifier.

A current-setting control is provided for optimizing the operating point of the input tube.

The main amplifier is conventional, and its gain is adjustable over a 16 to 1 range by factors of 2. No fine-gain control is used.

A precision pulser (mercury-wetted contact relay) is built into the main chassis.

¹C. Cottini et al., Nuovo Cimento 3, 473 (1956).

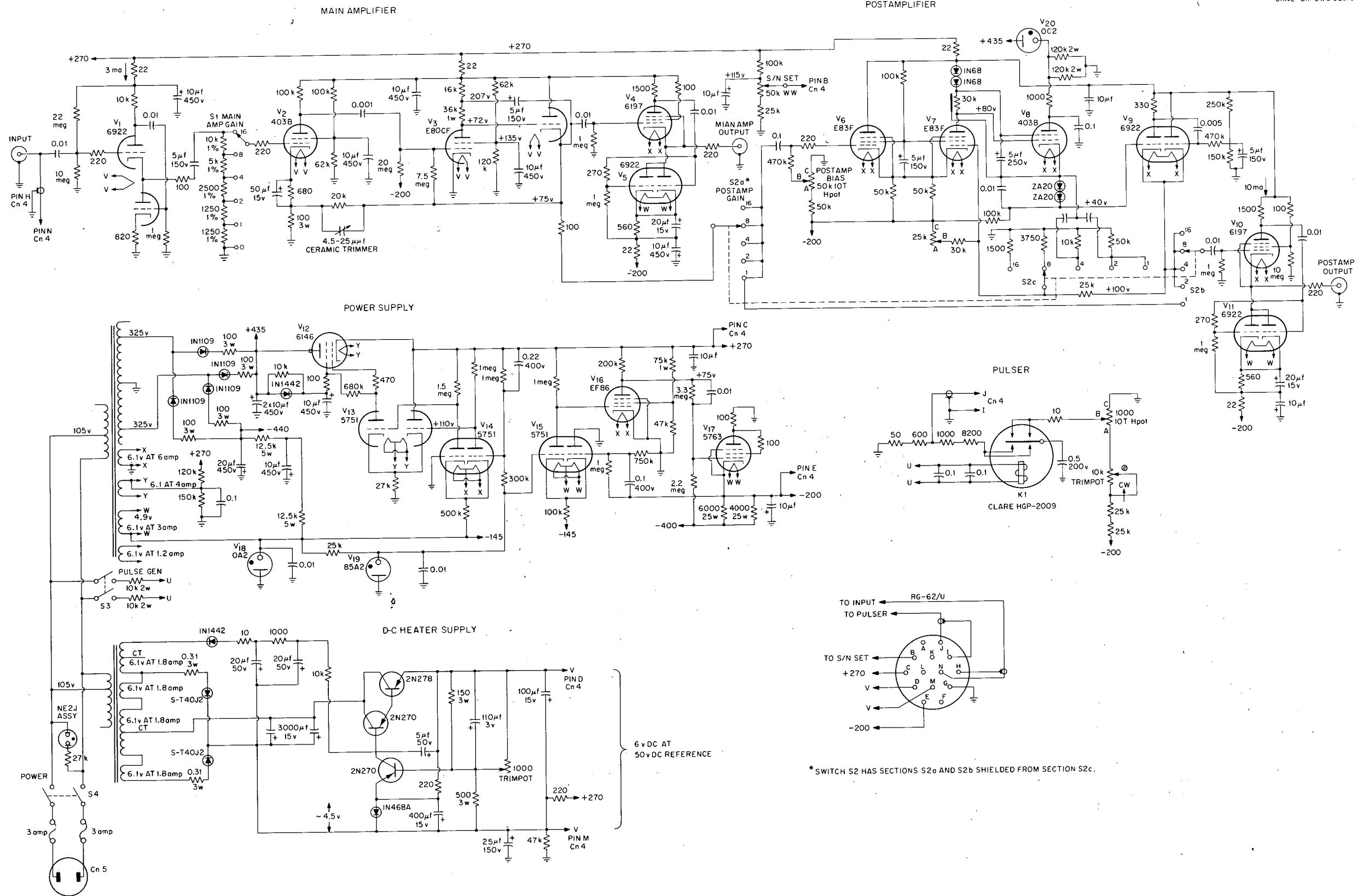


Fig. 6.2. Schematic of Main Amplifier Circuit.

The postamplifier is based on a design by Hutchinson,² but the circuit used here is a simplified version of the one published by him. The gain of the postamplifier assumes its normal value within 0.5 v of the threshold bias through the use of a biased-off cathode follower (V9) located at the output of the feedback loop. The current transition of this stage is augmented by a local positive-feedback loop (the 330-ohm resistor in the plate circuit of V9 and the 0.005- μ f capacitor which couples the plate to the following grid). The transition does not occur until the input tubes, V6 and V7, are in their linear operating range.

The postamplifier has a gain range of 1 to 16, adjustable by factors of 2.

The measured equivalent noise of the system with clipping and integrating times of 6 μ sec and a total input capacity of 20 pf (picofarads) is 240 ion pairs. This represents a full-width-at-half-maximum (FWHM) energy spread of 16 kev, assuming 28 ev per ion pair. In a test with a Frisch-grid ion chamber using a 5.3-Mev alpha-particle source, a measured FWHM of 31 kev was obtained.

The integral linearity of the amplifier is better than 1% in the output range from 5 to 100 v. Since the B supplies are regulated to better than 0.1% for a line change of $\pm 10\%$ and since all the tubes in the pre-amplifier and main amplifier are on a regulated d-c filament supply (1% for $\pm 10\%$ line change), the gain change with $\pm 10\%$ line changes is insignificant. Although no tests were made on long-term gain stability or gain drift rate, these should be excellent, since long-life, premium-grade tubes are used and since the feedback loops use temperature-stable components and initial feedback factors equal to or greater than 50.

²G. W. Hutchinson, Rev. Sci. Instr. 27, 592 (1956).

7. PERSONAL RADIATION MONITOR

R. H. Dilworth C. J. Borkowski

The objectives and general considerations of a fountain-pen sized personal radiation monitor weighing only 3.3 oz have been reported previously in this series.¹ This report presents the final form of the instrument after the completion of development. The circuit configuration of the original report has been retained in its essentials. The battery voltage has been reduced from 5 v to 4 v; the audible alarm has been made louder; and the range of temperature compensation has been increased. The mechanical construction has been changed considerably to improve ruggedness and to facilitate fabrication.

Figure 7.1 shows an exterior view. The case is of polished stainless steel, and a spring clip is provided for attachment to a pocket. The flashing neon warning lamp is protected by a molded Lucite cover, and the audible alarm is heard through an exit in the side of the case that is fashioned to resemble the familiar radiation safety symbol. When the screw cap at the bottom of the instrument is removed, the entire inner assembly may be withdrawn for battery replacement or inspection. Figure 7.2 shows the disassembled instrument.

The purpose of the instrument is to warn the user when he encounters an unexpected radiation field. This warning function must be distinguished from the problem of measuring radiation fields already known to exist. The characteristics of the instrument have been chosen expressly to favor the warning function. As a result, determinations of absolute intensity of radiation falling within the acceptable dynamic range are usually limited to establishing the order of magnitude. The warning signals given by the instrument are proportional in nature so that sources of radiation may be located or the best evacuation route chosen in exposure accidents.

Both visible and audible warning signals are produced. A neon lamp at the top of the instrument flashes at a rate proportional to radiation intensity. In the normal background of cosmic and natural radiation, the lamp will flash once every minute or two. In a field of 10 mr/hr the

¹R. H. Dilworth and C. J. Borkowski, Instrumentation and Controls Ann. Prog. Rep. July 1, 1959, ORNL-2787, p 55.



Fig. 7.1. Personal Radiation Monitor, Exterior.

lamp will flash about four times a second. The flashing rate increases with radiation intensity until a saturating flashing rate of three to four thousand flashes per minute is reached in fields of 1 to 10 r/hr. Above 10 r/hr the rate remains at this maximum. The dependence of flashing rate on radiation intensity is illustrated in the curve of Fig. 7.3.

The audible warning is produced by a hearing aid earphone at the base of an air column that exits through an opening in the side of the



Fig. 7.2 Personal Radiation Monitor, Disassembled

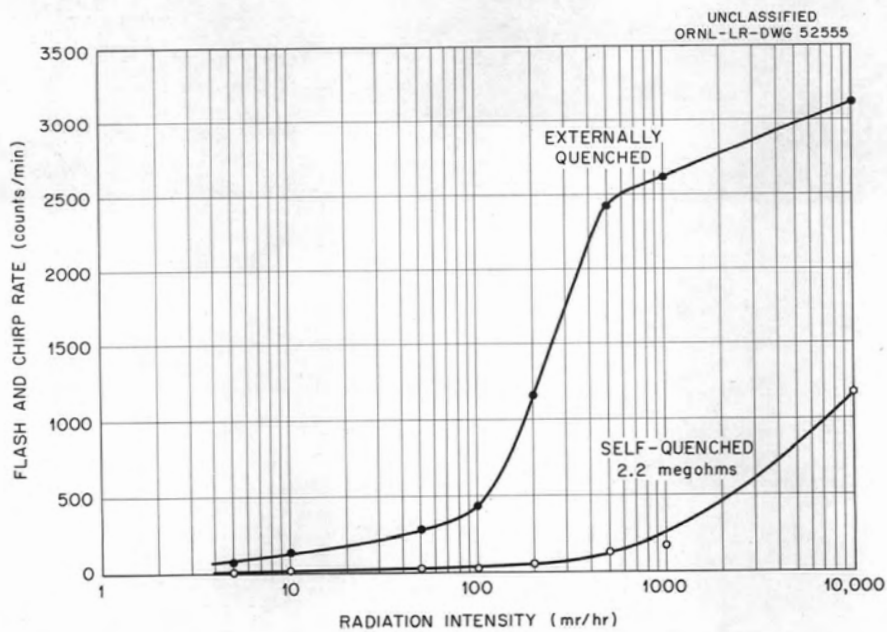


Fig. 7.3. Flash and Chirp Rate vs Radiation Intensity.

case. The sound is found somewhat complex when carefully analyzed; however, the subjective interpretation by the average user is always clearly understood. Each flash of the neon lamp is accompanied by a "chirp" from the earphone. This chirp consists of a sound which rises abruptly in amplitude and frequency and then decays more slowly again in amplitude and frequency. The maximum frequency of the sound at the abrupt start of the chirp is about 2000 cps when the chirp rate (which is also the neon lamp flashing rate) is of the order of a few per second. The decay of amplitude and frequency is exponential, with a time constant of about 0.1 sec. As higher radiation fields are encountered, the chirp rate increases proportionally, as shown in Fig. 7.3. The peak frequency of the chirp and the peak amplitude also increase with chirp rate. In a field of about 50 mr/hr the peak amplitude has increased to the point that the next chirp has occurred before the sound has decayed fully away, and the sound is now more nearly continuous. The peak frequency of the sound alarm rises with radiation intensity until a saturation is reached at about 3000 cps in fields of 0.5 r/hr and over. This relation is shown in Fig. 7.4. The air column that couples the earphone to the exterior of the case is dimensioned for quarter-wave resonance at this saturation frequency. As a result, the acoustical efficiency and therefore the apparent

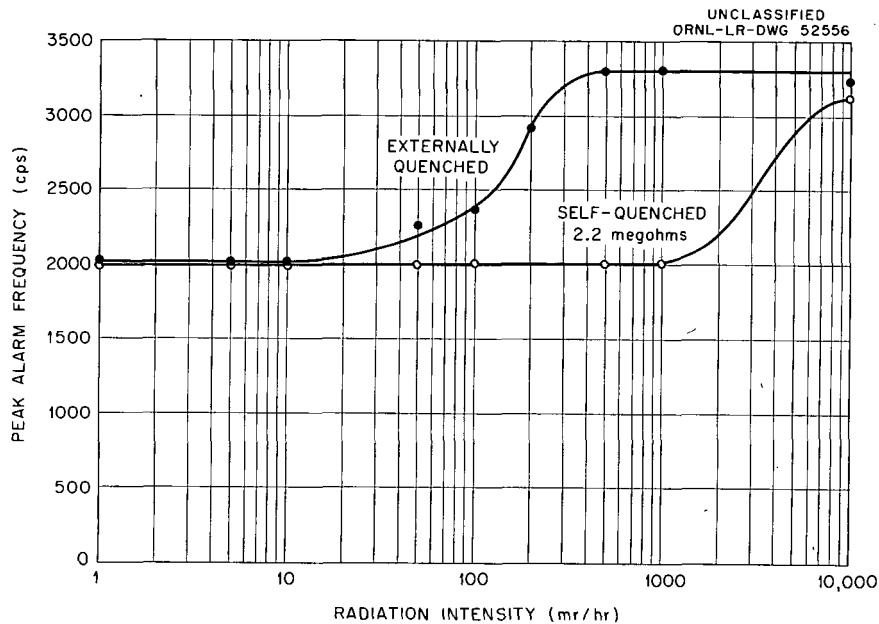


Fig. 7.4. Peak Alarm Frequency vs Radiation Intensity.

loudness of the alarm is greater for the higher and more dangerous radiation levels. The proportional information as to radiation intensity in the sound alarm is thus seen to be contained in a complex of chirp repetition rate, peak frequency, and amplitude. All three increase with radiation intensity. Even though the average user of the instrument probably will not recognize them definitively, his subjective interpretation of "increase" will be unailing.

An important characteristic of the monitor is the ability to maintain the alarm signals even when the radiation level has drastically exceeded the upper limit of its dynamic range of indication. Tests have shown that the saturated alarm rates that are reached between 1 and 10 r/hr are maintained as the intensity rises to at least 3×10^6 r/hr. In such fields a lethal dose is received in less than 1 sec; therefore the extension of the nonblocking range beyond this point is unjustified.

The loss of proportional indication when the radiation intensity has exceeded the saturating levels of 1 to 10 r/hr is a disadvantage when trying to locate the source of radiation or a safe exit route. A simple circuit change (unshorting a resistor) renders the instrument 100 times less sensitive and thereby raises the upper limit of proportional indication to about 100 r/hr. In the present design of the instrument this range change is possible only by removing the instrument from the case and making an irrevocable cut through the wire jumper that shorts the resistor in question. Consideration is being given to making this action simpler, with provisions for instantly changing the range. Such provision should remain irrevocable so that the loss of sensitivity would occur only in emergency situations when direly needed.

The instrument is powered by a 4-v mercury battery having a 1000 ma-hr capacity. The normal battery life is about six weeks of continuous use. There is no "on-off" switch. Battery life will be shorter if the instrument is subjected often to radiation greatly in excess of normal background. The cost of operation is somewhat less than 2 cents a day.

Circuit Description

The schematic diagram of the personal radiation monitor is shown in Fig. 7.5. The radiation detector is a miniature Geiger-Mueller counter.

of the halogen-quenched type. High voltage of about 500 v for operation of the counter tube and the neon lamp is obtained from a Cockcroft-Walton voltage quadrupler (diodes CR2 through CR5 and capacitors C3 and C4) which is driven through a step-up transformer from a transistor blocking oscillator, Q1. The voltage waveform at the collector of Q1 is shown in Fig. 7.6. Between blocking oscillations, Q1 is cut off and the collector rests

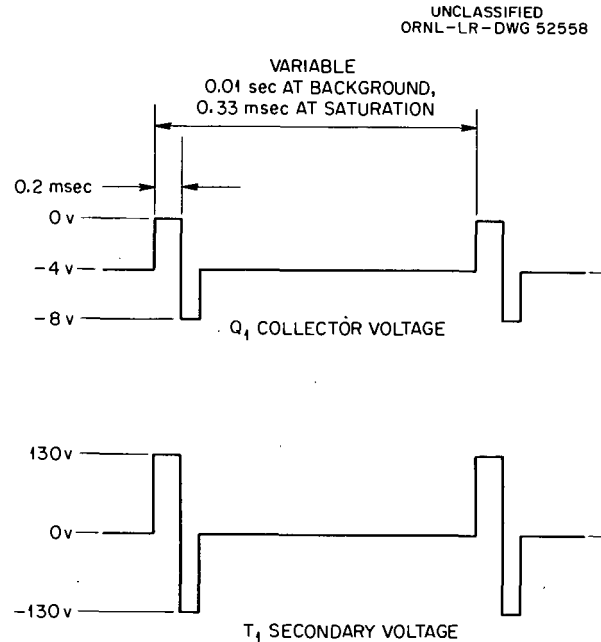


Fig. 7.6. Idealized Voltage Waveforms.

at -4 v. When the blocking charge on C1 has decayed sufficiently through R1 and R2, the base moves negatively to turn on Q1. The regenerative action of the feedback from the center-tapped primary of T1 is such as to strongly amplify the turn-on action until Q1 saturates. In so doing, the collector voltage has risen nearly to zero. The collapse of the magnetic field thus built up in T1 then initiates the reverse of the process in which the base of Q1 moves positively to turnoff. The regenerative action strongly amplifies the turnoff process. The transistor blocking oscillator Q1 is maintained in this cut-off condition because of the charge acquired by C1 during the brief on period. The collector voltage will begin to fall negatively as the collector current is removed and will fall considerably below the -4-v supply level because of the flyback action of the collapsing magnetic field in T1.

The effective turns ratio of T1 from the total secondary winding to the collector half of the primary is about 33 to 1. Therefore, the 4-v positive excursion of the Q1 collector produces a 130-v positive excursion in the T1 secondary, as shown in Fig. 7.6. Capacitor C3a is thus charged to 130 v through diode CR2. The flyback action would then, if unchecked, produce a negative excursion of 200 to 300 v in the secondary. The magnitude of this flyback excursion is strongly affected by load current variations in the quadrupler output, and a very poor voltage regulation would result. To circumvent this, the inverse breakdown of diode CR2 in the quadrupler is selected at about 260 v. The inverse diode voltage is the sum of the 130 v stored in C3a and the negative flyback excursion. The sum is limited by the inverse breakdown of CR2 to 260 v. Therefore the negative secondary excursion due to flyback in T1 is clamped to 130 v, and the secondary and reflected primary waveforms are symmetrical, single square waves. The output of the quadrupler is thus limited to twice the inverse breakdown voltage of CR2, or about 520 v. Since the selection of CR2 can be obtained only within ± 10 v of 260 v, the actual output voltage varies accordingly. The dissipation in CR2 due to this clamping action is well below the allowable rating.

The Philips 18509-02 G-M tube is intended for use in series with a large resistor (at least 2 megohms), and the radiation-induced discharges are quenched when the self capacitance of the tube - about 1 picofarad - is discharged from the original supply voltage to a certain extinguishing voltage, which is 350 v for this tube. For a small counter of this type, having a relatively small ratio of cathode to anode diameters, it is necessary for the actual terminal voltage of the counter to fall below this critical extinguishing voltage in order that each discharge be quenched. This is in contrast to the self-quenching action of larger tubes in which the larger diameter ratio permits a field reduction about the anode wire during discharge which quenches the discharge even though the terminal voltage of the tube is not allowed to fall significantly. The 18509-02 tube continues in discharge after being started until the terminal voltage is allowed to fall below 350 v.

In this circuit, the G-M tube is not operated in the conventional mode with a large series resistor. The resistor R5 is provided, but

it is normally shorted except when the emergency high range of indication is used. The circuit involving the tube can be seen to consist of a series connection of the output capacitors of the quadrupler, C4a and b; the G-M tube; resistor R4; capacitor C5; and diode CR1. The diode is connected for forward conduction with G-M tube current and may be neglected in this discussion. The 10,000-ohm resistor R4 is too small to provide conventional quenching by voltage drop. It is used to limit the peak discharge current and lengthen G-M tube life. The equivalent circuit for the G-M discharges is given in Fig. 7.7 in which the two series 0.005 mf capacitors in the quadrupler output are replaced by their single series equivalent of 0.0025 mf. The quantity of charge passed during a G-M discharge is equal in all three components of the circuit. The determination of this charge and the corresponding voltage steps on the capacitors are given in Fig. 7.7. When initiated by radiation, the G-M discharge continues until the voltage across the tube falls below 350. Capacitor C4, originally charged to 520 v by preceding blocking oscillator pulses, supplies the discharge current and in so doing discharges to 350 v. Capacitor C5 simultaneously charges to about 4.25 v. The quadrupler capacitor C4 must be recharged by the blocking oscillator before another G-M discharge is possible. Assuming that such recharging takes place, each successive discharge of the G-M tube imparts an additional 4.25 v of charging to C5. The magnitude of this voltage increment

UNCLASSIFIED
ORNL-LR-DWG 52559

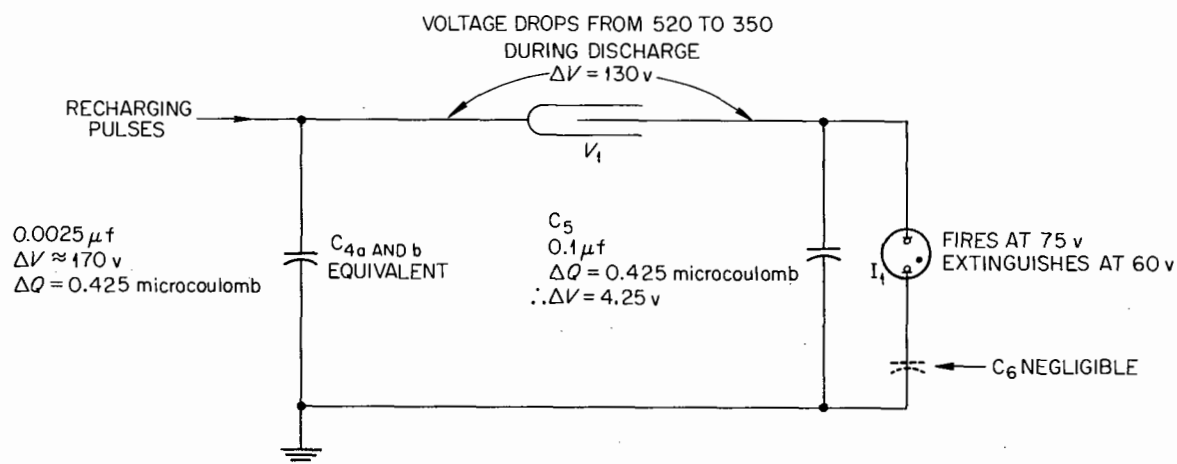


Fig. 7.7. Equivalent Circuit for G-M Tube Discharge.

decreases somewhat as the buildup of the voltage on C5 subtracts from the starting voltage across the G-M tube. When the instrument is started initially, with no residual voltage on C5, about 40 discharges of the tube are necessary before the voltage across C5 is sufficient to fire the neon lamp that shunts C5 in the full schematic, Fig. 7.5. About 75 v fires the neon lamp, and it then discharges C5 until the extinguishing voltage of the lamp is reached. This voltage is about 15 v below the firing voltage; therefore C5 is left with a residual of about 60 v after a recent G-M discharge. From this starting point, only six more G-M pulses are required to reach the firing point of the lamp gain. Thus it is seen that after the first flash is obtained, the neon lamp flashes once for each six discharges of the G-M tube, and a rudimentary scaler action is obtained. Operation of the tube in the unconventional manner just described results in a hundredfold increase in the output current when compared to conventional self-quenched operation in the same radiation field.

The discharge circuit of the neon lamp is extracted from the other circuitry and shown in Fig. 7.8. The source of energy is C5 being charged as described above. The diode CR1 is in forward conduction and therefore its resistance is negligible when C5 is being charged. However, for the discharge of C5, the diode does not conduct, and the path of current flow is through the emitter of amplifier transistor Q3. The polarity of the current is such as to turn on Q3 as if it were a grounded-base amplifier.

UNCLASSIFIED
ORNL-LR-DWG 52560

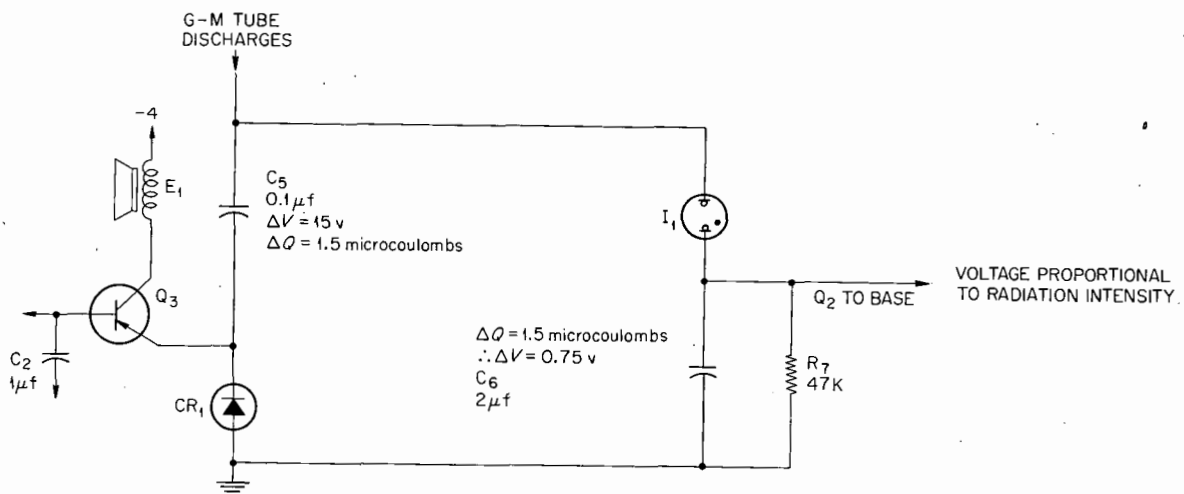


Fig. 7.8. Equivalent Circuit for Neon Lamp Discharge.

The base is effectively constrained by C2. The charge transfer is equal in C5 and C6, and the 15-v excursion at C5 results in a 0.75-v excursion at C6. The voltage placed on C6 in this manner is discharged exponentially by R7, with a time constant of 0.1 sec. If the neon lamp flash rate is great enough, the voltage across C6 is not depleted, and successive pulses add to the residual. The voltage across C6 is seen to be proportional to the flashing rate of the neon lamp. The flashing rate is in turn proportional to the current passed by the G-M counter. The counter current is proportional to radiation intensity. Consequently, the voltage across capacitor C6 is a measure of radiation intensity.

Transistor Q2 is an emitter follower that duplicates the voltage across C6 at a lower impedance. This voltage, which is proportional to radiation intensity, is fed back to the blocking oscillator through resistor R2. Resistors R1 and R2 are the discharge path for the blocking capacitor C1; therefore, as the voltage to which they are returned increases negatively, the repetition rate of the blocking oscillator increases. The net effect is that the repetition rate of the blocking oscillator is proportional to radiation intensity. This serves an essential function in providing a rate of recharging pulses to the voltage quadrupler circuit that is sufficient to maintain the output voltage to the G-M tube at a suitable level. A moderately good voltage regulation of the high-voltage supply is obtained in this manner, as is shown in the curve of Fig. 7.9. It should be remembered that the regulation at

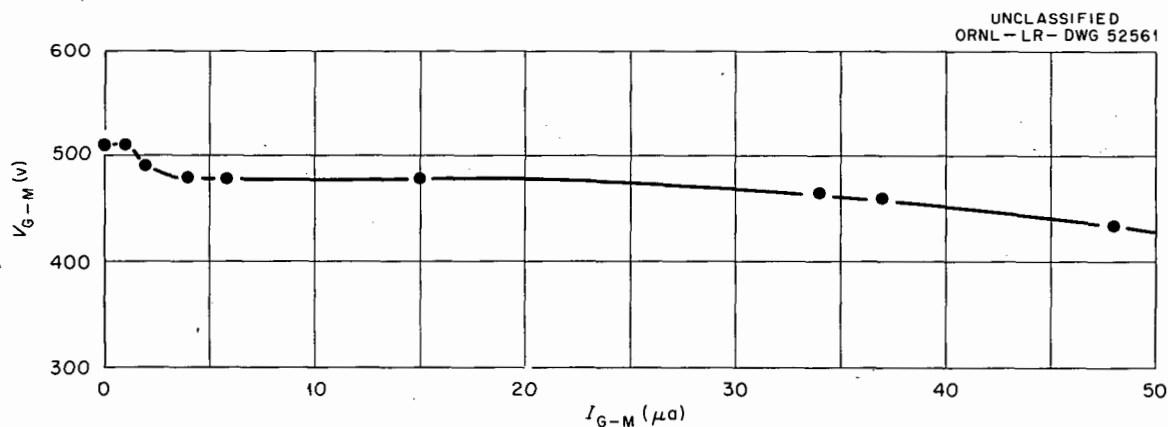


Fig. 7.9. G-M Voltage Regulation.

very low G-M currents is obtained by the clamping action of the inverse breakdown of diode CR2, as previously discussed.

Another important function of the compensatory feedback that controls the blocking oscillator rate is to automatically adjust the battery drain to the minimum value that ensures proper operation for a given radiation intensity. The duty cycle and therefore the battery current required by the blocking oscillator is much greater when the high-voltage supply is called upon to supply greater G-M currents in high radiation fields. Conversely, in background radiation the current output required of the high-voltage supply is negligible. The variation with radiation intensity of total battery current is given in Fig. 7.10. In order to provide the

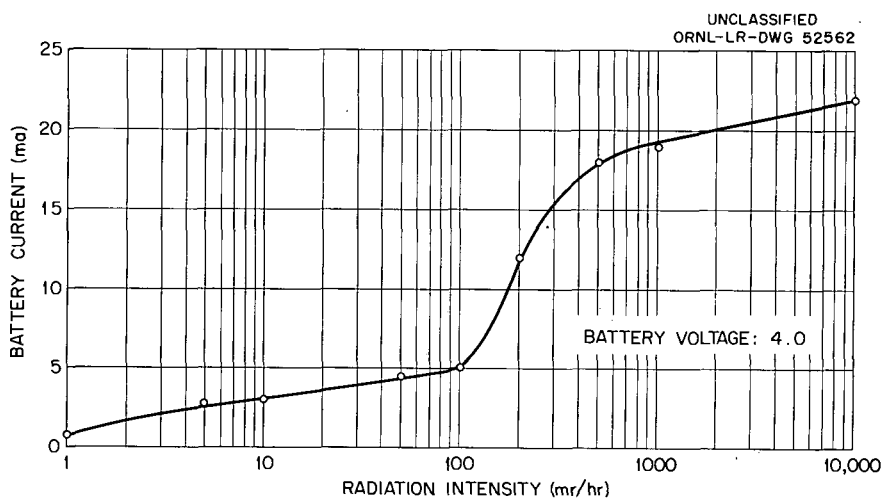


Fig. 7.10. Battery Current vs Radiation Intensity.

necessary minimum blocking-oscillator rate that will maintain the high voltage in readiness for possible radiation, resistor R6 sets a minimum voltage on C6 in the absence of radiation.

The range of repetition rate of the blocking-oscillator high-voltage supply has been chosen deliberately to lie in the lower audio frequency range from 100 to 3000 cps. Since this repetition rate is proportional to radiation intensity, as shown in Fig. 7.4, the warning may be had simply by listening to this rate. Transistor Q3 is an audio amplifier whose output drives a small earphone of the type used in eyeglass hearing aids. This earphone is at the base of an air column whose resonance occurs at the upper frequency limit of about 3000 cps in order to obtain greatest

loudness at the highest radiation intensity. Transistor Q3 is driven at its base by capacitor C2, which secures drive of the proper level and impedance from the base of the blocking oscillator transistor Q1. Bias current for Q3 is obtained through resistor R3 such that the operating current of Q3 increases with radiation level.

If the emitter of the amplifier transistor Q3 were returned to ground, the quiescent repetition rate of the blocking oscillator of about 100 pulses per second would be heard continuously. This would be annoying in offices or laboratories in which the instrument would be used. In order to provide muting of Q3 until the radiation level becomes significant, the emitter is returned to ground through a silicon diode CR1 connected for forward conduction when the transistor conducts. Such diodes have a forward-conduction characteristic in which there is very little conduction until the forward voltage has exceeded about 0.5 v. Since the base of Q3 is supplied bias through R3 from the emitter follower Q2, the forward-conduction voltage across diode CR1 will be below that necessary for conduction until radiation causes the emitter follower output voltage to rise above about 0.5 v. Above that level, Q3 will amplify in the usual manner. A further desirable audible effect is obtained by returning the lower side of C5 to the emitter of amplifier Q3. In this way, each discharge of the neon lamp pulses the emitter of Q3 positive with respect to the base and thus turns on Q3 in grounded-base fashion. Each single flash of the neon lamp now produces a chirp in the audible output even though the flashing rate is so low that the average voltage on C6 is insufficient to turn on Q3 continuously. This chirp, occurring once every minute or so in normal background, is a source of reassurance that the instrument is functioning properly. Furthermore, in high radiation fields where the audible alarm has become continuous, the connection just described produces an amplitude modulation of the alarm tone at the flashing rate of the neon lamp. This modulation adds a distinctive quality to the sound and adds to its warning nature.

In the quiescent condition of operating in normal background radiation, the battery drain is almost entirely that drawn by the blocking oscillator operating at its minimum rate of about 100 pulses per second. The audio amplifier is biased off by the muting diode, and the emitter

follower is being driven with only the minimum voltage level set by resistor R6 and thermistor R7. Under these low-current conditions the collector leakage currents of Q1 and Q2 contribute significantly to the operating currents. As a consequence, the operating currents decrease significantly when the instrument is operated in a colder environment in which the collector leakage currents are diminished. In fact, if the quiescent blocking oscillator rate were set to the minimum possible to sustain oscillation at room temperature, then the oscillation would cease when the instrument became cooler, and the instrument would be inoperative. This tendency to failure upon cooling is eliminated by setting the room-temperature oscillator rate high enough so that the decrease in rate upon cooling to the lowest temperature desired does not reach the point of failure. The amount of excess current thus needed at room temperature is reduced by the use of thermistor R7. The negative temperature coefficient of this device causes the room temperature resistance of 47 kilohms to triple at 0°C, and the voltage division ratio of R6 and R7 changes so as to compensate for the loss of operating current due to cooling. The thermistor also provides compensation in the same manner when the instrument is subjected to temperatures higher than normal. The compensation is not complete, and the battery current decreases when the instrument is cooled and increases when it is heated.

The alarm indications are also affected by temperature in that the absolute flashing and pitch rates will change. Figure 7.11 illustrates these temperature effects. However, the relative indications are always proportional to radiation intensity, and the basic warning function of the instrument is preserved over an ambient temperature range of 0 to 50°C. At the higher temperatures within this range the muting diode CR1 as well as the voltage placed across it have been affected so as to initiate a barely audible indication of the quiescent pulse rate of the blocking oscillator even in the absence of radiation. The resulting sound can be interpreted as a warning that the instrument is approaching the upper limit of its temperature range. This sound need not be confused with the audible indication of radiation, since it is of a steady nature instead of pulsating in amplitude, and also since the neon lamp will not be flashing.

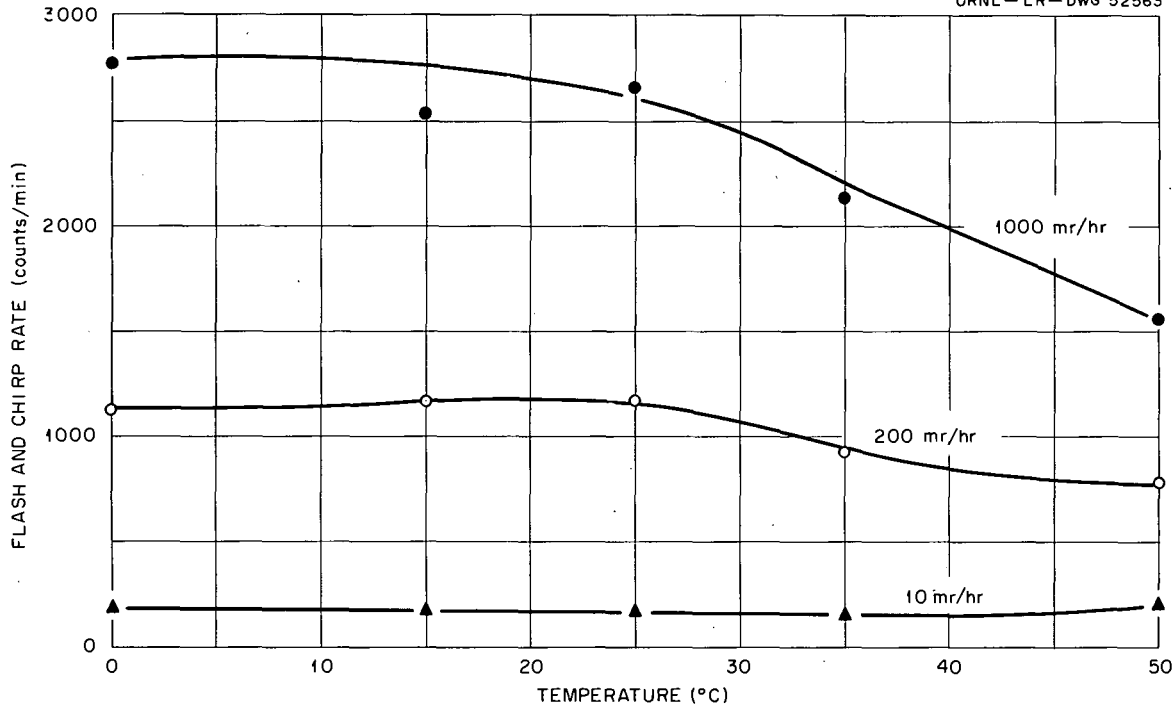


Fig. 7.11. Flash and Chirp Rate vs Temperature.

The battery current in a normal background is 0.75 ma. This current is set during final assembly of the instrument by the choice of resistor R6. Such a selection is necessary because the collector leakage currents of the transistors have a considerable variation as manufactured. These leakage currents affect the operating current as described above, and the usual types of circuits that would permit complete transistor interchangeability are too wasteful of battery current for use in this application. If the instrument is operated in a normal background of radiation for the life of a battery, about six weeks of operation is obtained. Under these circumstances the battery may be replaced routinely once a month to ensure operation. If the routine radiation intensity is higher, the battery life is shorter, and appropriate means for testing and battery replacement must be provided. The flat discharge characteristic of mercury cells provides normal operation over the effective life of the battery except for the relatively short final period of voltage decline. During this period the internal resistance will rise and the instrument can give an erroneous indication. In a low radiation field, the current drain is

low enough so as not to cause an appreciable drop in the terminal voltage of the battery, and indications will appear normal. But if the instrument is now placed in a strong radiation field, the increased battery current will drop the terminal voltage low enough to affect the G-M voltage, causing the flashing rate and peak frequency to fail to indicate as high a field as they should. This dependence of indications on battery voltage is shown in Fig. 7.12. From this it may be inferred that the best legitimate check of the instrument and its battery is to place it in a strong

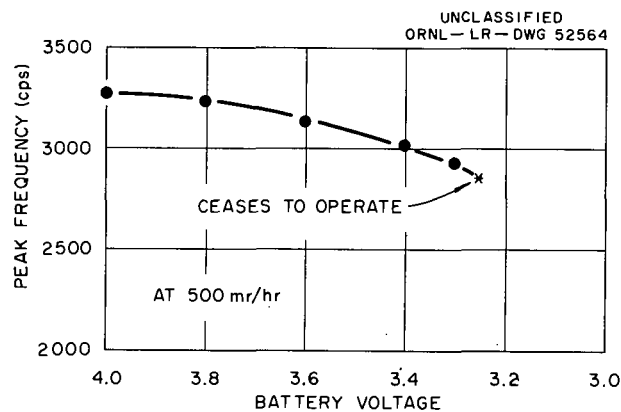


Fig. 7.12. Peak Alarm Frequency vs Battery Voltage at 500 mr/hr.

radiation field and observe the indications. The instrument lends itself to insertion into well-shielded test sources of suitable strength, for example, 10 μc of Sr^{90} . The G-M tube wall and the instrument case are thin enough to allow the use of hard beta radiation for testing if desired. Provision should be made for such strong source testing at point of use of the instrument or for routine battery replacement at a rate known to ensure operation. The 33-mf capacitor C7 across the battery provides peak current on demand and increases the effective life of the battery.

Mechanical Description

The basic mechanical features of the instrument were shown in Fig. 7.2. The case is made of type 304 stainless steel tubing having an outside diameter of 0.71 in. and a wall thickness of 0.015 in. The top flange is made by spinning, and the threads at the bottom and on the cap are rolled. The sound opening is formed by the Elox process. The

battery contacts are plated with gold to ensure reliability. The positive battery contact is made through a phosphor-bronze plated leaf that extends from the instrument assembly alongside the battery and around the end to make contact. In this way the very troublesome problem of making a reliable contact through a spring and cap and then back to the assembly has been eliminated. The strong spring in the screw cap provides a high pressure on the contacts. The main assembly of the instrument is shown before encapsulation in Fig. 7.13. A molded or machined Lucite molding

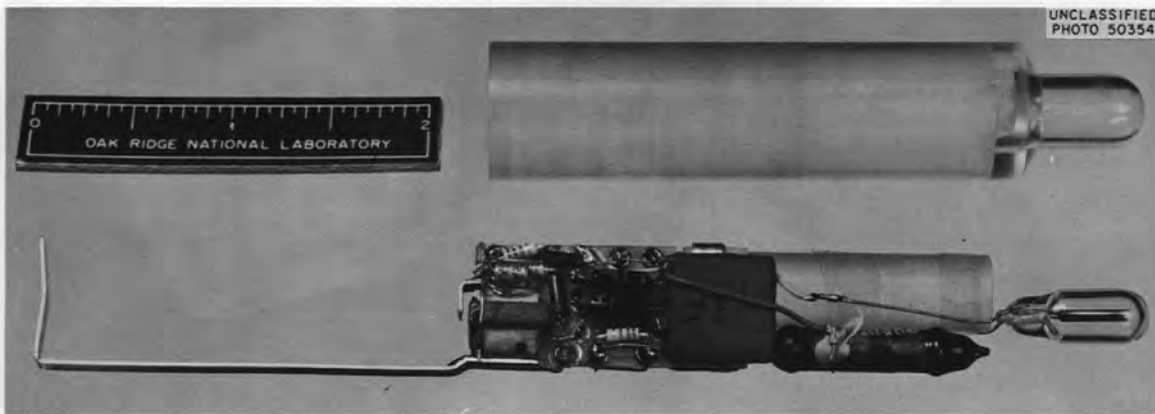


Fig. 7.13 *Internal Construction*

form is provided into which the electronic assembly is fitted. The top of the Lucite form is a protective cover for the neon lamp. The epoxy resin encapsulation is done in two steps. First the tip of the mold tube is filled with a few drops of epoxy resin and the assembly with the attached neon lamp is gently pressed into position. The tip of the form is heated to about 50°C for an accelerated cure of the epoxy. Upon cooling, the Lucite will contract upon the epoxy and counteract the effect of shrinkage in the resin when cured. In this way the Lucite does not separate optically from the resin and cloud the view of the neon lamp. In the second step, the entire remaining void in the molding tube is filled with epoxy and allowed to cure at room temperature. Some refilling of the end around the battery contact may be desirable to counteract the shrinkage as curing takes place.

The resonant air column is formed by cementing an entirely sealed, hollow, Lucite column of the proper dimensions to the earphone sound-output tube before the encapsulation process. After the epoxy is cured, the air column is opened to the outside with a ball end mill. Orientation of the milled hole with the case hole is assured by a wire key, spot welded inside the case top that engages a matching slot in the Lucite molding form. Araldite epoxy resin has been used in prototype instruments.

The electronic assembly is also seen in Fig. 7.13. An epoxy-fiberglass board, 0.020 in. thick, is used as a mechanical foundation. The larger components are cemented to the board during assembly, and the smaller components are supported on their own leads which are soldered into miniature gold-plated eyelets. The component placement has been arranged so that nearly all the component leads meet directly together at eyelets. Only four wires are used to connect the earphone, G-M tube, and neon lamp to the chassis board. Since only one of these could be placed on the chassis board, it was felt that the use of a printed circuit on the board was not justified. It is obvious that careful soldering technique is necessary to fabricate such an assembly without damage to the semiconductors. Experience has shown that the average technician familiar with more ordinary electronic construction can quickly acquire the skills needed for this type of assembly.

Prototype Experience

Experience obtained with prototype instruments of the monitor has been in two categories: (1) that dealing with the general usefulness of an instrument of this type in protecting personnel from radiation exposure, and (2) that relating to the reliability and performance of the particular prototype instruments that have been fabricated. Experience in the first category has been uniformly enthusiastic among field users of the instrument. The instrument has not been involved in any emergency situations, but its usefulness in routine operations has been well demonstrated. Users have located unknown beams of radiation around reactors and process plants easily. Those who do manipulations of radioactive objects from the shadow of shielding find that the instrument permits drastic reduction in accumulated doses by giving instant warning when the safe shadow

has been exceeded. Most users find it possible to identify the order of magnitude of unknown radiation after brief prior experience in known fields. Those who have made routine use of the instrument report a considerable confidence in their ability to protect themselves from accidental exposure. This tendency on the part of the user to place such reliance on the instrument obviously places a more stringent requirement of operational reliability on the circuit design.

The experience gained with regard to operation of prototype instruments is not subject to simple interpretation. The first types of instruments built began field service in March 1959. They used the same circuit essentials as the present model, but the circuit details and the components were quite different. These early instruments were made without encapsulation, so as to facilitate changes; therefore, they were very delicate mechanically. As this final preferred circuit evolved, six successive designs were made. Some of these stages involved unsuccessful innovations, and the experience thus obtained had no bearing on the present model. Mechanical failure due to dropping the instrument accounted for the removal of many instruments from service before the present rugged design was achieved. Of the 69 instruments made over the development period, an average of about 20 has been in field service at any one time. Older-design instruments have been gradually replaced with newer models as the older ones were mechanically damaged or as circuit failure occurred. The present distribution of field instruments consists of about half of the final design and half of earlier models. The oldest types now in service have been in constant use for over a year.

This ever-changing distribution of instruments in field experience precludes exact numerical data on the reliability of a specific design. However, careful logs of causes of failure were kept, and a useful pattern of experience evolved. Certain components and circuit features were eliminated when their failures were noted. The present design involves no components or circuits that do not have some basis of reliability in the composite experience of past models. Of all the components in the present design, only two have a history of nonmechanical failure in the entire experience period. One of these is the 0.1-mf capacitor, C5; two

failures have been noted. This capacitor is operating at its rated voltage of 75 v. A search for a more conservatively rated unit having suitable size and cost has been unsuccessful. In future construction, this component will be subjected to a breakdown and leakage test at three times rated voltage in an attempt to preclude this failure. The other component with a history of failure is the G-M counter tube. Type 18509-01 tubes have been used in all instruments in field use up to the time of this report. The unconventional external quenching previously described to obtain hundredfold-greater current output has resulted in a tendency to "afterpulse" after a strong irradiation in about half the tubes tested. Selection was necessary to ensure elimination of these tubes. Experimental evidence indicated that adsorption of the bromine quenching agent on the cathode wall was the probable cause. The manufacturer has just made available an improved tube, the 18509-02, which has a higher bromine content and a better cathode surface. The few samples of this new tube that have been tested do not evidence any of the previous difficulties. Although unproved by field experience, the laboratory tests justify confidence that the 18509-02 tube will be reliable. It should be noted that the G-M counter reliability is without history of failure when operated in the less-sensitive conventional mode with resistor R5 unshorted. In application where size is not so critical, the somewhat larger Philips 18550 G-M counter tube will operate the circuit shown in Fig. 7.5 in the conventional self-quenched mode with R5 unshorted and have an over-all sensitivity about five times less than the 18509-02 in the high current mode.

At this writing, the Laboratory is procuring a large quantity of personal radiation monitors for routine use.

The considerable improvements in the mechanical ruggedness of the present design and the encapsulation techniques are due to R. J. Fox. The prototype instruments were constructed by J. L. Hutson. Grateful acknowledgment is made of their essential contributions to this development.

8. SILICON SURFACE-BARRIER NUCLEAR-PARTICLE SPECTROMETER

J. L. Blankenship C. J. Borkowski

Abstract

Gold-silicon surface-barrier counters which give good resolution at room temperature have been made. Counters from 150-ohm-cm material have given 15-keV ($\sim 1/4\%$) resolution for Cm^{244} (5.801-MeV) and Am^{241} (5.477-MeV) alpha particles. A large-area (1-cm²) counter has given 19-keV (0.35%) resolution for Am^{241} alpha particles. The detector has resolved alpha-particle groups which previously had been unresolved with Frisch-grid pulse-ion chambers.

Introduction

A grown p-n junction diode was first used by McKay in 1949 to detect alpha particles.^{1,2} This diode had poor energy resolution and a very small effective area. Orman and others at Purdue achieved similar results in 1950.³ Gossick and Mayer in 1956 made a small-area germanium surface-barrier diode which operated at room temperature with rather poor energy resolution.^{4,5} Shortly thereafter, Walter *et al.* at ORNL began making germanium surface-barrier counters for cryogenic physics experiments.⁶ Russian scientists did similar work shortly thereafter.^{7,8}

¹K. G. McKay, Phys. Rev. 76, 1537 (1949).

²K. G. McKay, Phys. Rev. 84, 829 (1951).

³C. Orman *et al.*, Phys. Rev. 78, 646 (1950).

⁴J. W. Mayer and B. R. Gossick, Rev. Sci. Instr. 27, 407 (1956).

⁵J. W. Mayer, J. Appl. Phys. 30, 1937 (1959).

⁶F. J. Walter *et al.*, Phys. Semiann. Prog. Rep. Mar. 10, 1958, ORNL-2501, p 73; Study of Germanium Surface Barrier Counters, ORNL CF-58-11-99 (Nov. 28, 1958).

⁷A. V. Airapetyants and S. M. Ryvkin, Soviet Phys. - Tech. Phys. 2, 79 (1957).

⁸A. V. Airapetyants *et al.*, Soviet Phys. - Tech. Phys. 2, 1482 (1957).

McKenzie and Bromley at Chalk River also made germanium surface-barrier diodes which operated at liquid-nitrogen temperatures.⁹⁻¹¹

In the spring of 1959 the groups at RCA-Montreal, Chalk River, Bell Telephone Laboratory, California Institute of Technology,¹² ORNL,¹³ and Hughes Aircraft^{14,15} began work on silicon diodes which would detect alpha particles at room temperature. Except for the early work at Chalk River and the California Institute of Technology on the silicon surface barrier, the other groups have been working with the diffusion technique for making a p-n junction diode for alpha-particle detection. At ORNL emphasis has been placed on surface-barrier diodes because of the possibility of superior performance for large-area devices. This potential advantage is due to the difference in fabrication techniques. The surface-barrier technique does not require the use of high temperatures and, consequently, the finished device has the same minority carrier lifetime as the starting material. The reverse leakage current, which is a noise source and which affects energy resolution, is due to diffusion of minority carriers to the barrier and is given by $I_{\text{REV}} \propto \rho/\tau^{1/2}$, where ρ is the resistivity, and τ is the minority carrier lifetime.¹⁶ It is seen that long lifetimes give reduced leakage current. The total barrier leakage current is proportional to diode area, and for large-area counters long minority-carrier lifetime becomes important.

The formation of a p-type inversion layer on the silicon surface is accomplished by treatment of the surface to produce a high density of

⁹J. M. McKenzie and D. A. Bromley, Phys. Rev. Letters 2, 303 (1959).

¹⁰J. M. McKenzie and D. A. Bromley, "International Convention on Transistors and Semiconductor Devices," Spec. Suppl., Proc. Inst. Elec. Engrs. (London), Pt. B. (May 1959).

¹¹J. M. McKenzie and D. A. Bromley, Bull. Am. Phys. Soc. [2] 4, 422 (1959).

¹²E. Nordberg, Bull. Am. Phys. Soc. [2] 4, 457 (1959).

¹³J. L. Blankenship and C. J. Borkowski, Bull. Am. Phys. Soc. [2] 5, 38 (1960).

¹⁴S. S. Friedland, J. W. Mayer, and J. S. Wiggins, Hughes Aircraft Technical Memorandum 626 (1959).

¹⁵S. S. Friedland et al., Rev. Sci. Instr. 31, 74 (1960).

¹⁶J. N. Shive, The Properties, Physics and Design of Semiconductor Devices, p 350, Van Nostrand, Princeton, 1959.

electron traps.^{17,18} An etched and washed silicon crystal surface exposed to ambient air develops surface states which have produced good surface barrier diodes.

Since a reverse-biased diode has a space charge region in which an electric field exists, any charge carriers produced in this region by ionizing radiation can be swept out and collected. The space charge region depth and capacitance per unit area depend on the applied bias voltage and the resistivity of the starting material. The space charge region depth X , in microns, is given by $X^2 = (V/N) \times 1.33 \times 10^{15}$, where V is the sum of the applied voltage and the barrier height potential, and N is the uncompensated carrier concentration in atoms/cm³.

The capacitance per unit area, C/A in 10^{-12} farads per cm², is given by $C/A = 1.06 \times 10^4(1/X)$. The uncompensated carrier concentration is given by $N = 1/\rho\mu e$, where ρ is the resistivity in ohm-cm, μ is the mobility of the majority carrier, and e is the electronic charge, 1.6×10^{-19} coulomb; μ (p type) = 450 cm² volt⁻¹ sec⁻¹, and μ (n type) = 1200 cm² volt⁻¹ sec⁻¹.

The above equations can be solved graphically with the aid of the nomograph shown in Fig. 8.1. Thus for 3600-ohm-cm n-type silicon with 45 v reverse bias, the effective barrier depth is 200 μ and the capacitance is 52 picofarads for a 1-cm²-area detector. This depth corresponds to the range of a 5-Mev proton.

Construction Methods

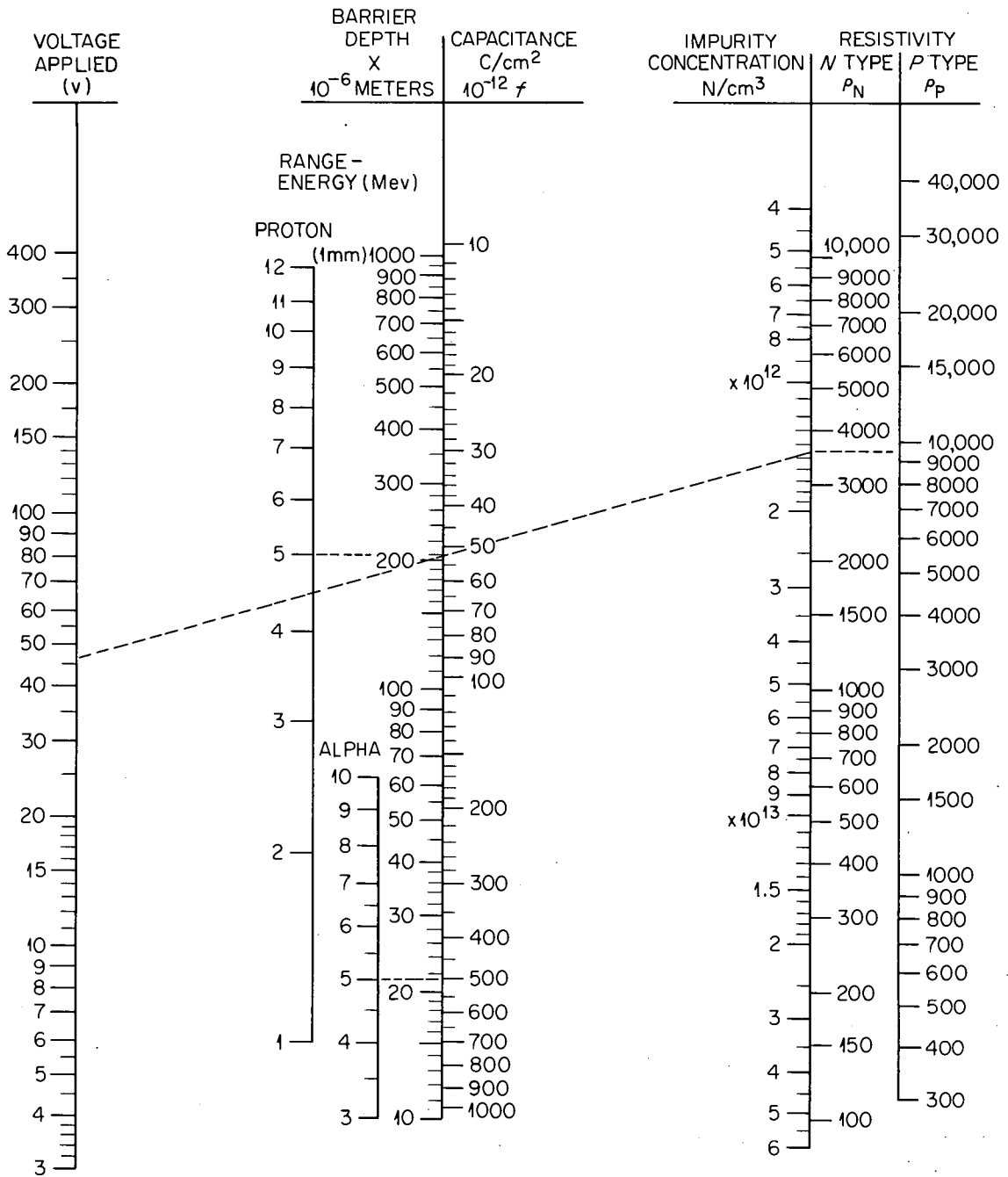
Conventional semiconductor technology is used in fabricating the surface-barrier counters.^{19,20} Figure 8.2 shows several of the steps in the preparation of counters. The silicon is purchased in single-crystal ingots of about 1-in. diameter and in assorted lengths, and then sliced to about 0.050-in. thickness with a diamond-impregnated-steel abrasive

¹⁷H. Statz et al., Phys. Rev. 106, 455 (1957).

¹⁸J. I. Pantchechnikoff, Rev. Sci. Instr. 23, 135 (1952).

¹⁹H. E. Bridgers, J. H. Schaff, and J. N. Shive (eds.), Transistor Technology, Vol I, Van Nostrand, Princeton, 1958.

²⁰F. J. Biondi (ed.), Transistor Technology, vols 2 and 3, Van Nostrand, Princeton, 1958.



$$X^2 = V \cdot \frac{1}{N} \cdot 1.326 \times 10^{15}, \quad C/A = 1.061 \times 10^4, \quad \frac{1}{X} \cdot \rho = \frac{1}{N\mu e}$$

$$\mu_N = 1200 \text{ cm}^2/\text{volt}\cdot\text{sec}, \quad \mu_P = 450 \text{ cm}^2/\text{volt}\cdot\text{sec}$$

Fig. 8.1. Nomograph for Silicon Diode Barrier Equation.

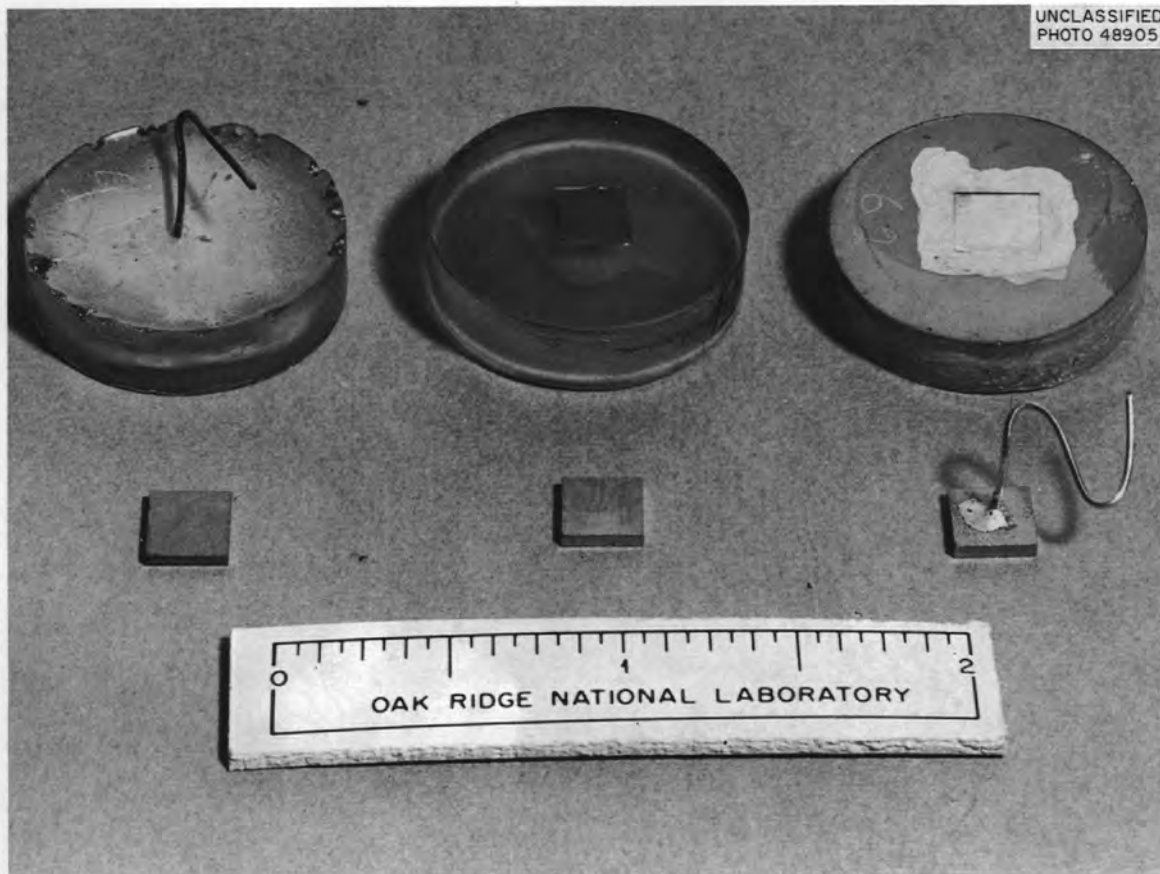


Fig. 8.2. Several Steps in the Construction of Surface-Barrier Diodes.

disk. Water is used as lubricant and coolant. The wafers are then diced to the required size, lapped with 400-mesh silicon carbide, and thoroughly washed. Then the wafers are nickel plated, using the electroless nickel plating method.²¹ A copper wire is attached to one side by soldering to the nickel plating with ordinary Pb-Sn eutectic solder. The solder joint, nickel plating, and wire comprising the ohmic contact are masked with a protective coating such as polystyrene dissolved in toluene or Apiezon W dissolved in trichloroethylene. The unprotected nickel plating is stripped off, and the crystal is then etched lightly in CP-4.²²

²¹M. H. Sullivan and J. H. Eigler, *J. Electrochem. Soc.* 104, 226 (1957); see also ref 20, vol 3, p 173.

²²CP-4 has the following composition: concentrated nitric acid, 5 parts by volume; concentrated hydrofluoric acid, 3 parts by volume; glacial acetic acid, 3 parts by volume; liquid bromine, 10 drops per 50 cc of acid mixture.

The silicon wafer is cast in an epon resin such as Ciba Araldite, with one face of the silicon wafer flush with the plastic. The silicon and plastic are lapped through several grades of silicon carbide abrasive in water slurries until a fine matte finish is obtained. Then the silicon is etched in CP-4 until a smooth, specular surface is obtained. The etch rate may be modified by varying the amount of acetic acid in the CP-4 in order to obtain the best surface appearance. The crystal assembly is then washed several times in deionized water and dried. A thin layer of a solution of polystyrene dissolved in toluene is painted around the edges of the silicon face in order to reduce surface-leakage current across the edges of the space charge region.

A thin layer of gold ($50-100 \mu\text{g}/\text{cm}^2$) is then deposited by vacuum evaporation²³ onto the entire face of the crystal assembly, thus forming a conductive sheet over the silicon face and plastic. Here a pressure contact can be made without stressing or scratching the silicon crystal surface. Stable diode characteristics have been obtained by allowing the crystal to remain in typical room ambient conditions for two or three days, either before or after depositing the gold film. This process of aging perhaps permits the formation of an oxide layer and adsorption of water on the freshly etched silicon crystal surface. Both oxygen and moisture are known to serve as trapping sites for electrons, thus forming a p-type inversion layer. This aging can be accelerated by exposing crystals to H_2O_2 , wet oxygen, ozone and steam, or oxygen and steam.

Evaluation Methods

The counter diode characteristics should be tested for low forward resistance and low reverse current over the desired voltage range. A good 5×5 -mm counter will have a reverse current less than $0.05 \mu\text{a}$ at 20 v bias. A high value of resistance ($\sim 10^5$ ohms) should be in series with the counter when measuring reverse current characteristics so that when the avalanche "knee" is reached, the current will be limited to a safe value. An acceptable counter diode characteristic has always been

²³L. Holland, Vacuum Deposition of Thin Films, Wiley, New York, 1958.

accompanied by good energy resolution, although a counter with higher reverse current may still give acceptable energy resolution.

Connections are made to the lead wire on the back and to the gold film on the front of the plastic. The bias voltage, which is usually supplied by a battery, is applied through a resistor of a suitable value, ~ 1 megohm, with the pigtail lead (ohmic contact) positive. A low-noise preamplifier of the type which is used with Frisch-grid pulse-ion chambers is satisfactory for counters whose capacitance does not exceed ~ 50 picofarads.

Since the collection time for both electrons and holes is less than 10 nanosec for alpha particles, the clipping time of the amplifier may be adjusted for best signal-to-noise ratio. Clipping times of 0.5 to 2 μ sec are suggested. At ORNL the Q-2069B (-1 and -3) "linear amplifier and preamplifier for alpha energy analysis" has been used; special features are a 417A in a low-noise cascode input stage, capacitance feedback to the input grid,²⁴ and a postamplifier with adjustable bias.²⁵ The spectra were taken with a 256-channel analyzer.

The noise contribution to resolution spread can be measured in two ways: The first method requires the insertion of a charge at the preamplifier input which produces the same pulse amplitude as the alpha particle. This is accomplished by applying a large voltage pulse from a mercury pulser through a capacitor which is small compared to the total input capacitance of the preamplifier and counter. The pulse-height distribution of the artificial pulses will show the effect of noise on the resolution. A second method consists of measuring the pulse height produced by alpha particles of known energy and then measuring the rms output noise in the absence of the alpha source. If amplifier gain is linear with amplitude, then the resolution spread due to the noise is given by $(E \text{ noise rms}/E \text{ pulse}) \times 2.355 \times 100\% = \text{full width at half maximum (FWHM)}$.

²⁴G. G. Kelley, Phys. Semiann. Prog. Rep. Sept. 10, 1956, ORNL-2204, p 55.

²⁵Instrumentation and Controls Div. Drawing Q-2069B (-1 and -3).

Discussion of Results

The alpha spectra shown in Fig. 8.3, taken with a 1-cm² counter made from 3600-ohm-cm n-type silicon, gave a resolution of 0.35%, limited by the inherent detector noise and not by the amplifier. Figure 8.4 displays the beta spectra of Hg²⁰³ taken with a 1-cm² counter made from 3600-ohm-cm material. Counters made from 3600-ohm-cm silicon with 2.6-cm² sensitive area have given 1.8% resolution for 5.5-Mev alpha particles. Counters

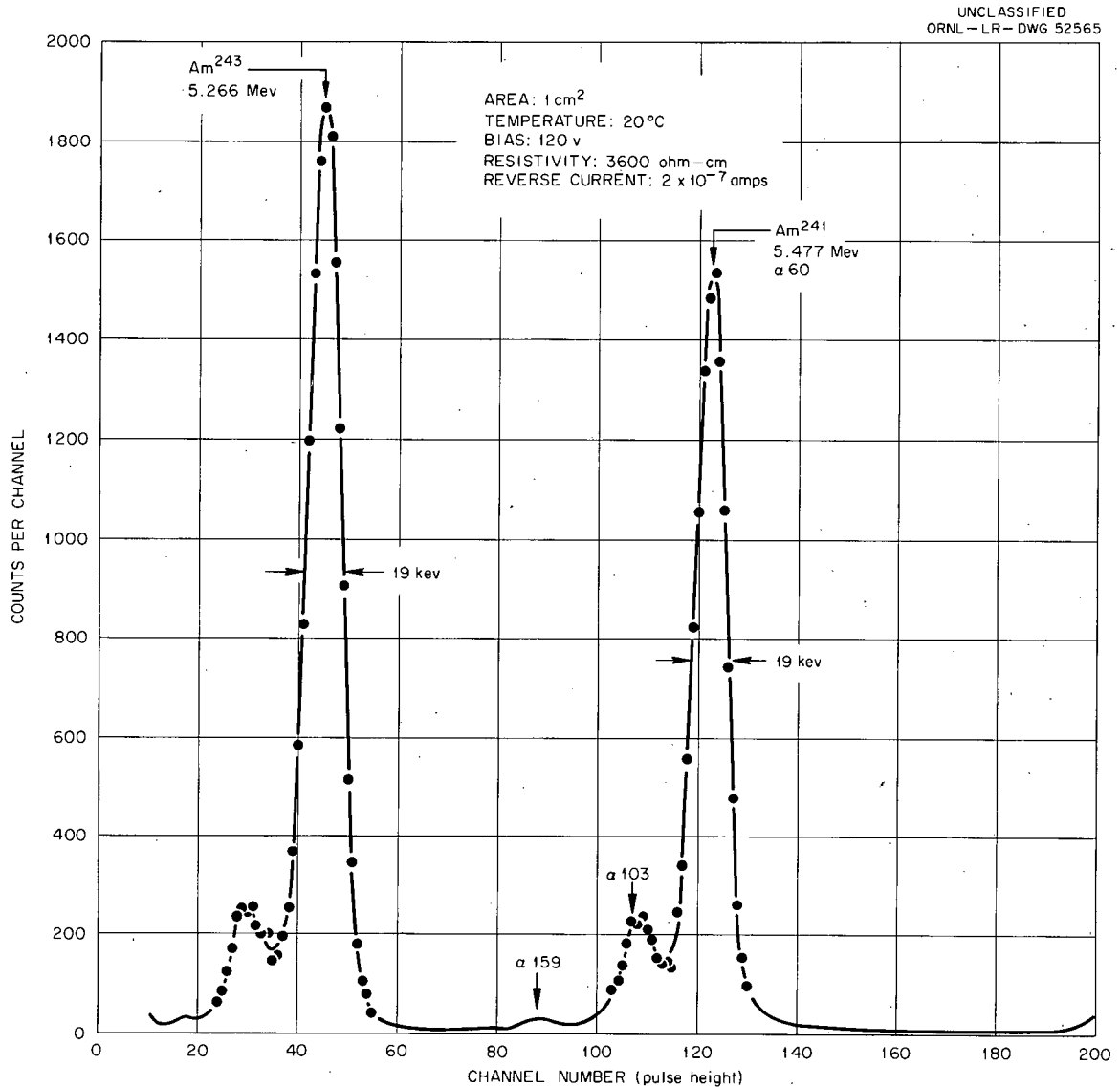


Fig. 8.3. Pulse-Height Spectra of Am²⁴¹ and Am²⁴³ Taken with a Detector of 1-cm² Sensitive Area.

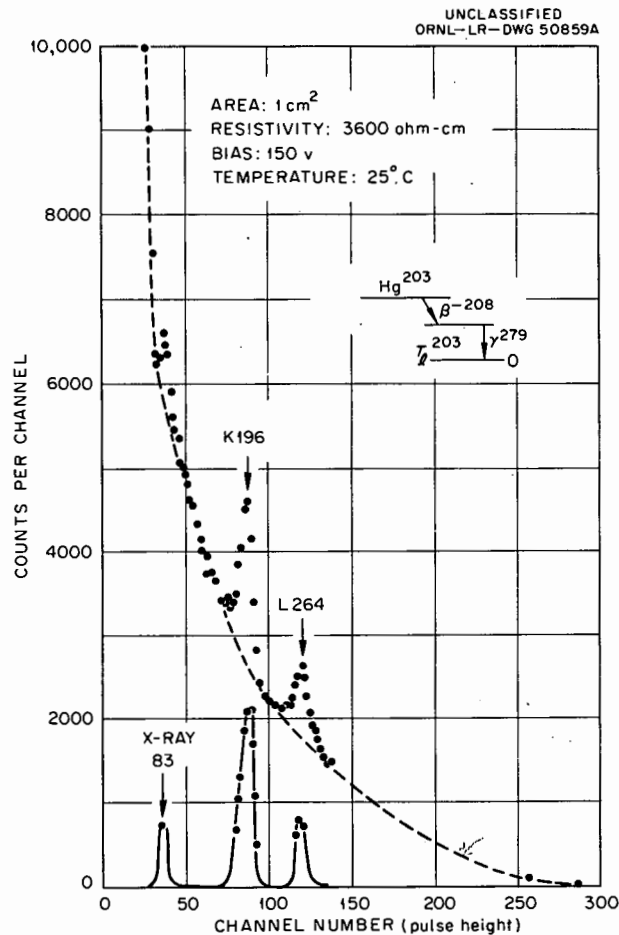


Fig. 8.4. Silicon Surface-Barrier Detector Beta Spectra of Hg^{203}

with areas of 25 mm^2 have given 16-kev resolution for 5.5-Mev alpha particles when operated at room temperature. The alpha spectra displayed in Fig. 8.5 were taken with a 25-mm^2 detector cooled to dry-ice temperature. The total resolution is 13.5 kev; the electronic noise contributed only 4 kev.

Figure 8.6 shows the best resolution that has been achieved with a 6.3-mm^2 counter. The resolution of 15 kev was limited by factors other than amplifier noise, since the equivalent input noise of the amplifier was 7.5 kev (FWHM) for a total input capacitance of 50 picofarads. Therefore, the intrinsic resolution of this counter was 13 kev. The fine structure may be seen for the α_0 , α_{60} , α_{103} , and α_{159} lines. The ratios of the areas under these lines are in agreement with magnetic spectrograph data.

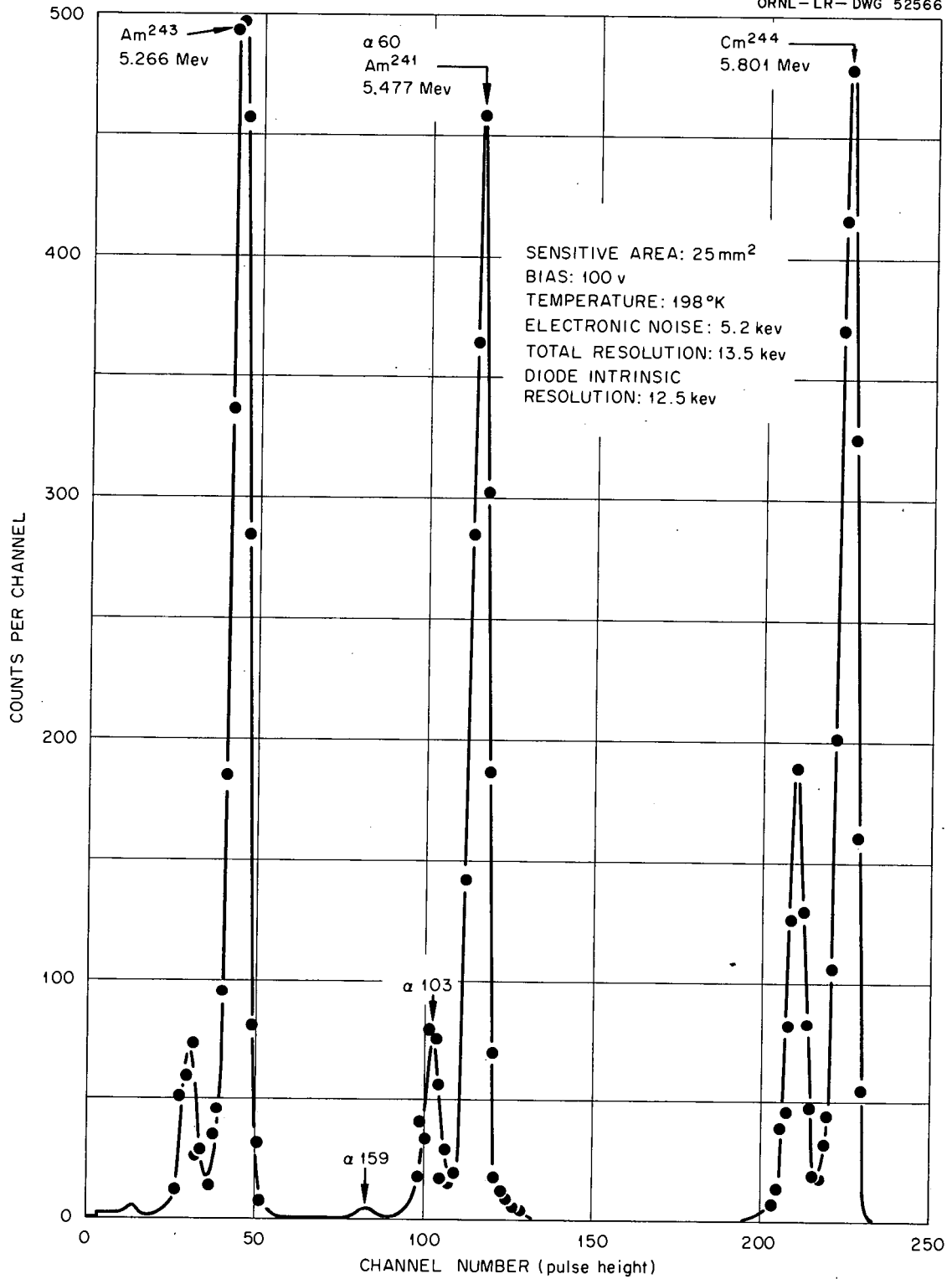


Fig. 8.5. Pulse-Height Spectra of Am²⁴¹-Am²⁴³-Cm²⁴⁴ Taken with a Detector of 25-mm² Sensitive Area, at Dry-Ice Temperature.

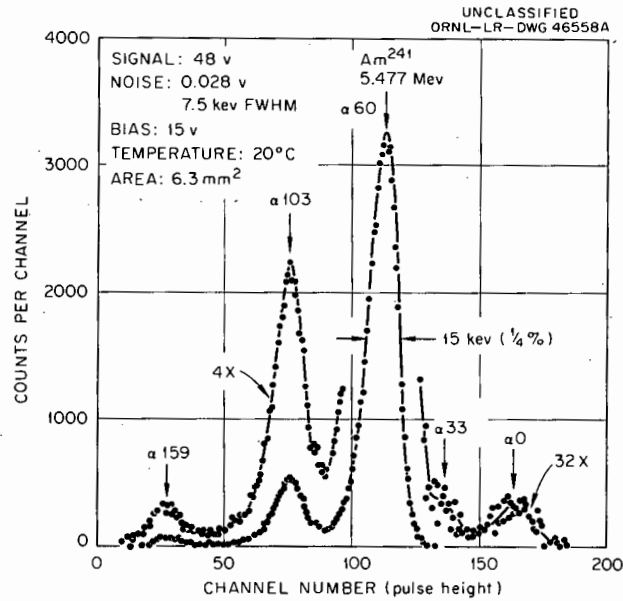


Fig. 8.6. Pulse-Height Spectra of Am^{241} Taken with a Detector of 6.3-mm^2 Sensitive Area.

The peak-to-valley ratio for the $\alpha 103$ line is a useful measure of resolution in the range of 15 to 20 kev. These lines would not be seen with a Frisch-grid pulse-ion chamber, since the best energy resolution that has been obtained with this type of detector is about 26 kev. Shown in Table 8.1 is the principal reason for the superior resolution of silicon counters over gas-ionization chambers. Since silicon requires only one-eighth as much energy to produce an electron-hole pair as argon gas requires per ion pair, eight times as much charge will be produced in the silicon. The signal is eight times as large if the capacitance remains comparable to

Table 8.1. Resolution Spread Due to Statistics for a 5.3-Mev Alpha Particle

In a Gas	
$\epsilon = 28 \text{ ev/pair}$	
$\sigma = 270 \text{ pairs}$	
$\sigma = 7.5 \text{ kev}$	
$\text{FWHM} = 2.36 \times \sigma = 19 \text{ kev}$	
	Fano Factor = F
	$1/3 < F < 1/2$
In Silicon	
$\epsilon = 3.5 \text{ ev/pair}$	
$\sigma = 1200 \text{ pairs}$	
$\sigma = 4.4 \text{ kev}$	
$\text{FWHM} = 10 \text{ kev}$	
	Assume F = 1

that of the ion chamber. The standard deviation, based on the number of charge carriers produced, is reduced by a factor of $1/\sqrt{8}$. Since the Fano factor²⁶ for silicon is not known, the resolution spread produced by statistics may be as low as 6 to 10 kev. Table 8.2 shows the combined benefits of increased signal and improved statistics in silicon counters, and how the resolution of silicon counters compares with the Frisch-grid chamber.

Table 8.2. Sources of Resolution Spread for a Frisch-Grid Pulse-Ion Chamber and a Silicon Surface-Barrier Spectrometer

In Argon-Methane Frisch-Grid Chamber	In Silicon Surface-Barrier Spectrometer
Statistics, 19 kev	Statistics, 10 kev, $F = 1$
Electronic noise, 13 kev	Statistics, 6 kev, $F = 1/2.5$
Theoretical performance, 23 kev	Electronic noise, 3.5 kev, 40 μ f total
State of the art, 26 kev	Theoretical performance, 11 to 7 kev
	State of the art, 15 kev

Summary

Counters having a 1-cm² area with reverse voltage breakdown in excess of 500 v have been made from n-type silicon having resistivities ranging from 150 to 3600 ohm-cm. As can be seen from Fig. 8.1, the higher-resistivity materials yield deeper barriers and lower capacitance per unit area for a given bias voltage. A deeper barrier is useful for the more energetic alpha particles, protons, and electrons. Lower capacitance per unit area improves the signal-to-noise ratio for large-area counters.

The counters have been used to detect alpha particles, fission fragments, electrons, protons, energetic heavy ions²⁷ and neutrons, using an

²⁶U. Fano, Phys. Rev. 72, 26 (1947).

²⁷M. L. Halbert and J. L. Blankenship, "Response of Semiconductor Surface-Barrier Counters to Nitrogen Ions and Alpha Particles," to be published in Nuclear Instruments.

Li⁶ radiator.²⁸ The availability of higher-resistivity silicon will extend the particle-energy range over which the device would be linear.

Acknowledgment

The authors are especially indebted to C. E. Ryan, who performed many of the steps in the fabrication and testing of these detectors.

²⁸T. A. Love and R. B. Murray, Use of Silica Surface-Barrier Counters in Fast-Neutron Detection and Spectroscopy, ORNL CF-60-5-121 (May 31, 1960).

9. ALPHA-SURVEY PROBE

M. M. Chiles R. K. Abele

A large-area alpha-survey probe has been designed to speed up the surveying of areas of low alpha contamination. This probe (see Fig. 9.1) is designed around the RCA 6655A 2-in. photomultiplier tube which is used in previous models. This allows the use of the new probe with existing electronics as well as with the Q-1975A and Q-2091.



Fig. 9.1. Alpha-Survey Probe.

The alpha-particle-sensitive phosphor, zinc sulfide (silver activated), is deposited with a thickness of 20 mg/cm^2 on a Lucite plate ($4\text{-}1/4 \times 4\text{-}1/4 \times 1/2 \text{ in.}$) which acts as a light piper. Actual sensitive area of the phosphor is 75 cm^2 , due to a 75% open-area protective grill (shown in Fig. 9.2) centered on 100 cm^2 of phosphor. The light-tight window (shown in Fig. 9.2) is a 0.00025-in.-thick Melinex film, double coated with aluminum to give a combined thickness of 1 mg/cm^2 . The in-

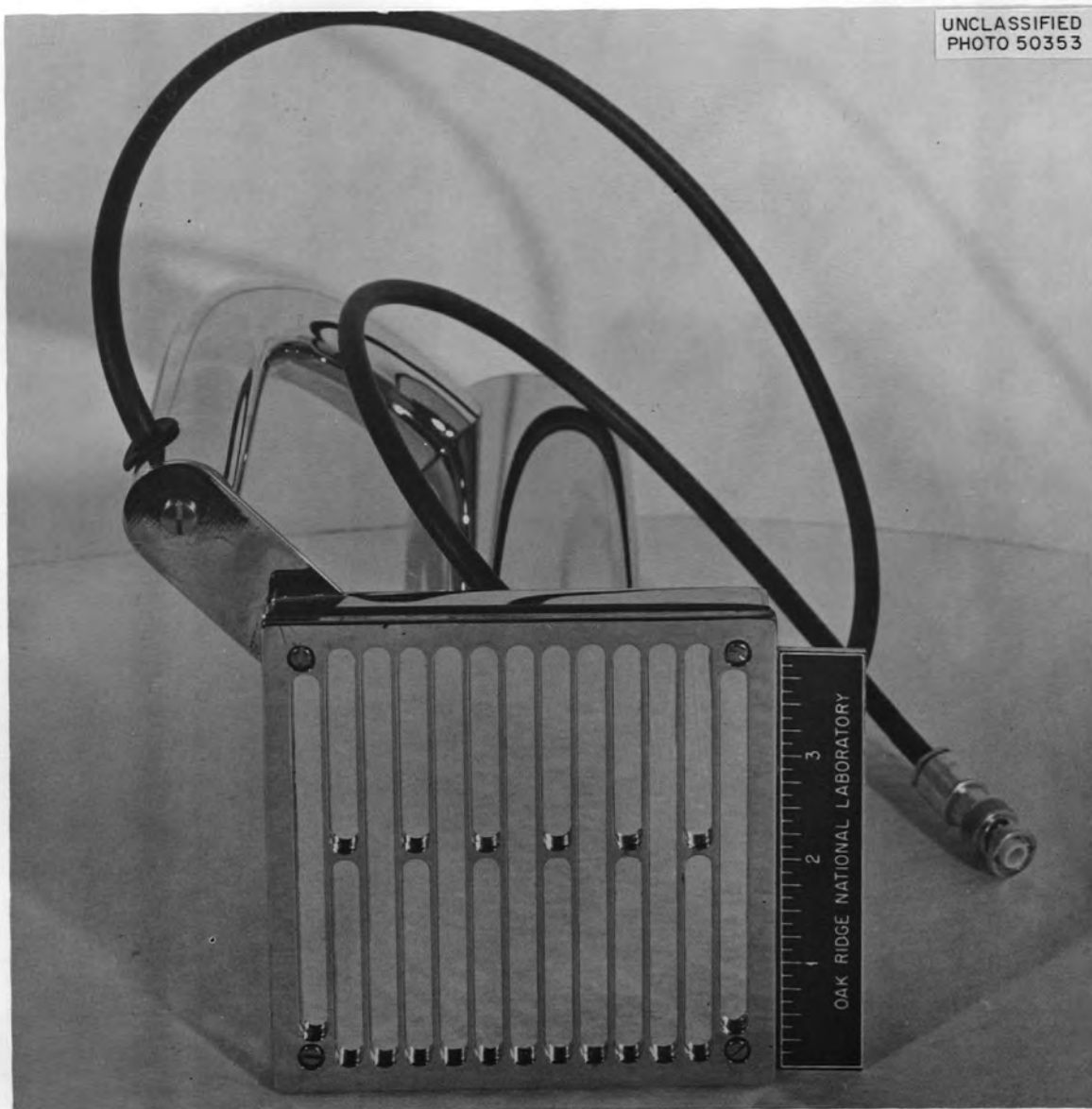


Fig. 9.2. End View of Protective Grill and Foil Window on Alpha-Survey Probe.

side of the housing surrounding the Lucite plate is sprayed with α -alumina for better light collection from the phosphor.

The phototube, phosphor, and grill are in a light-tight subassembly which can be readily separated from its voltage-divider network and cable for independent checking.

The counting rate from an alpha source located at any corner of the phosphor was compared with the counting rate of the source located at the center of the phosphor. With the electronics adjusted so as to reject all pulses from Cs^{137} x rays, the corner counting rate was at least 80% of the center counting rate. (Intensity of the cesium source used for these tests was 10^7 disintegrations/min.) With special care in the adjustment of the electronics, this corner counting rate could be made 90% of that at the center. As a matter of interest, this center-to-corner counting rate ratio is achieved under conditions for which the ratio of corner pulse amplitude to center pulse amplitude is from 1/3 to 1/5.

The square, flat, Lucite plate was chosen as a first approach to a light piper. It is simple in design and needs no finishing on its two large surfaces. It proved satisfactory under test and thus saved the cost of a more elaborate light piper. Several thicknesses of Lucite sheet were tested. Thicknesses from 3/8 to 3/4 in. proved adequate. The final thickness of 1/2 in. was chosen to simplify mechanical design and assembly.

Mechanical design of this probe is covered by drawing Q-2101. Fabrication and performance specification No. SF191 is a source of more detailed information for its manufacture.

10. ZENER-DIODE REGULATED POWER SUPPLIES FOR
MINNEAPOLIS-HONEYWELL AND LEEDS & NORTHRUP RECORDERS

J. L. Horton

Zener-diode regulated power supplies are now available from most electronic recording potentiometer manufacturers for the replacement of the standard cell and standardizing mechanism. The advantages of such continuous standardizing of the potentiometer bridge are numerous, provided that performance is not sacrificed.

Minneapolis-Honeywell and Leeds & Northrup, the most widely used makes of recorders at ORNL, have such supplies available. Minneapolis-Honeywell are building their own unit, and Leeds & Northrup are buying theirs as a package from Performance Measurements Co. The circuits of each are shown in Figs. 10.1 and 10.2 and are quite similar -- each uses a conventional rectifier supply with cascade shunt regulator stages of Zener diodes. Both utilize bridge-type output stages to compensate for dynamic impedance of the Zener diode used in that stage. Since the Zener diodes used regulate in the range of 6 to 9 v, series resistors are used to drop the voltage, thus making loading critical. Both the Leeds & Northrup and Minneapolis-Honeywell are designed for specific constant loads. A bridge-type output stage is used and allows good compensation

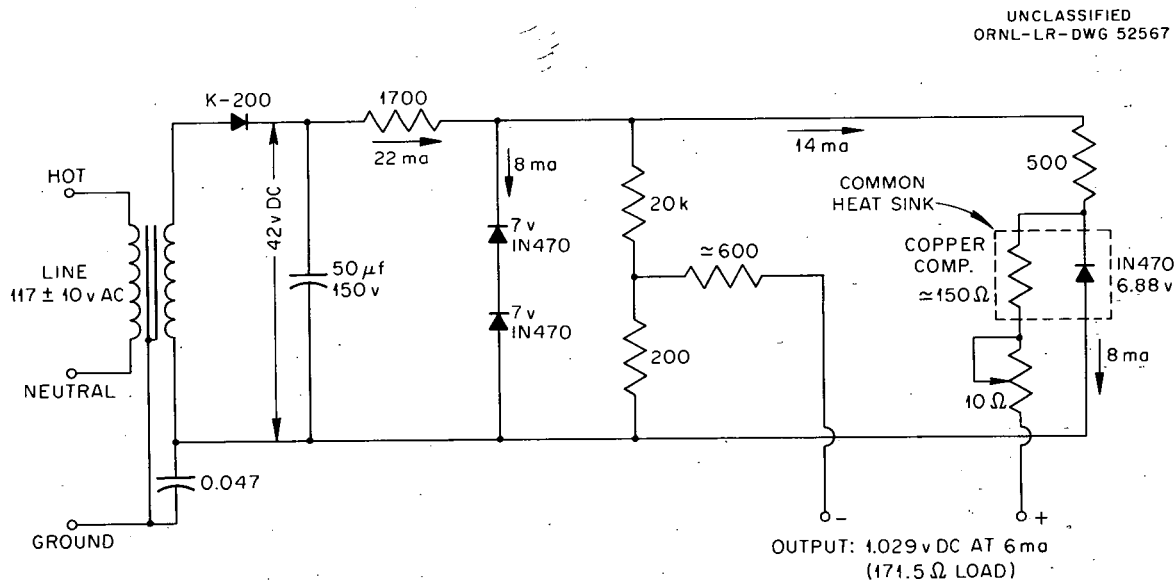


Fig. 10.1. Minneapolis-Honeywell Regulated Power Supply. M-H part No. 365389-1.

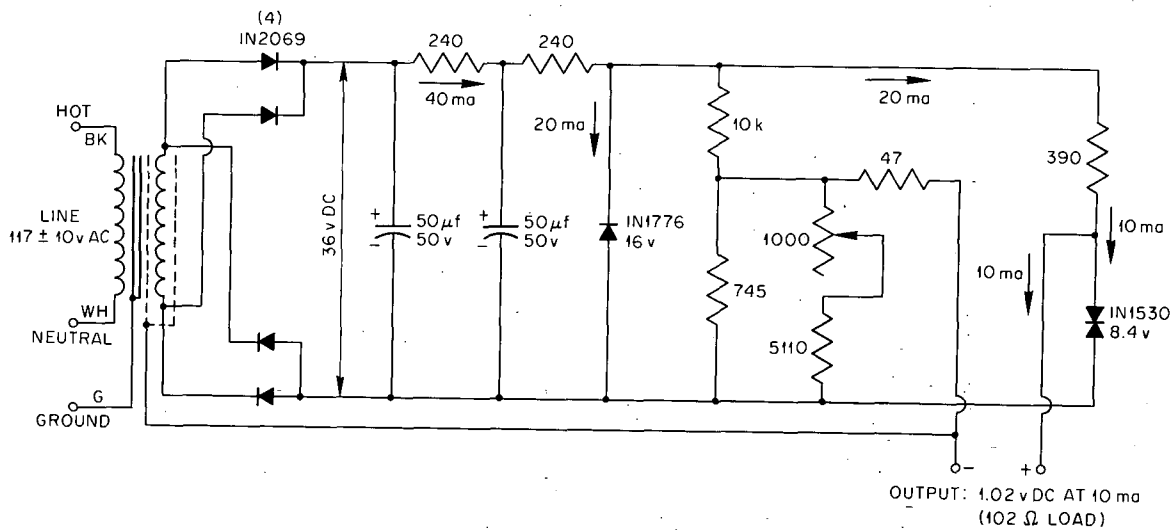


Fig. 10.2. Leeds & Northrup Regulated Power Supply. Manufactured by Performance Measuring Co., L&N part No. 099005.

against input line-voltage fluctuations. For temperature compensation, the Minneapolis-Honeywell unit uses a simple Zener diode with a positive temperature coefficient which is matched at rated output current by a copper compensating resistor. The Leeds & Northrup unit utilizes a commercial temperature-compensated diode combination in which compensation is achieved by use of two forward-biased diodes in conjunction with the Zener diode.

The Minneapolis-Honeywell unit is rated at $\pm 0.03\%$ output voltage change for a line-voltage variation of ± 10 v from 117 v or $\pm 0.15\%$ for the same line variation plus a temperature variation of $\pm 55^\circ\text{F}$ from 85°F (from Minneapolis-Honeywell specification S900-5a). No specifications are available from Leeds & Northrup on their unit.

Four Minneapolis-Honeywell units were tested with a constant 6-ma load and compared with an Eppley (catalog No. 100) standard cell. At constant temperature, the output voltage change vs a ± 10 -v line-voltage fluctuation varied from 0.02 to 0.04%, with an average of slightly less than 0.03%. Combined line and temperature fluctuation as specified gave output voltage fluctuations ranging from 0.12 to 0.17%, with an average of 0.14%.

Eight Leeds & Northrup units, factory installed in Speedomax type H recorders, were checked by using the same standard-cell arrangement. Line-voltage fluctuations from 107 to 127 v produced output voltage fluctuations ranging from 0.002 to 0.04%, with an average of 0.02%. Combined line and temperature fluctuations from 40 to 120°F ($\pm 40^\circ\text{F}$ vs $\pm 55^\circ\text{F}$ for Minneapolis-Honeywell units) produced voltage fluctuations from 0.02 to 0.29%, with an average of 0.15%. Figure 10.3 shows the typical regulating characteristics of a Leeds & Northrup and a Minneapolis-Honeywell unit.

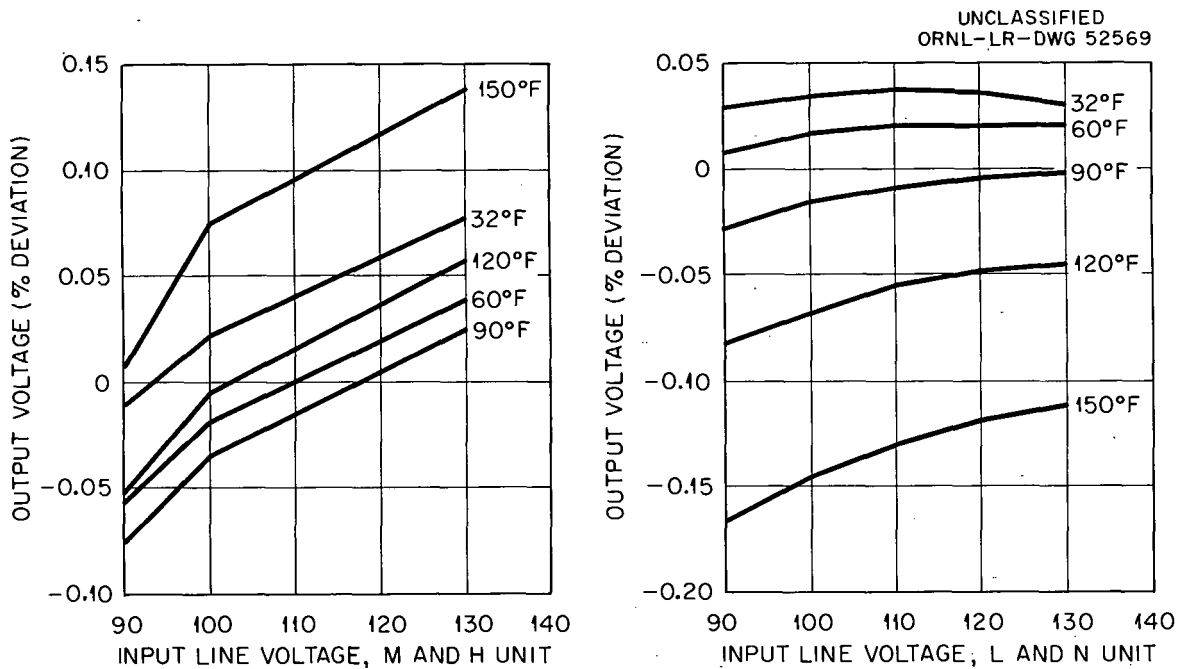


Fig. 10.3. Typical Regulating Characteristics.

Both the Minneapolis-Honeywell and the Leeds & Northrup units were checked for line-noise interference. Noise spikes up to 50 v peak (as recorded on a Sanborn recorder) were induced on the 117-v line. No spikes over 0.05% were observed in the output voltage of either make of power supply.

The general conclusions reached on the basis of these tests are: (1) there is considerable variation from unit to unit in the regulation against line voltage and temperature fluctuations; (2) the Minneapolis-Honeywell units on an average meet the specifications; and (3) the Leeds & Northrup units are practically the same in performance as the Minneapolis-Honeywell

unit except that they are possibly slightly inferior with respect to temperature fluctuations. The line-voltage fluctuations at ORNL are low (under 10 v, peak to peak), and most instruments are used where temperature fluctuations are not too large. Under these conditions these units far exceed the stability required to maintain the rated accuracy of either Minneapolis-Honeywell or Leeds & Northrup recorders. However, under adverse line or temperature fluctuations a recorder with a large zero suppression may suffer loss of accuracy if one of the poorer performance units is used.

The units make excellent voltage sources for "bucking voltage" units, calibration units, etc., provided that they are properly loaded.

11. TEMPERATURE CONTROL OF THE 30-Mw COOLING SYSTEM FOR THE ORR

B. C. Duggins J. L. Horton

The cooling system for the Oak Ridge Research Reactor (ORR) is being expanded to allow continuous operation of the reactor at a maximum 30-Mw power level. A two-section cooling tower has been installed with a three-unit water-to-water heat exchanger to isolate the reactor loop. Figure 11.1 shows an instrument flow sheet of the modified cooling system flow plan and components, including temperature-control instrumentation. The cooling tower is rated at 30.78 Mw at design conditions of 10,500 gpm flow, 78°F wet-bulb temperature, 104°F water-inlet temperature and will be used for normal operation up to 30 Mw. The eight water-to-air heat exchangers which were used to cool the reactor cooling water in the past will remain for emergency service and to allow possible 45-Mw reactor operation in the future.

The design objectives for the temperature control system are listed below:

1. Maintain steady-state (constant power level) control of the inlet temperature to the reactor within $\pm 0.25^\circ\text{F}$ limits. (a) It is important to minimize the fatiguing of the reactor structure which results from stresses produced by temperature cycling. (b) The most accurate method of obtaining reactor power is to compute it from coolant flow and the temperature rise across the reactor. If the inlet temperature is changing, and since there is a transport delay across the reactor, the measurement of the temperature difference and consequently power is incorrect. At ORR a 0.5°F error in ΔT will cause a 4% error in calculated power.

2. Provide a system of sufficiently fast response such that reactor operation would not be inhibited by the temperature-control system. (a) Good transient response reduces the danger of overheating the fuel, especially on a power increase. The operating conditions in ORR at 30 Mw are such that very limited temperature overshoot is permissible before the possibility of surface boiling at the fuel elements exists. (b) The recirculation of temperature transients has always been a problem at ORR due to the long loop time and low natural damping. Fast response of the

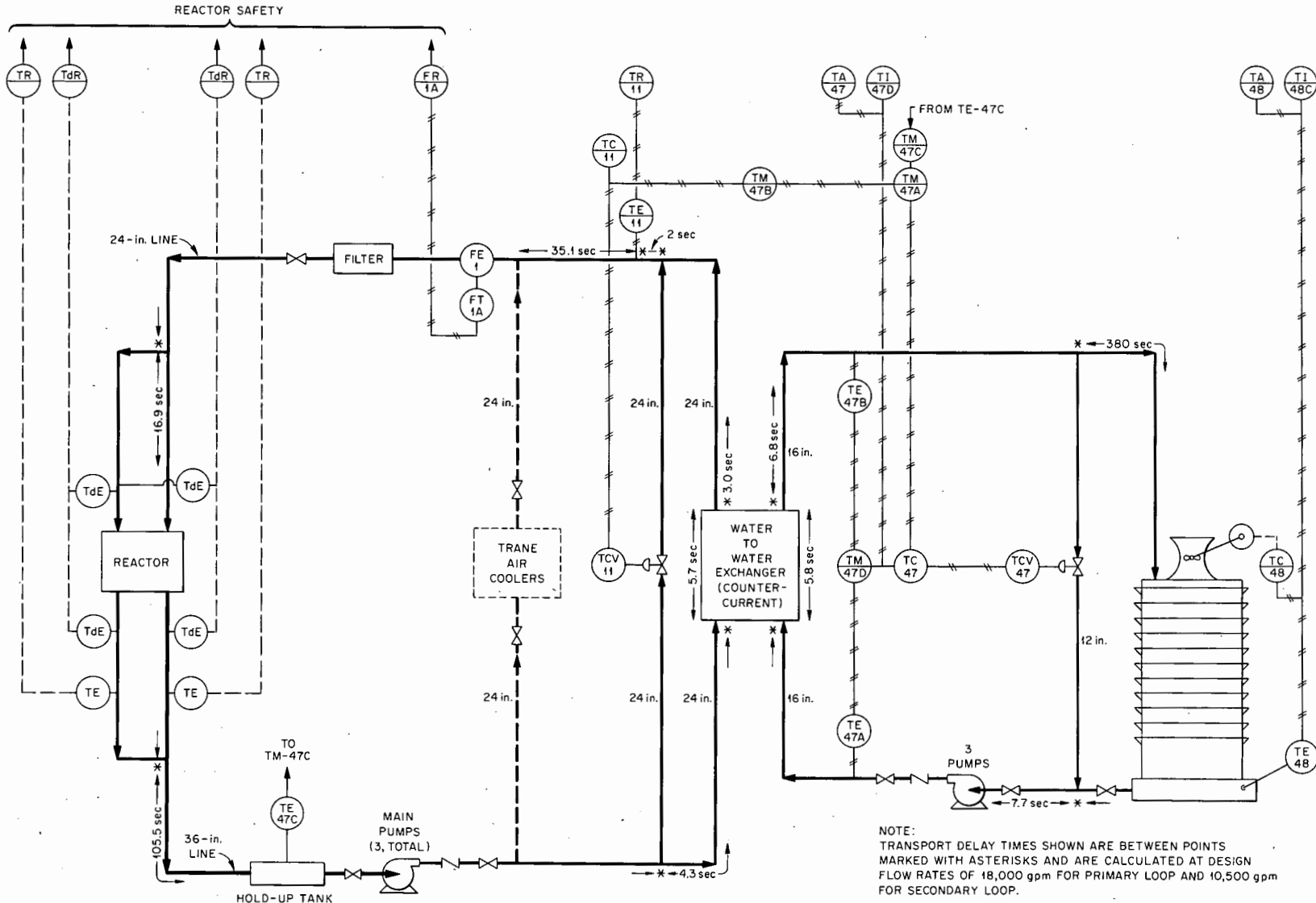


Fig. 11.1. ORR 30-Mw Cooling System Flow Plan and Partial Instrument Flow Sheet.

temperature controls is required to damp out these disturbances as they occur. (c) When the reactor is unexpectedly shut down by abnormal conditions, xenon poisoning makes it mandatory to return to power within a short time; otherwise, a 6-hr delay for changing fuel is required. The cooling system must therefore be capable of going from 30 to less than 1 Mw and then back again at a rate equal to that of the reactor in order not to hinder this operation and thereby cause unnecessary down time.

3. Provide a design that could be used with both the cooling tower and the air exchangers for 45-Mw operation.

4. Provide a design such that the failure of the control valves would not result in an abrupt loss of cooling to the reactor. This point dictated the use of fail-closed bypass valves rather than throttling valves in the cooling loops. Thus, potential failure would be in the direction of maximum cooling.

The design of the temperature-control system presented two fundamental problems:

1. to adapt the sluggish thermal response characteristics of the cooling tower to the extremely fast response of the reactor,
2. to synchronize changes in reactor power level with changes in cooling capacity after an appropriate delay. According to Fig. 11.1, there is approximately 1.5 min of circulation time between the reactor outlet and the water-to-water heat exchanger inlet. Therefore it will be 1.5 min after a reactor power change before it will be necessary to change the cooling rate. Failure to properly synchronize this action-reaction will lead to recirculating temperature transients throughout the system.

Due to the unusual nature of the reactor cooling system as described, and also due to the rather severe temperature control requirements, it was decided to study the problem on the Instrumentation and Controls Divisions analog computer. Once the cooling system was simulated on the computer, it was possible to try various configurations of control equipment and to observe the response of the system to each. Thus, an optimum combination of control components could be selected along with the proper location in the system for each. Also, once the correct combination was chosen, approximate controller adjustments could be found, thereby minimizing the amount of test operation of the reactor required for this purpose during the check-out period following installation. The pneumatic controllers

to be installed on the cooling system were coupled to the analog computer for these tests.

The temperature-control system as designed consists of three loops:

1. cooling-tower-basin temperature control,
2. water-to-water heat exchanger secondary (tower side) mean-temperature control,
3. reactor inlet temperature control.

Tower-Basin Control

The difficulty arising from the slow thermal response of the cooling tower was overcome by operating it essentially as an infinite heat sink. A control loop that senses the tower-basin temperature will step the two, two-speed tower fans as necessary in order to maintain the basin sufficiently cool to absorb 30 Mw at all times.

This control of basin temperature has side advantages: It (1) improves the control precision in the secondary and primary loops, (2) helps to alleviate the problem of tower freeze-up in cold weather, and (3) improves operating efficiency by eliminating unnecessary cooling.

Secondary Mean Temperature Control

The rate of heat transfer from primary to secondary of the water-to-water heat exchanger is given by the equation

$$Q = UA\Delta t_m \quad , \quad (1)$$

where

Q = heat transfer rate (Mw),

U = over-all heat transfer coefficient,

A = area for transfer of heat,

Δt_m = logarithmic mean temperature difference between hot and cold liquids.

The design of the ORR exchangers is such that this logarithmic mean temperature difference can be equated to the difference between the mean temperatures on the primary and secondary sides. The conditions on the primary side are determined by the reactor outlet and the desired exchanger

outlet temperatures. Therefore, at constant flow rates, the secondary mean temperature required to give the desired primary outlet temperature may be approximately calculated from the reactor outlet temperature.

As indicated in Fig. 11.1, the reactor outlet temperature is used to provide the set point for the secondary mean temperature control loop. This mean is measured by averaging inlet and outlet temperatures. The 12-in. tower bypass valve mixes cool water from the basin with hot water from the exchanger to maintain the mean temperature at the set point. The valve is able to bypass practically the entire secondary flow and thereby provide zero to maximum cooling.

The problem of synchronizing changes in reactor power with changes in cooling rate was solved by locating the sensor for reactor outlet temperature at an appropriate point on the piping such that secondary-valve action would coincide with the arrival of the hot or cold wave front at the primary side of the heat exchanger.

Reactor Inlet Temperature Control

Although it would seem that the cooling tower bypass valve should be sufficient to control the rate of heat transfer in the exchanger, there is good justification for installing a second bypass valve across the primary side of the exchanger. It has been pointed out that the secondary valve gives excellent rangeability, but rangeability always comes at the expense of resolution. The heat exchanger primary, unlike the tower, has a pressure drop which is a function of flow rate; so, the 24-in. bypass valve indicated in Fig. 11.1 will bypass only about half the main-stream flow with the valve full open. For a fixed secondary mean temperature, this change in flow will result in a reduction in heat transfer rate of about 2 to 1 in the steady state because of a change in film coefficient and saturation effects. This valve therefore gives excellent resolution to the control of reactor inlet temperature.

Improvement in transient response is the most important function of the primary valve. The primary-valve actuating signal will be fed back to the secondary system to adjust the secondary set point as necessary to keep the primary valve in the center of its throttling range. It will

then always have the ability to respond quickly to damp out small-amplitude transients in order to prevent them from recirculating through the system.

A third function of the primary valve would be to materially reduce the magnitude of the potential "cold slug" that could be given to the reactor by failure of the secondary control.

Conclusion

The over-all control philosophy emerges as more precise and faster control of temperature as one considers, in turn, the tower basin, the secondary system, and finally the primary system or inlet to the reactor. It has been demonstrated by the analog computer studies of the system that it is indeed possible to achieve the desired control precision and dynamic response. Also, it is possible to make appropriate control adjustments to prevent any interaction between the various components other than that required by stability or precision requirements. Figure 11.2 shows test results from the computer of the response of the three loops of the system to load changes. A period of steady-state operation is also shown.

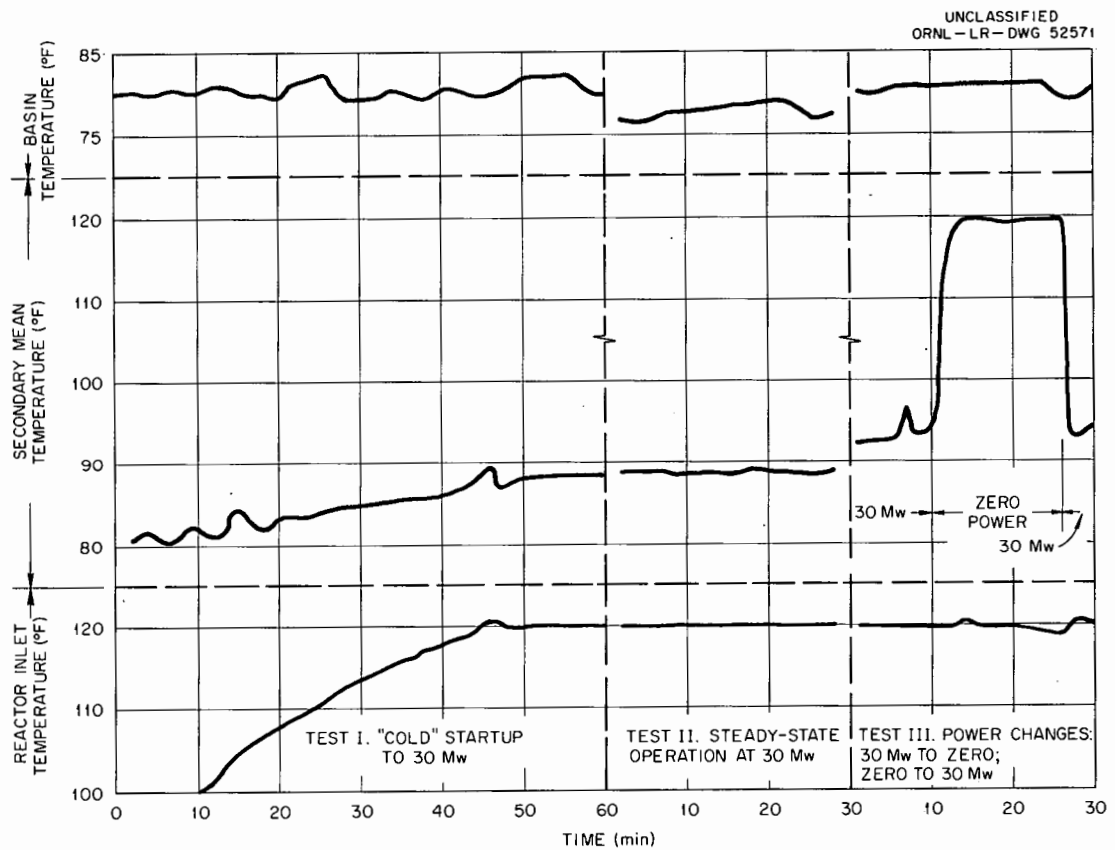


Fig. 11.2. Response of the ORR 30-Mw Cooling System to Load Changes. Curves taken from analog computer tests.

An unusual feature of the control circuit which couples the primary valve signal to the secondary-loop set point was recognized during the analog study. The purpose of this coupling, as stated before, is to keep the primary valve in its throttling range at all times. When the reactor was shut down for a prolonged period (with the controls operating) the integrating action of the controller in this circuit caused a large signal to accumulate, thereby shifting the secondary-system set point an erroneous amount. This, in turn, caused abnormal temperature overshoot on startup. This problem was overcome by sensing a shutdown from the reactor outlet temperature and eliminating the integrating action of the controller during the down period.

12. MODIFICATION OF A BAUSCH & LOMB SPECTRONIC 20
COLORIMETER-SPECTROPHOTOMETER FOR IN-LINE APPLICATIONS

T. M. Gayle

The Bausch & Lomb Spectronic 20 is an inexpensive colorimeter-spectrophotometer covering the region of 350 to 950 μ . Figure 12.1 shows the basic optical arrangement of the instrument. The even diffraction and dispersion at all wavelengths provided by the diffraction grating, together with the excellent mechanical construction of the device, prompted the development of the unit as an inexpensive in-line instrument.

Amplifier-circuit changes were made primarily to provide an output signal sufficient to drive standard potentiometric recorders, that is to say, a suitably clean d-c signal of about 10 mv, preferably within a few volts of ground potential. It was desired that this voltage be provided in addition to whatever signal was required to drive the existing meter. Figure 12.2 shows the original amplifier with the meter in the plate circuit. Surprisingly enough, this amplifier was extremely stable, due in great part no doubt to the excellent inherent balance of the 5751 tube. Modification of this amplifier proved impractical and, accordingly, a new amplifier assembly shown in Fig. 12.3 was designed. The additional gain required to put the meter and the recorder in the cathode circuit necessitated using an aged and selected 6201 instead of the 5751. High-voltage

UNCLASSIFIED
ORNL-LR-DWG 45220A

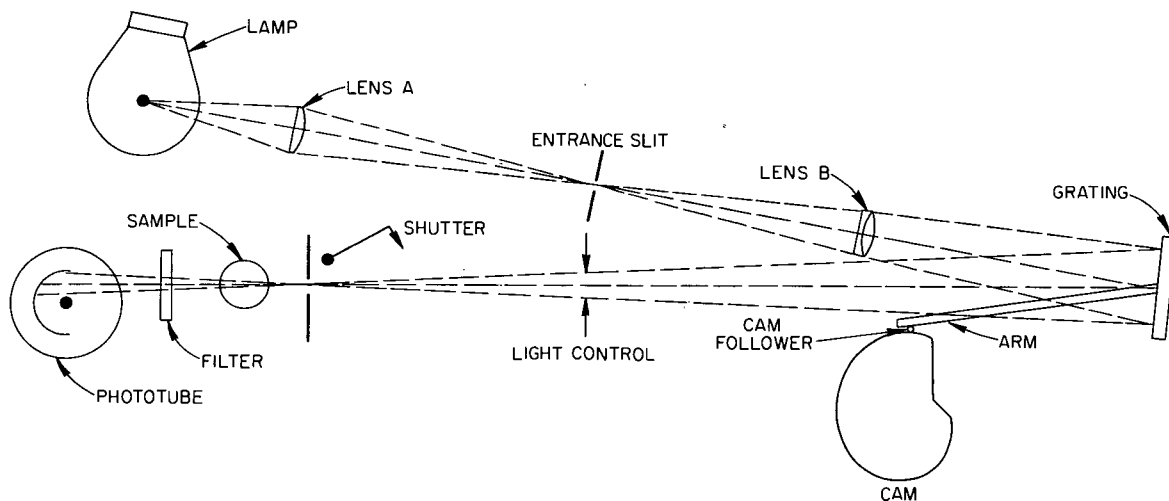


Fig. 12.1. Basic Optical Arrangement of Bausch & Lomb Spectronic 20.

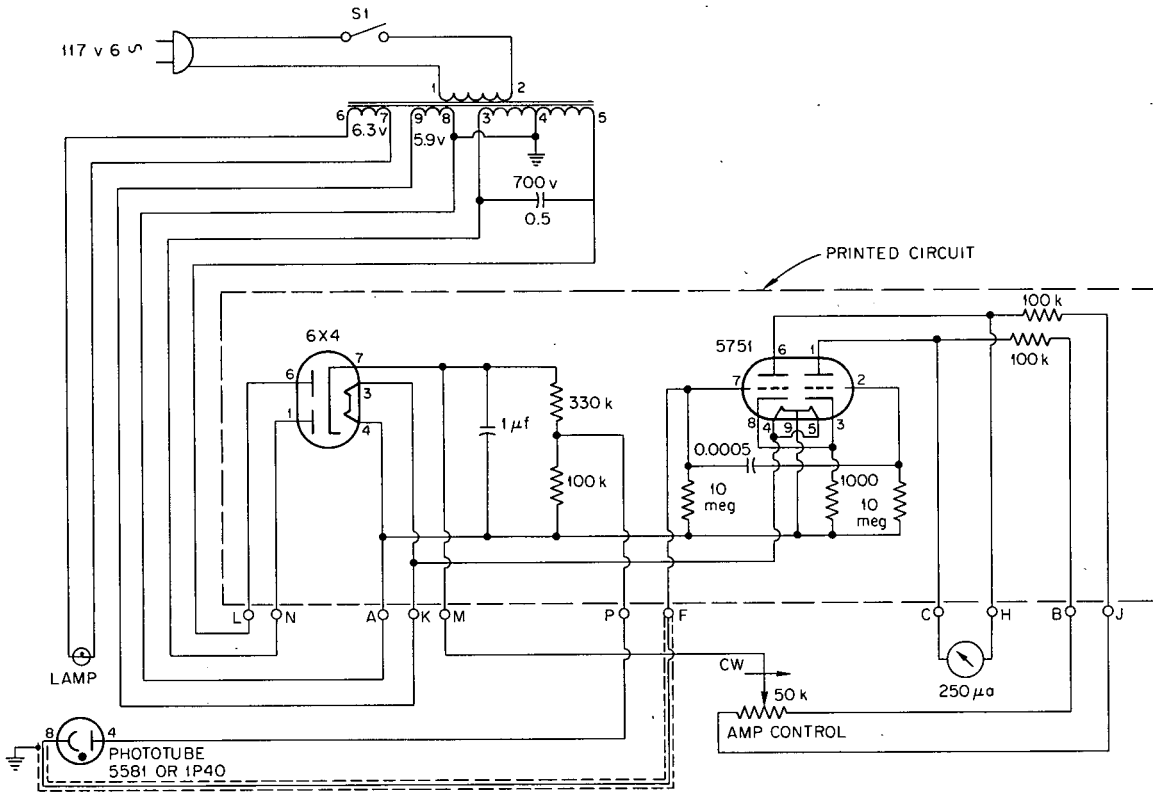


Fig. 12.2. Original Amplifier with Meter in Plate Circuit.

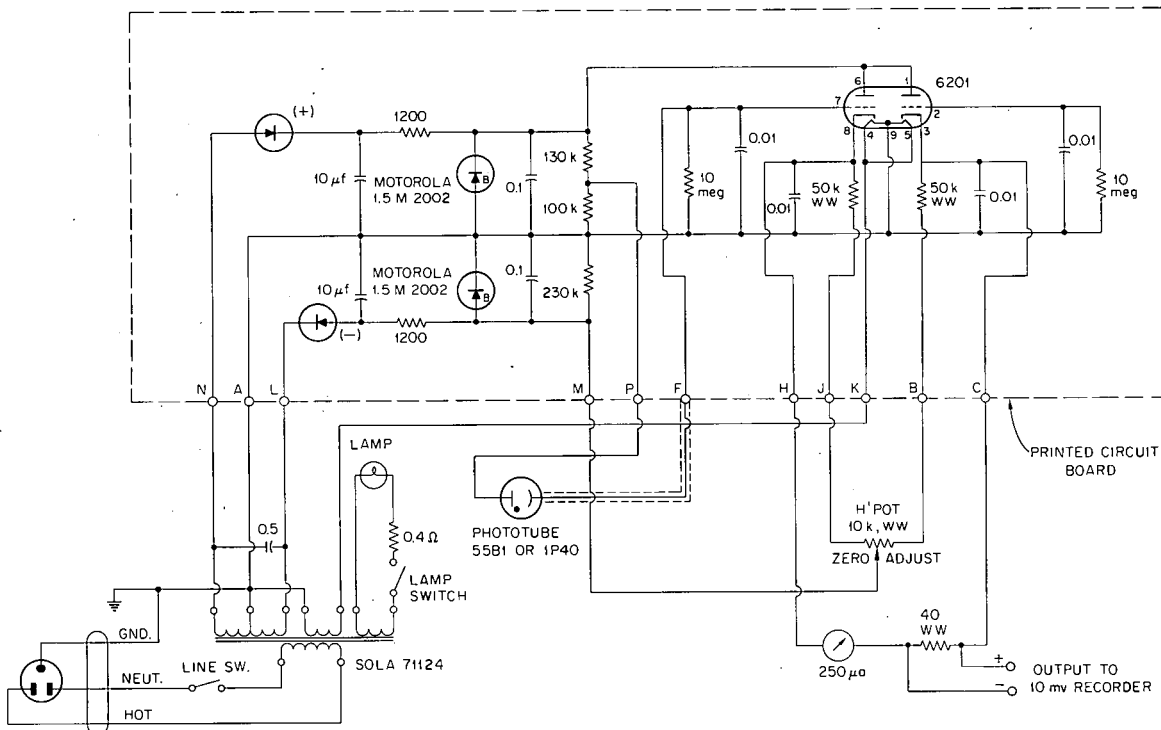


Fig. 12.3. Circuitry of New Amplifier Assembly.

Zener diodes were employed for both positive and negative supply regulation. Figure 12.4 shows the new amplifier assembled on its plug-in module. Component size and use were held to a minimum in order to meet the physical requirements of the original housing and to make the ribbon connector terminals interchangeable for either amplifier.

Other modifications included dropping the lamp voltage approximately 10%, replacing the balance-control potentiometer with a multiturn wire-wound unit, providing separate lamp and amplifier power switches, and mechanical modification of the shutter to permit manual operation for optical zero adjustment with the flow cell in place.

Two types of flow cells were designed for use in the original holders. A cuvette-cell assembly is shown at the bottom in Fig. 12.5, while a longer-path 1-in. tube cell is shown at the top. The cuvette cell is completely glass sealed, with optically flat sides, while the less expensive tube cell is slightly less desirable optically but easy to disassemble and clean. Figure 12.6 shows the complete unit with cuvette cell installed.

Performance of the unit indicates that the stability is from 1 to 2% after initial warm up. Line voltage fluctuations of $\pm 5\%$ give a calibration shift of $< 1\%$.



Fig. 12.4. New Amplifier Assembled on Plug-In Module.

UNCLASSIFIED
PHOTO 48555

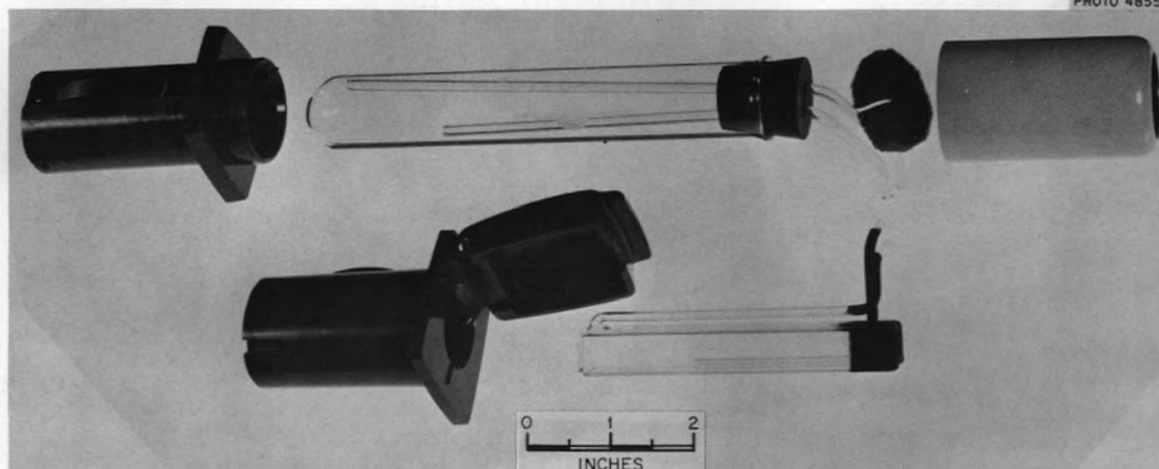


Fig. 12.5. Cuvette Assembly (bottom) and Longer-Path 1-in. Tube Cell (top).

UNCLASSIFIED
PHOTO 48553

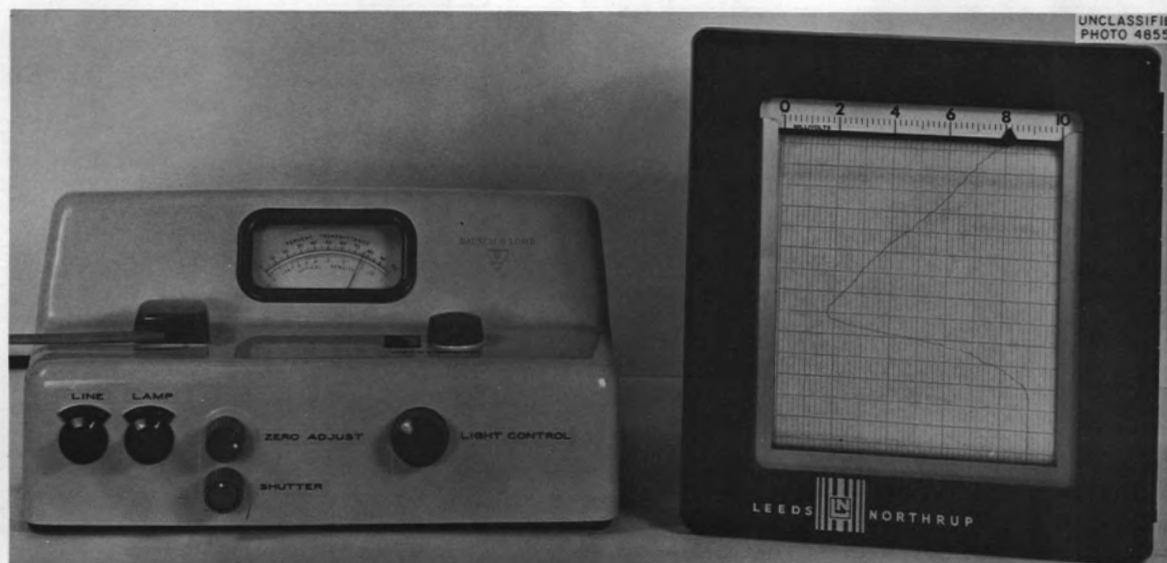


Fig. 12.6. Complete Unit with Cuvette Cell Installed.

13. INSTRUMENTATION FOR SALT FIELD EXPERIMENT

T. M. Gayle

The ORNL Health Physics Division Salt Field Experiment for the disposal of radioactive liquid wastes is currently being conducted in a Carey Salt Co. mine near Hutchinson, Kan. Instruments built or assembled at ORNL included a 144-point temperature and data logger, over 100 specially designed thermocouple probes, a 24-point salt-conductivity monitor with special conductivity probes, together with a variety of standard instruments for other measurements. A special requirement of the instrument panels was that all assemblies would be required to be broken down into modules approximately $2 \times 2 \times 6$ ft in order to reach the operating level via the mine elevator. Accordingly, all connections to the panels and interconnections between panels were made of the plug-in coded type for ease of assembly.

The thermocouple probes for the boiling waste pits were designed to use only Teflon in contact with the waste sludge, due to the high concentration of both nitrates and chlorides in the aqueous solution. Teflon tubing (1/4-in. OD) was pulled over 3/16-in.-OD Inconel tubing to form these probes. A new experimental trifluorochloroethylene film (DuPont FEP film) was employed to make a fused end seal between the tubing and a Teflon plug inside the tubing. Operating experience proved this new technique of Teflon-to-Teflon bonding to be quite satisfactory.

The 144-point logger was a commercial unit purchased from Minneapolis-Honeywell Regulator Co. While the unit has proved satisfactory, the relatively high maintenance required initially has suggested a number of changes which could be made in the input switching system of future logging systems of this type.

Salt-conductivity probes were designed to detect the penetration of liquid into the salt at various points from the pits. The probes were inserted into 12-ft-deep holes bored in the salt formation. The probes were constructed from Monel pipe, with slots milled in the pipe walls 180° apart for the entire length of the probe in order to provide two electrically insulated sections. The probe was held together by casting the inside of the pipe with epoxy resin. This construction is shown in Fig. 13.1. The 24-point salt-conductivity monitor which is actuated by these

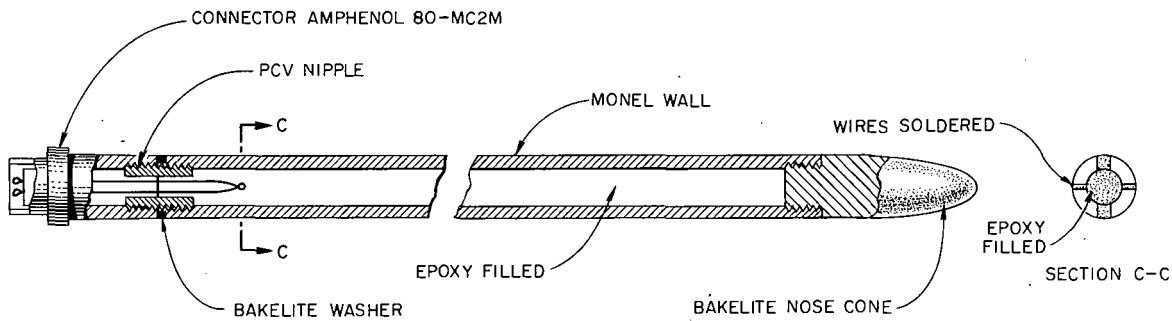


Fig. 13.1. Salt Conductivity Probe. Split-shell type.

probes is a low-gain solid state device terminating in mercury-wetted relays and giving instantaneous alarm if salt conductivity reaches a preset high level due to seepage from a pit. Outputs are also provided from the monitor for recording conductivity on the logger.

Annunciators were provided on a number of signals. An annunciator repeater was provided on the surface in the mine office, over 600 ft from the operating level. A d-c transmission system via cable up the elevator shaft was provided for this repeater. A transistorized, battery-operated intercommunicator was also provided via this cable for communication with the surface. Figure 13.2 shows a view of the operating panel.



Fig. 13.2. Operating Panel.

14. STATUS REPORT ON AUTOMATIC EXPERIMENTAL DATA HANDLING
AND COMPUTATION AT ORNL

R. K. Adams G. H. Burger

The Instrumentation and Controls Division's program in data handling and computation has been concentrated in three main areas, as listed below:

1. investigation and survey of the needs of the Laboratory and the Division,
2. application and development of suitable instruments to perform such data-reduction tasks as may be uncovered by the surveys and investigations,
3. data-reduction programming assistance to the users of the instruments applied or developed by the division.

The three functions are interlaced with educational activities both within the Division and with other divisions.

Investigation and Survey

In July 1959 the Division undertook a study of manufacturers of data-logging equipment in order to determine their competency to produce equipment suitable for use at the Laboratory and to bring itself up to date on the latest techniques for experimental-data acquisition. Early in this study it was realized that an entirely new concept was being applied in many experimental and laboratory applications. That concept was the on-line computer concept, in which a small general-purpose digital computer is used to process the data from an experiment (as the data is produced by the experiment), thereby allowing immediate access to the experimental results in reduced form or perhaps even the control of the experiment by means of the reduced results and computed control parameters. This concept so contrasted with the more common data-logging concept that it was decided that further investigation was necessary.

This new concept resulted in a study contract between the Laboratory and the Thompson Ramo Wooldridge Products Co. to investigate further the applicability of the on-line-computer idea to the EGCR loops, the HRE-2, the HFIR, and the several chemical processing pilot plants at the Laboratory. This study was intended to assess the benefits to be anticipated

by the application of the computing control and computing data processing application. The study contract with the Thompson Ramo Wooldridge Products Co. is completed, and an interim report¹ based on the applicability of the on-line computer to HRE-II has been written. A report on the applicability of the concept to the Experimental Gas Cooled Reactor loops has also been written.²

One example of the usefulness of a computer connected directly to the HRE-2 may be of interest here. The inventory of the various materials in the reactor varies with fuel instability and corrosion rate. Uranium sometimes leaves solution when the power is increased and re-enters solution when the power is reduced. An on-line computer can be made that will calculate the inventory of the various metals in solution and predict a tendency toward losses in inventory by comparing past inventories with past nuclear average temperature (computed from nuclear and heat-balance data) and present nuclear average temperature. It is even possible that a computer could materially aid in deducing the causes of this noncirculating uranium buildup. This is but one example of the many reasons the study recommends an on-line computer system for HRE-2.

The investigation of data handling and computation needs, as concerned with large-scale digital computers, has been receiving increased attention. A committee composed of two members of the Mathematics Panel and two members of the Instrumentation and Controls Division was formed to assess the state of the Laboratory in this regard. By far, the most significant finding of the committee is the accelerated upward trend of computer requirements by ORNL staff members. This is partly the result of an increased awareness in the potential of the digital computer, and partly due to the increasing use at ORNL of equipment which automatically accumulates experimental results in a form that can be fed directly into

¹R. K. Adams et al., Interim Report to Oak Ridge National Laboratory Relating to a Digital Data Acquisition System for Use with the Homogeneous Reactor Test Facility, ORNL CF-60-3-159 (Mar. 29, 1960).

²R. K. Adams et al., Final Report to Oak Ridge National Laboratory Relating to a Digital Data Collecting and Computing System for the EGCR Test Loop Facility, intralaboratory communication, June 22, 1960.

a large-scale digital computer. Some examples of the successful application of this technique are listed below:

1. The Solid State Division has been using for about two years an "events per unit time" meter with punched-tape output for general-purpose pulse-rate recording.

2. The Physics Division is using a punched tape unit on its 2048-channel neutron time-of-flight analyzer.

3. Multichannel pulse-height-analyzers in the Electronuclear Research Division and the Neutron Physics Division produce punched cards and punched tape, respectively.

4. The Chemical Technology Division Volatility Pilot Plant will shortly install a process data system which logs 120 process variables, such as temperature, flow, pressure, etc., on punched paper tape.

5. H. Levy of the Physics Division will soon put into use a neutron diffraction apparatus which produces punched paper tape from its neutron detector and scaler and which will orient the diffracting crystal in three dimensions as commanded by an input punched paper tape produced by the Oracle.

6. G. P. Smith of the Metallurgy Division has used a digitizing system with an optical or infrared spectrophotometer (Applied Physics model 11MS) to produce a punched paper tape of the absorbance values.

Application and Development of Instruments

In this area, the Division has accomplished during the past year the engineering and checkout of a standard paper-tape punch "black box" which can be connected to an experimenter's equipment to provide automatic data acquisition in a form compatible with computer input requirements. Under development at present is equipment to provide punched-card data recording similar to the punched-paper tape unit. The Division has also re-engineered and rebuilt a data-logging device which accumulates experimental data from the process plants, such as the Volatility Pilot Plant or the Thorex Pilot Plant, and logs the temperature, pressure, flow and liquid level data on punched paper tape which can be fed into the Oracle. The Division is providing this equipment to the Chemical Technology Division so that they may better evaluate the extent to which automatic

data acquisition and data reduction by the off-line concept can be of benefit to their processes. The devices mentioned earlier were applied or developed by the Instrumentation and Controls Division.

The Division has also assisted the other research divisions in the specification of automatic data-plotting and data-acquisition equipment to ensure that instrumentation of sound design and reliable performance is procured.

Data-Reduction-Programming Assistance Function

The Instrumentation and Controls Division has engaged in this work because of the particular requirements of automatically accumulated data. The reduction of such data by an automatic computer demands an intimate knowledge of the experimental methods and instrumentation. In addition to valuable assistance to the users of data-acquisition equipment, this function serves to keep the Division personnel well-versed in computing methods and recent developments in numerical techniques, both necessary to effective instrument application and development. The Division has made important contributions to the "spectrum stripping" problem.³ In addition to the spectrum stripping effort, members of the Chemical Technology Division and Volatility Pilot Plant personnel have been assisted with their data-reduction programming needs.

³R. O. Chester, "Computer Processing of Gamma Spectra," in Proceedings of Total Absorption Gamma Ray Spectrometry Symposium, Gatlinburg, Tennessee, May 10-11, 1960.

15. HOMOGENEOUS REACTOR PROJECT INSTRUMENTATION AND CONTROLS

R. L. Moore

S. J. Ball	D. G. Davis
A. M. Billings	P. G. Herndon
J. R. Brown	H. D. Wills

Instrument Development

Electric Systems Evaluation

During recent years several new process-instrumentation systems which feature electric transmission and, in some cases, solid state components, have been developed and placed on the market by leading instrument manufacturers. Many of the features appear desirable in instrumentation systems for nuclear reactors and associated reactor experiment systems. However, there is a natural reluctance on the part of the reactor-systems engineer to replace time-proven equipment with new equipment, even though the new equipment is predicted to be more reliable.

In order to gain more experience with the new systems and to gain data which can be used for comparative evaluation of the various systems available, a test-and-evaluation program was initiated. A survey of the field was made, and four systems were selected for testing. The selection was based on the completeness of the system, availability, versatility, and desirability for use in reactor systems. Representative components of these systems were placed on order, and tests are proceeding.

In general, the results of tests on one system indicate that the performance of components is within the manufacturer's specification; however, some "bugs" have been discovered. For example, the input impedance of the emf-to-current converter was of the order of 18 kilohms instead of the 50 kilohms specified, and the alarm switch had what appeared to be a preact or derivative action under certain conditions of operation. Also, the range of the emf-to-current converter could not be changed by a simple interchange of the range-unit assembly, as had been expected. Furthermore, in some cases, emf-to-current converters having the same range were not interchangeable in the same housing. These difficulties were brought to the attention of the manufacturer and have been or are in the process of being corrected. Examples of data obtained from a typical component are shown in Figs. 15.1 and 15.2 and in Table 15.1.

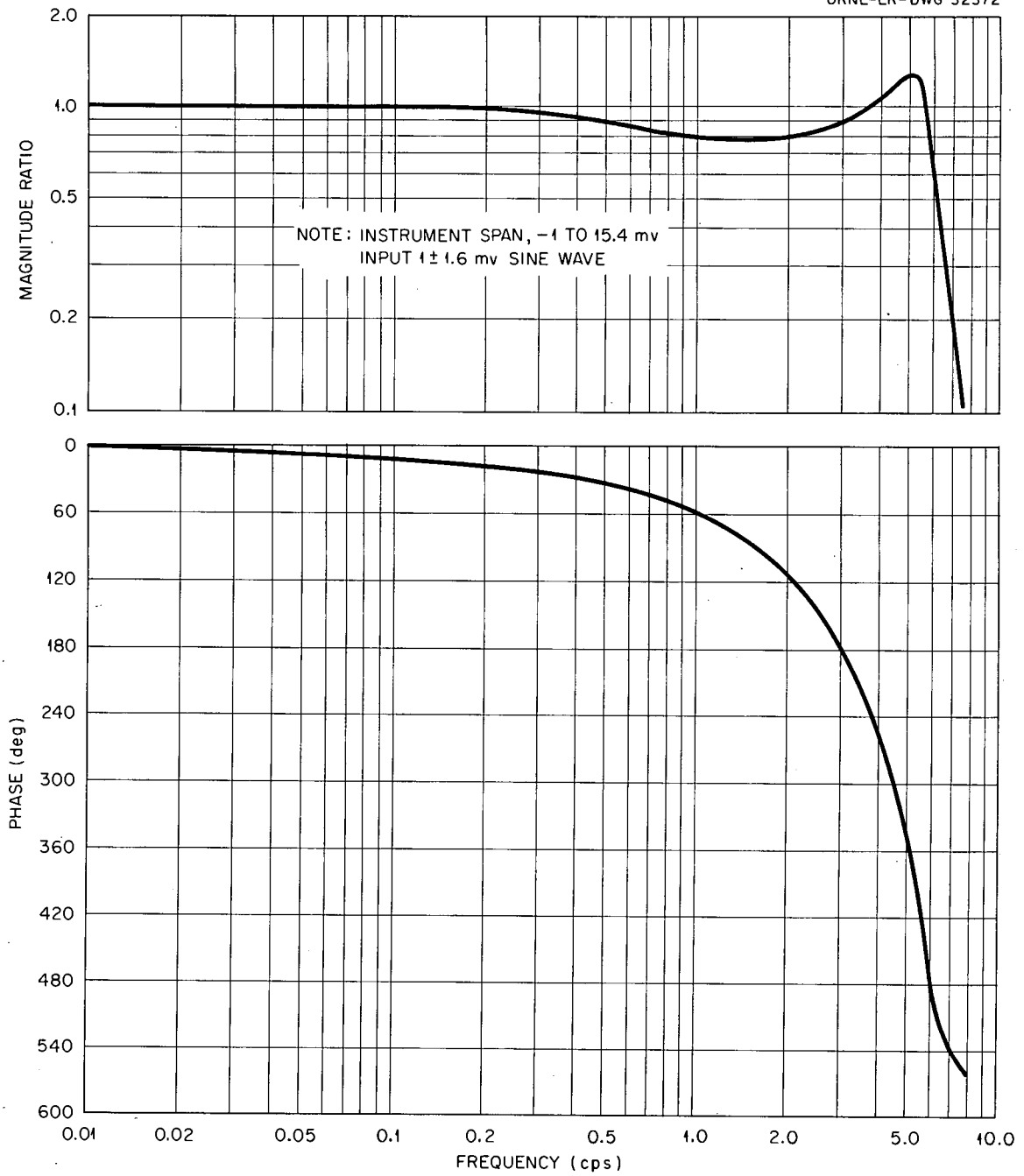


Fig. 15.1. Frequency Response of an EMF-to-Current Converter.

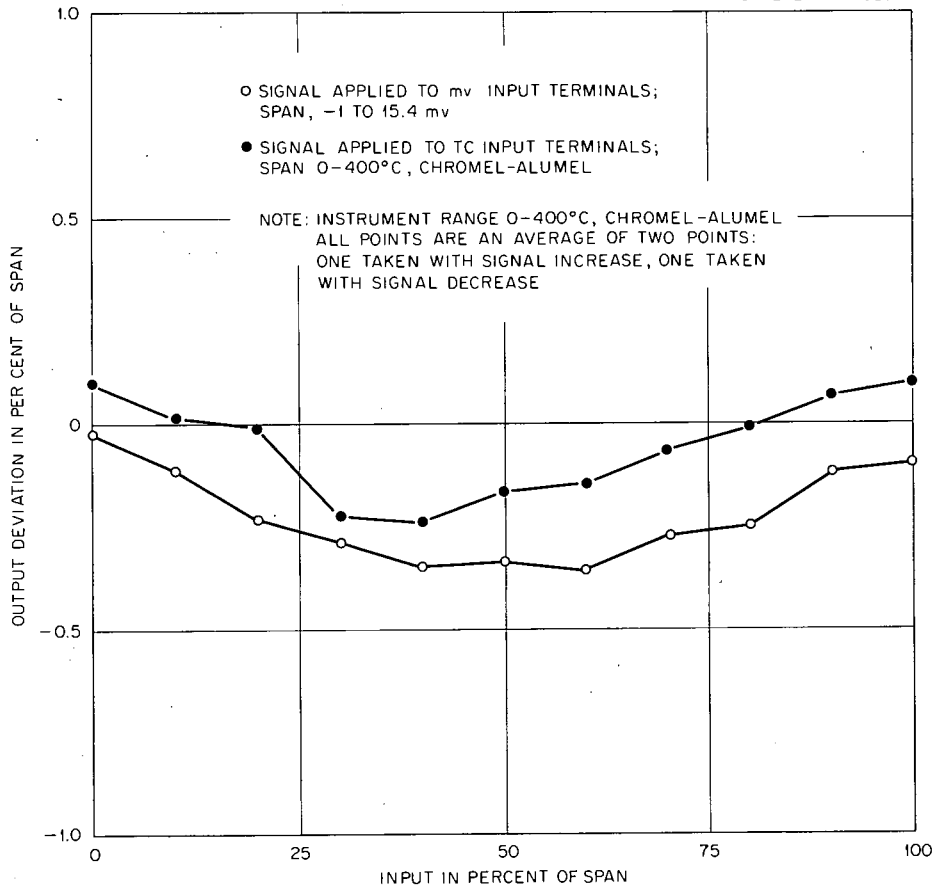


Fig. 15.2. Output-Signal Deviation from Linearity vs Input Signal - EMF-to-Current Converter.

Some operational experience has been gained with components of this system. As previously reported,¹ a pressure-control system, composed of a pressure transmitter and transmitter amplifier, a recorder, a controller, and a current-to-pneumatic converter were tested in 1959. This system, which was placed in service in May 1959, has given little trouble. The major trouble experienced was due to a loose screw-terminal connection in the transmitter amplifier. Some difficulty was experienced with the recorder inking system; however, it is believed to have been corrected by the installation of a new type of plastic ink sac, supplied by the manufacturer.

¹D. S. Toomb et al., Instrumentation and Controls Ann. Prog. Rep. July 1, 1959, ORNL-2787, p 122.

Table 15.1. Effects of Line Voltage and Frequency Variations on EMF-to-Current Converter (Range 0-400°C C/A -1 to +15.4 mv)

	% Output Deviation with Constant Input		
	At 10% Input	At 50% Input	At 90% Input
Volts at 60 cps			
95	-4.7	-4.5	-4.9
100	-3.5	-3.6	-3.8
105	-2.3	-2.5	-2.3
110	-1.2	-1.3	-1.0
115	0.0	0.0	0.0
120	+0.95	+1.2	+1.3
125	+1.9	+2.1	+2.3
130	+3.8	+2.9	+3.3
Frequency (cps) at 115 v			
45	+4.3	+3.6	+3.7
50	+2.4	+2.1	+2.2
55	+0.8	+0.53	+0.85
60	0.0	0.0	0.0
65	-1.2	-1.5	-1.1
70	-2.2	-2.2	-2.0
75	-2.9	-3.0	-2.7

Flush-Diaphragm Differential-Pressure Transmitter

A prototype differential-pressure transmitter of the type described in an earlier report² was received and tested. Results indicate that the transmitter was linear within 1/2% of full scale and had a hysteresis of 1% of full scale when mounted in the horizontal position. Hysteresis was negligible in the vertical position. Zero shift due to pressure was 2% of full scale at 2000 psi; zero shift due to temperature was negligible

²D. S. Toomb et al., Instrumentation and Controls Ann. Prog. Rep. July 1, 1958, ORNL-2647, p 84.

at 100°C. During these tests, the range of the instrument was set at 100-0-100 in. H₂O.

The transmitter was accidentally damaged during the elevated-temperature tests, and the results of tests above 100°C were inconclusive; the instrument is being repaired. After repairs are completed, the effects of temperature on zero and span over the temperature range from 100 to 300°C will be determined.

Transistorized Electropneumatic Converter

The transistorized electropneumatic converter described previously³ was redesigned to eliminate recurrent zero shift and drift troubles experienced with this prototype. Analysis of the circuitry and bench tests of the prototype model indicated that the basic circuit design was satisfactory and that the shifts and drift were due to such factors as poor contacts in printed-board connectors, leaky and intermittently open condensers, poor solder joints, and the arrangement of the wiring.

The redesigned model, shown in Fig. 15.3, is designed for rack mounting of the main chassis in a standard 19-in. relay rack. The associated electropneumatic and pneumatic-to-electric transducers are connected to the main chassis by cables and may be field mounted. Printed wiring has been eliminated, and the number of plug-in connections has been reduced to one connector, located at the rear of the chassis. High-grade components, including silicon transistors and tantalum capacitors, are used throughout.

Basic operation of the instrument is the same as that of the University of Virginia prototype model except that the automatic phasing feature of the prototype has been eliminated, and the d-c amplifier is of the direct-coupled type instead of the chopper type previously used. A block diagram of the revised circuitry is shown in Fig. 15.4.

The redesigned model utilizes 18 transistors, compared to 26 required in the prototype model. This reduction resulted from the elimination of the automatic phasing circuitry and from redesign of the d-c amplifier

³Ibid., p 81.



UNCLASSIFIED
PHOTO 35140

Fig. 15.3. Transistorized Electropneumatic Converter.

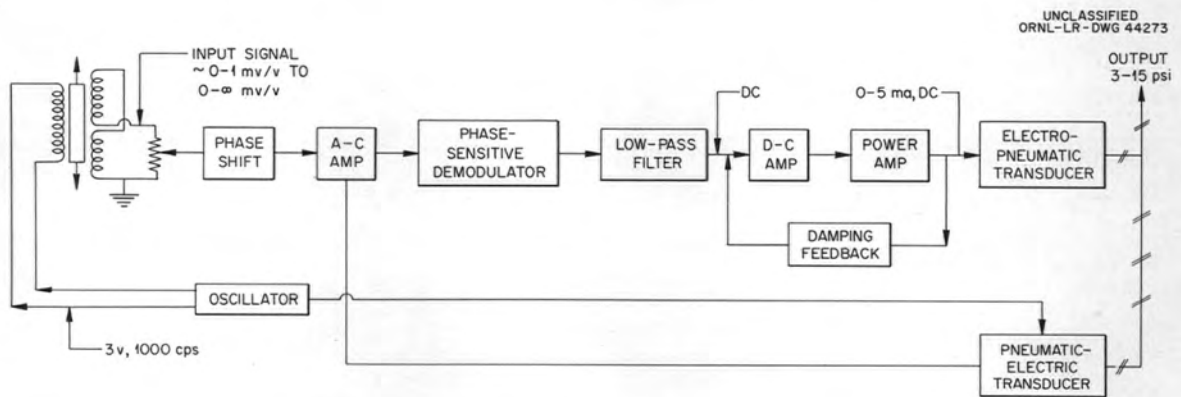


Fig. 15.4. Block Diagram of Transistorized Electropneumatic Converter.

circuit. Significant reductions were also made in the number of other components required.

Tests to date indicate that the redesigned instrument has an accuracy of $\pm 1/2\%$ of span under the following conditions:

Range	5 mv/v, full scale (1000 cps)
Output	3 to 15 psig air
Supply voltage	40 to 50 vdc
Ambient temperature	50 to 120°F

Remote Viewing Equipment

Radiation Tests of a Miniature Television Camera. - Radiation tests of the Dage 2-in.-dia television camera^{4,5} were repeated, using a Wollensak 1-in., f/2.5 nonbrowning lens. The camera was exposed to a gamma radiation field of 3.9×10^5 r/hr, produced by Co⁶⁰ slugs in the canal at the Graphite Reactor. The only radiation effect observed was a gradual loss of sensitivity, which was compensated by adjustment of the target control. The test was continued for 248.5 hr; total integrated dose was 9.6×10^7 r. At the end of the test, the target control had been advanced to its maximum position, and there was a slight loss in resolution of the picture.

Inspection of the camera, after removal and decontamination of the test assembly, showed that the loss of sensitivity was due primarily to browning of the Vidicon tube and the lamp bulbs. Comparison tests of the lens indicated that the light transmission of the lens had been reduced by only 6%. Further tests showed that 14% of the loss of sensitivity was due to browning of the lamp bulbs which supplied illumination for the test pattern. The remaining 80% loss in sensitivity is apparently due to loss of Vidicon sensitivity, since its replacement restored the original sensitivity of the equipment. This loss of Vidicon sensitivity is believed to be due to browning of the glass on the Vidicon face plate. The browned Vidicon has been shipped to the Dage Television factory, where tests will be

⁴Ibid., p 114.

⁵D. S. Toomb et al., Instrumentation and Controls Ann. Prog. Rep. July 1, 1959, ORNL-2787, p 124.

performed to determine the nature and extent of the radiation damage. Two additional tubes have been exposed to 10^8 r of gamma radiation. These tubes, which were pretested, have been forwarded to the Dage Television factory for test.

HRT Core Viewing Manipulator. - A manipulator was developed to enable the 2-in.-dia Dage camera to be used for viewing the inside of the HRT core.⁶ In this application the camera is required to pass through a 2-1/8-in. access hole in the top of the reactor and to be manipulated from a point above the shield blocks which is 20 ft above the center line of the reactor. The manipulator, which is shown in Fig. 15.5, supports the

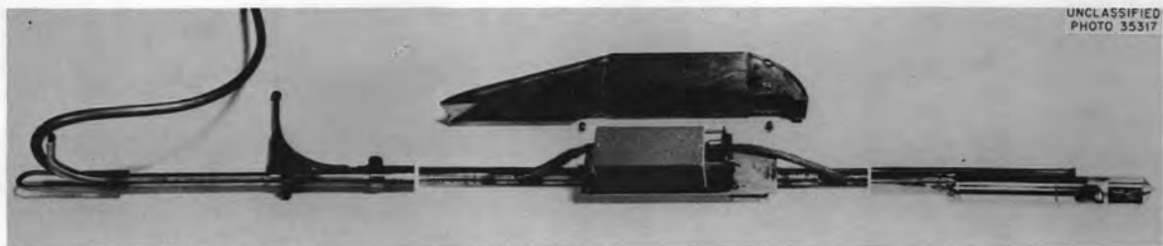


Fig. 15.5. Television Camera Manipulator.

camera on a vertical tube which can be raised or lowered to provide vertical scanning. Horizontal scanning is provided by rotating the tubular support.

To provide clearance for other tools it was desired that the camera be swung out of the way after insertion into the core vessel. It was also desirable to provide a means of focusing the camera after insertion. Both these requirements are met by the support mechanism which allows the assembly to be folded into a compact 2-in.-dia assembly for insertion and then rotated away from the axis of the access hole. A focusing assembly can then be unfolded, pushed down past the camera and rotated to engage a gear on the lens of the camera. Illumination is provided by a lamp mounted behind a mirror. The preamplifier is mounted on the tubular support rod at a point 10 ft above the camera and outside the reactor vessel.

⁶J. S. Culver, Viewing Equipment for Use in the HRT Core and Blanket Vessels, ORNL-2886, p 14.

Pump Impeller Viewing. - Another adaptation of the 2-in.-dia camera is shown in Fig. 15.6. This assembly was developed for use in viewing the impeller of an HRT canned-rotor pump. In this service, the camera was required to pass through the 3-in.-ID inlet pipe of the pump assembly with sufficient clearance to allow passage around the two 45° bends in the pipe. Other requirements include:

1. a means for pushing, pulling, and twisting the camera,
2. provision for shadowless illumination of the impeller by lights outside the field of view of the camera,
3. an air purge in order to prevent overheating of the camera,
4. protection in order to prevent contamination of those parts of the camera which could not be easily decontaminated or which would be costly to replace.

The camera was tested on the bench by using a spare pump impeller. The impeller of a spare fuel-circulating pump was also viewed; the pictures



Fig. 15.6. Miniature Television Camera Modified for Pump Inspection.

were clear and sharp. The portions of the impeller seen were the same as would be seen by looking into the center of the impeller with the eye 3 in. from the edge of the impeller hub.

Analog Computer

A Donner model 3400 electronic analog computer, shown in Fig. 15.7, was acquired for use in training personnel in the uses of analog computers and in closed-loop process-control theory.

The computer incorporates ten stabilized operational amplifiers, two electronic multipliers, and one diode function generator. The computer is finding use in solving various HRP problems which are sufficiently simple to be within its capacity. It is also very useful in setting up and checking analogs of portions of large systems prior to setting up the complete system analog on the Reactor Controls Analog Facility.

High-Temperature Radiation-Resistant Differential Transformers

The development of differential transformers for sensing the primary-element motions of instruments and capable of operating for long periods at high temperatures and in radiation fields was continued.

The transformer described previously⁷ was operated for three months at 300°C and then subsequently temperature cycled several times between 25 and 300°C. A zero drift of about 5% was accumulated over the three-month period. The drift was determined to be due to expansion of the test jig; no other changes in characteristics were noted over this period. A second transformer was constructed and has performed satisfactorily.

Profilometer

In the study of the heat transfer properties of EGCR fuel-rod clusters, rods in simulated clusters are first coated with naphthalene. Heated air is directed over the clusters at a controlled rate, causing sublimation of the naphthalene. The rate at which it sublimates at a given point is directly related to the heat transfer rate at that point. Therefore, if the

⁷D. S. Toomb et al., Instrumentation and Controls Ann. Prog. Rep. July 1, 1959, ORNL-2787, p 119.

UNCLASSIFIED
PHOTO 35148

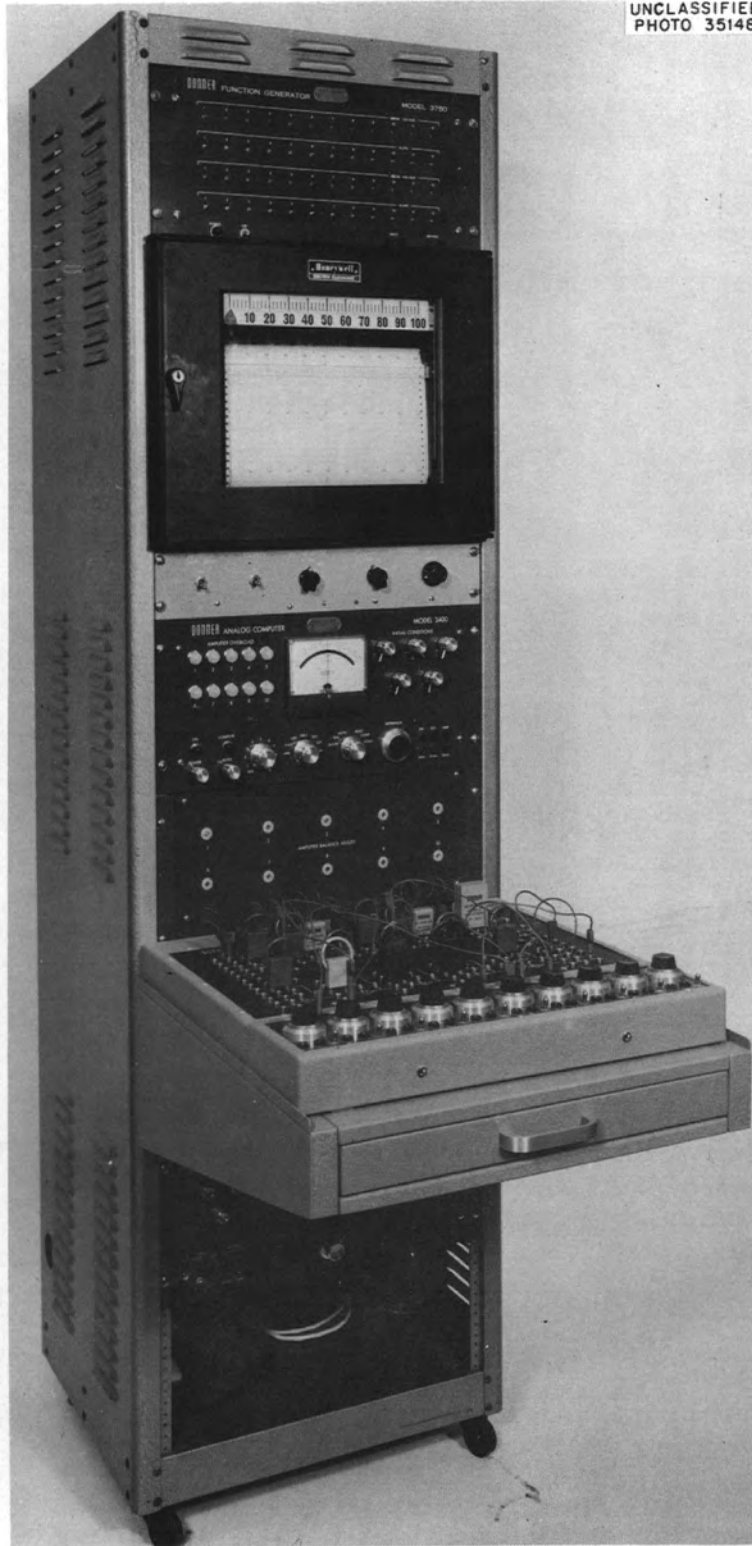


Fig. 15.7. Donner Model 3400 Electronic Analog Computer.

profile of the rod before and after heating is known, a profile of the heat transfer rate over the surface of the rod can be obtained.

In the initial experiments the profile was obtained by mounting the rod on bench centers and measuring the profile with a dial test indicator. This procedure was lengthy and tedious and was subject to errors due to the continuation of sublimation of the naphthalene at room temperature and to indentation of the naphthalene caused by the spring force of the dial test indicator. In order to eliminate those errors and reduce the amount of labor required in the experiments, the instrument shown in Figs. 15.8 and 15.9 was developed. It consists of a carriage bed with mounting centers, a profile feeler mounted on a carriage, an angular-position indicator, and a turning mechanism. In operation, the sample rod is mounted between centers and rotated at 3 rpm by a turning mechanism consisting of a gear train and a clock motor. A profile-feeler arm rides on the surface of the rod and positions the core of a differential transformer, the output of which is recorded on one channel of a two-channel Sanborn recorder. The angular position of the rod is detected by a stylus which follows the contour of the teeth on the driven gear. Motion of the stylus is transmitted through a rocker arm to a differential transformer, the output of which is recorded on the second channel of the Sanborn recorder as a series of "pips" corresponding to the angular position of the rod. The position of the carriage on which the profile feeler is mounted can be set accurately in 1/10-in. increments over a longitudinal distance of 12 in.

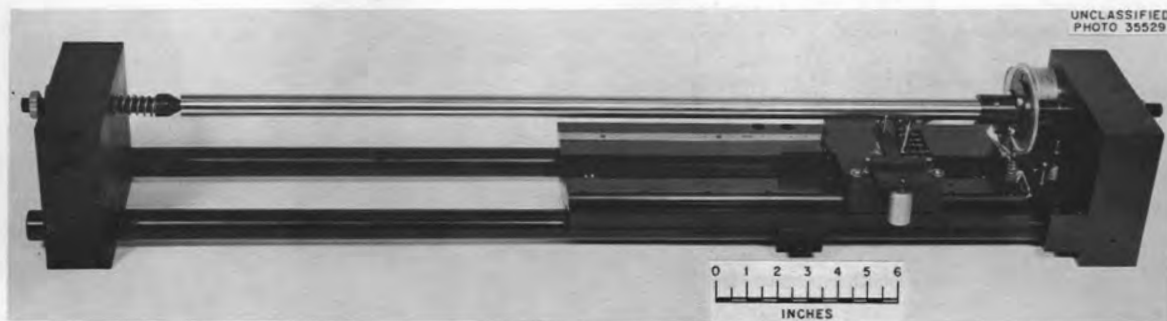


Fig. 15.8. Profilometer.

UNCLASSIFIED
PHOTO 35527

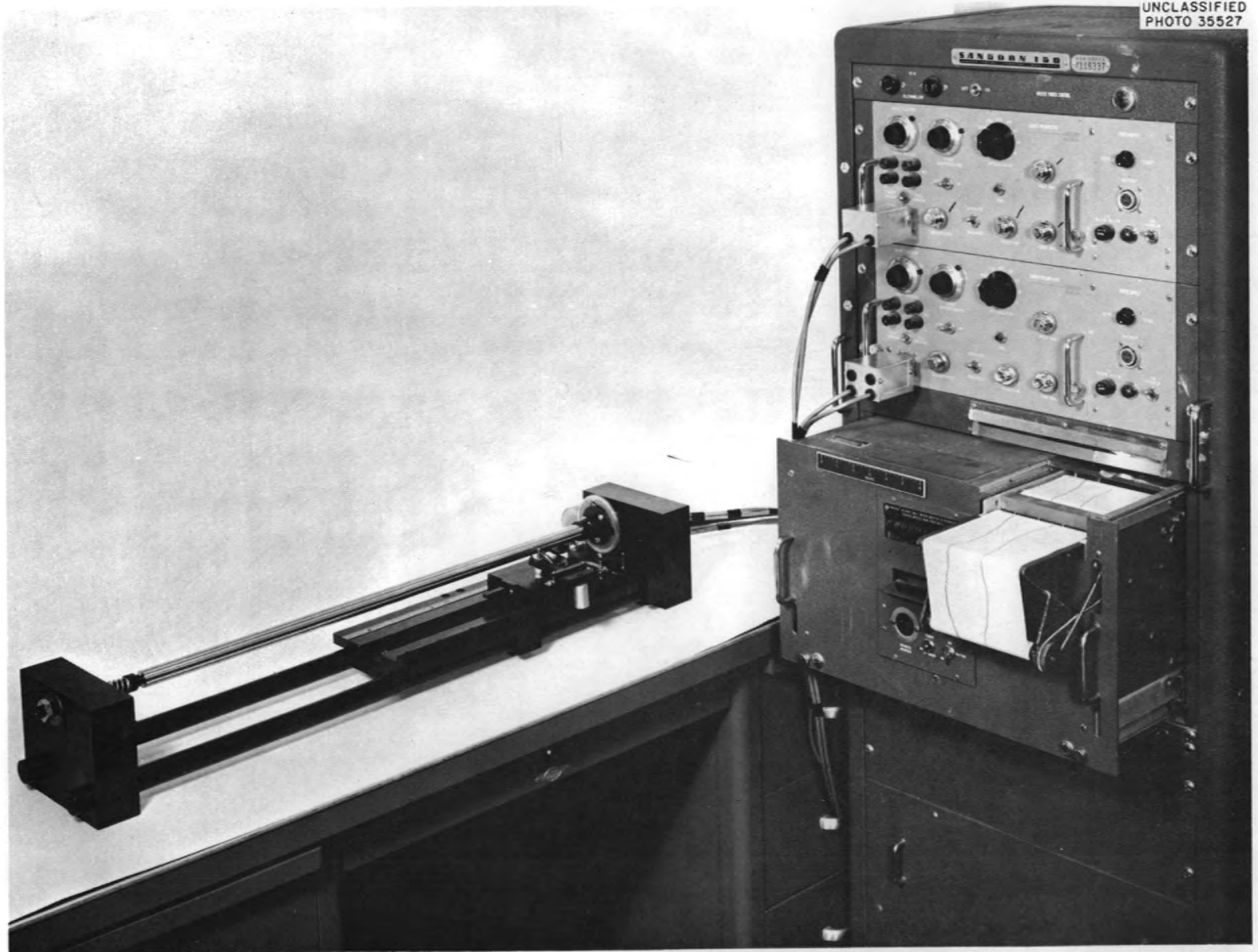


Fig. 15.9. Profilometer and Associated Recorder.

The first step in the operation of the device is to calibrate each rod by making a record of the circular profiles at those longitudinal positions of interest. The rod clusters are then assembled and exposed to the hot air stream for a known time, after which the rod clusters are disassembled and the circular profiles of the rods re-recorded at the same longitudinal positions. The two records are then compared, and the amount of naphthalene sublimed from the points of interest is calculated.

The reproducibility of this instrument is 0.0002 in. The span of the instrument can be set as low as 0.001 in., full scale; however, a span of 0.01 in. is usually used.

Valve Development

Hammel-Dahl High-Pressure Slurry Control Valve

Upon conversion of the 30-gpm loop to solution service, the flushed-bellows Hammel-Dahl valve⁸ was removed from service. Examination of the Zircaloy-2 plug and seat after removal revealed considerable pitting in the seating area of the valve seat. The pits appeared uniformly sized and were spaced around the periphery of the seating area. Erosion of the guide region of the plug shank, although rather extensive, appeared uniform. This damage, although considerable, was not catastrophic. The plug and seat are shown in Fig. 15.10.

This set of trim was installed for approximately 5500 hr of slurry service time. For high-temperature, low-differential-pressure slurry applications, Zircaloy-2 appears to be the most favorable valve-trim material tested to date.

Inspection of Slurry Mockup Loop Valves

As part of the scheduled modifications to the 300-SM system, all valves isolating the high-pressure system from the low-pressure system, plus several other more critical valves, were removed from the loop for leak testing and modification as required.

⁸D. S. Toomb et al., Instrumentation and Controls Ann. Prog. Rep. July 1, 1958, ORNL-2647, p 100.



Fig. 15.10. Plug and Seat from Hammel-Dahl Valve After Test.

Of six valves isolating the high-pressure system from the low-pressure system, only one was found with a gross leakage rate. The lower letdown valve, HCV-1281, with a Stellite No. 6 plug and a Stellite No. 12 seat, had such a high leak rate as to be useless for tight-shutoff purposes. The plug and seat, after removal, are shown in Fig. 15.11.

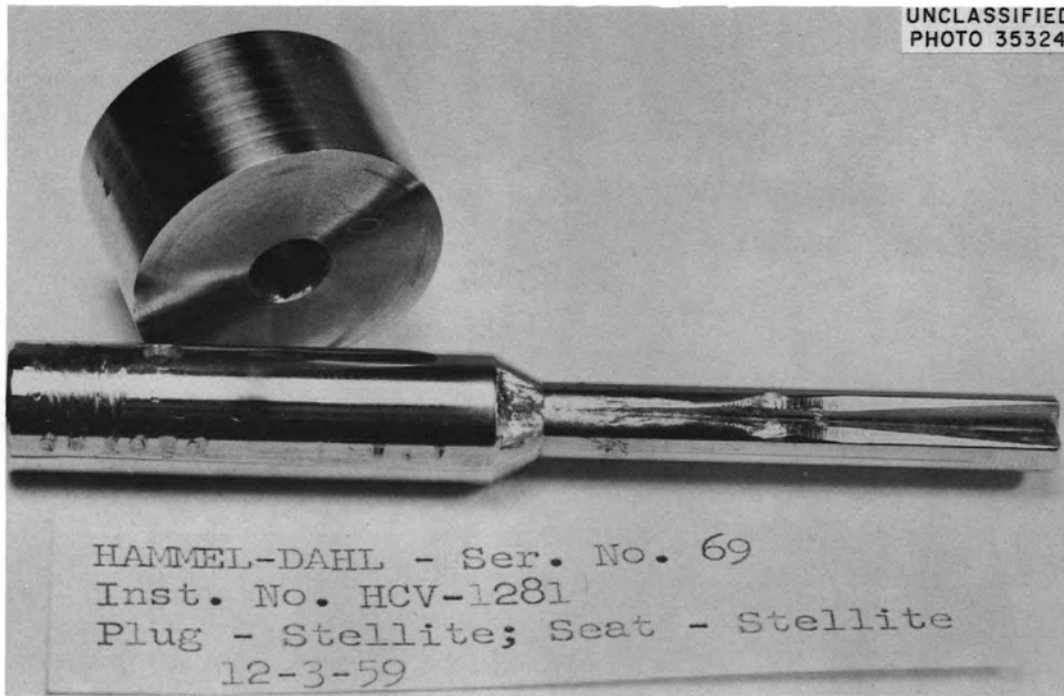
Leakage to the low-pressure system through HCV-1281 was prevented by HCV-1271, the upper letdown valve. Figure 15.12 shows essentially no wear on the Zircaloy-2 plug or the Armco 17-4 PH seat.

Since the Annin Co. split-body valves used in isolating the high-pressure system from the low-pressure system have poorly designed gasketing between the split-body sections, three valves for the more critical applications were modified to accept a standard ring-gasket between the body sections. These modifications are illustrated in Fig. 15.13.

Tungsten Carbide Trim in Slurry Service

A High Pressure Equipment Co. handwheel-type valve, fitted with tungsten carbide trim, was used for "letting down" slurry from 1500 to 500 psig. Total operating time was 45 hr, including 22 hr of slurry flow.

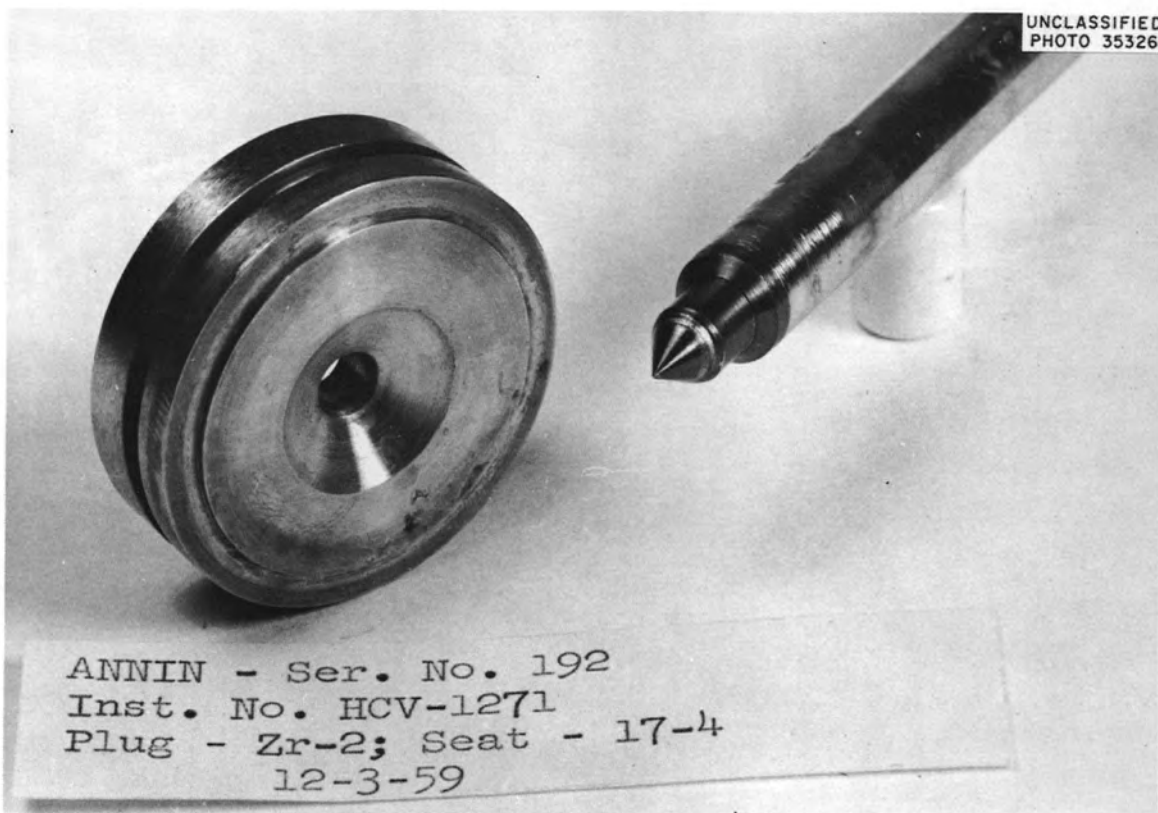
UNCLASSIFIED
PHOTO 35324



HAMMEL-DAHL - Ser. No. 69
Inst. No. HCV-1281
Plug - Stellite; Seat - Stellite
12-3-59

Fig. 15.11. Plug and Seat from Valve HCV-1281 After Service in Slurry Mockup Loop.

UNCLASSIFIED
PHOTO 35326



ANNIN - Ser. No. 192
Inst. No. HCV-1271
Plug - Zr-2; Seat - 17-4
12-3-59

Fig. 15.12. Plug and Seat from Valve HCV-1271 After Service in Slurry Mockup Loop.

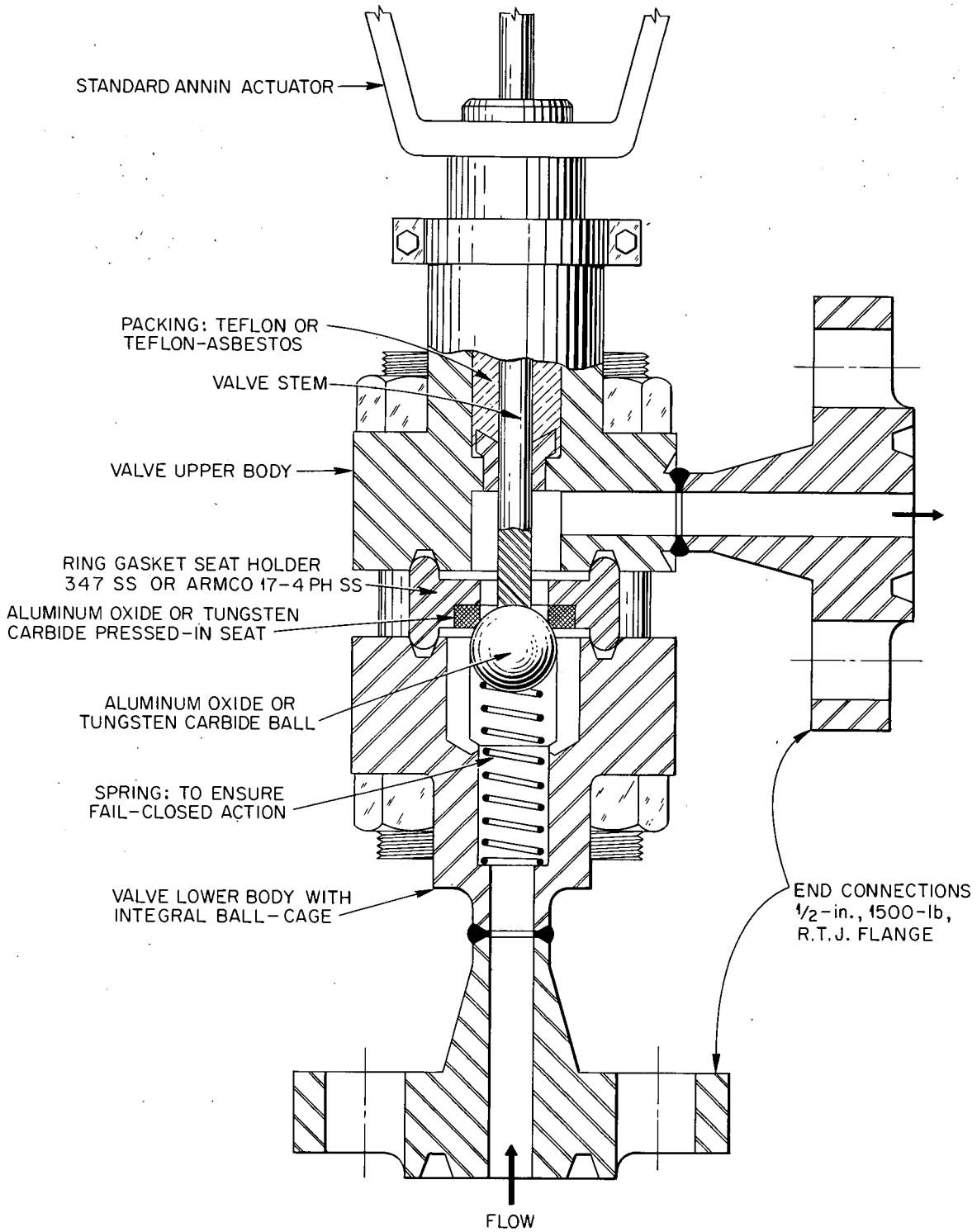


Fig. 15.13. Modified Annin Split-Body Valve.

The valve had to be removed because of severe attack on plug and seat. Figure 15.14 shows the eroded condition of the plug and seat.



Fig. 15.14. Tungsten Carbide Plug and Seat After Slurry Letdown Service.

Stem-Sealing Bellows

Titanium Stem-Sealing Bellows. - Life testing of the titanium stem-sealing bellows⁹ developed by the Fulton Sylphon Co. for ORNL has been completed. Average life of the 12 production assemblies was 24,362 cycles, with failure always occurring at the root of a convolution near a seal weld, indicating the occurrence of annealing in the heat-affected zone. Figure 15.15 shows a typical assembly after testing; the flattened convolutions are the characteristic result of having subjected the bellows to high pressure. The usual points of failure by cracking at the root of a convolution are indicated.

Fulton Sylphon Bellows Slurry Tests. - Three HRT-type valve-stem sealing bellows (Fulton Sylphon No. 10716-R3) have been cycled to destruction in a thoria slurry (400 g of ThO₂ per kg of H₂O) at 2300 psig, 285°C, with a 1/8-in. stroke. Average life of the three units was 75,598 strokes. No further testing is planned since bellows life does not seem adversely affected by the ThO₂ slurry.

⁹D. S. Toomb et al., Instrumentation and Controls Ann. Prog. Rep. July 1, 1959, ORNL-2787, p 125.

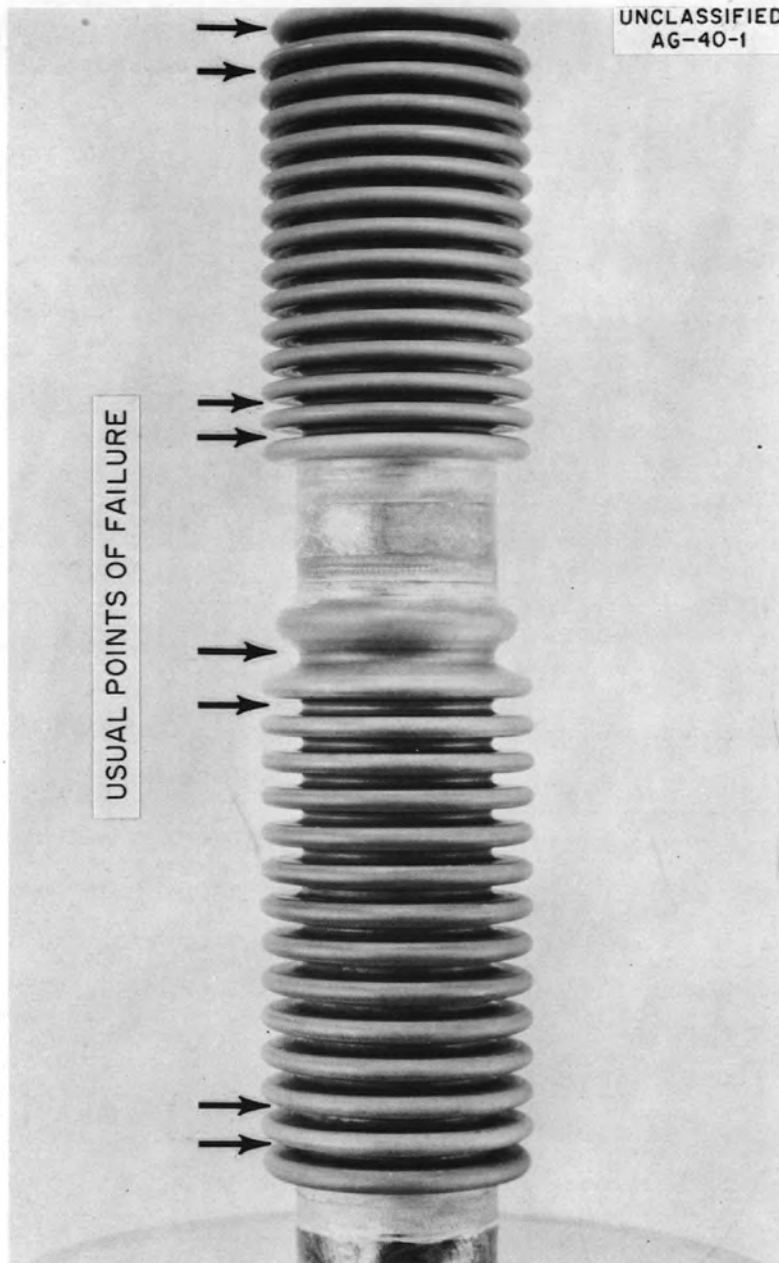


Fig. 15.15. Titanium Stem-Sealing Bellows After Test.

Life Tests of HRT Isolation-Chamber Bellows. — Life tests were performed on five Fulton Sylphon bellows of the type which are to be used as replacements for Clifford bellows which failed in service.

Four test assemblies were cycled to destruction in water at 1000 psig, 225°C, with a stroke of 1/8 in. At a cycling rate of 10/min the average life was 3950 cycles. Since all the failures occurred near the seal weld on the plug end of the test assembly, it appears that lighter

seal welds would improve the life. (Bellows life is markedly increased by light seal welds, as noted in previous tests.¹⁰)

HRT Instrument and Controls System

HRT Valves

The fuel-feed shutoff valve, HCV-337, serial No. K-03, was replaced during October 1959. Radioactive contamination has prevented disassembly of the valve; however, preliminary tests indicate that there may be mechanical binding between the valve stem and its guide bushing. Plug-to-seat leakage was negligible. This is the first low-pressure-system valve of the integral flange face, through-bolted type to require replacement since the valves were tested and reinstalled in the reactor, approximately two years ago.

The 1/4-in.-dia letdown port valve, which controls the reactor pressurizer level, continues to give satisfactory performance after approximately 5657 hr.

HRT Instrumentation and Controls System Modification

During the past year the HRT has been operated as a 1.4-region machine, that is to say, with some power generation in the blanket. This method of operation, which was necessary because of the formation of a hole in the core, was accomplished by constant purging through the hole from the blanket to the core. This was accomplished by the following:

1. eliminating blanket feed and letdown flow;
2. filling the blanket system full, thus eliminating the vapor space in the blanket pressurizer;
3. operating the blanket purge pump continuously;
4. continuous transfer of D₂O from the fuel low-pressure system to the blanket low-pressure system.

Although a number of changes were required in the control system external to the reactor cell and in the operation procedures, no major changes in instrumentation were required within the reactor cell. This

¹⁰A. M. Billings, Life Test of Stem-Sealing Bellows for HRT Valves, ORNL CF-58-3-39, p 3, 6, 7, 18.

was because most of the changes required the elimination rather than the addition of control. During this period no major difficulties were experienced with the HRT instrumentation and controls system. However, after a recent shutdown, it was found that many of the Thermo Electric Co. thermocouple connectors in the HRT cell were deteriorating. This is believed to be due to the combination of radiation damage to the Bakelite, plus immersion in water, which occurs when the reactor cell is flooded during maintenance operations.

A number of additions and revisions were made to the HRT instrumentation and controls during the past year. These include the addition of a second generator to provide stand-by power for the d-c control circuitry, installation of an emergency power system to provide power for the public address system in the event of loss of normal (TVA) power, installation of two Eberline model RM-2 radiation monitors to give better coverage of the radiation monitoring of hazards to personnel, revision of the control system to permit operation of the turbine from reactor steam, revision of the instrument-cubicle emergency-blocking system, the addition of instrumentation and control for a newly installed recombiner superheater, and installation of a reactor-cell sump-level measurement system.

At present, operations are being performed on the HRT system to remove the core screens, reverse the direction of flow through the core, and patch the holes in the core. After these revisions and repairs, the reactor will be returned to two-region operation.

The reactor instrumentation and controls system is being revised to conform to the new method of operation. The changes involve modifications in the reactor safety-control circuitry, revision of the blanket level-control system, revision of the blanket temperature-control system, revision of the blanket pressure-control system, and the addition of a system to provide automatic control of the transfer of D₂O from the fuel to the blanket low-pressure system.

Other changes in the reactor instrumentation and controls system which are being made, but which are not related to the change in method of reactor operations, include (1) the addition of two steam-vent valves which will be interlocked with the steam-pit activity monitors in order

to return contamination to the reactor cell in the event of a heat exchanger leak, with subsequent leakage of the steam safety block valves, and (2) addition of a safety block valve on the cell jet line. This valve will be interlocked with radiation monitors to prevent jetting of radioactive liquids from the reactor cell.

16. PERFORMANCE TESTS OF ORNL FAST SAFETY SYSTEM
FOR POOL-TYPE REACTORS

J. R. Tallackson R. E. Wintenberg
R. T. Santoro J. B. Ruble

Operational testing of the complete ORNL safety system, from sensing chambers to safety rods, installed in the Bulk Shielding Reactor II (BSR-II),¹ was completed early in 1960. (The tests were conducted at NRTS, Idaho Falls, Idaho. They were a joint effort shared by the Reactor Controls Department and the Neutron Physics Division of ORNL, and the SPERT-I Project at NRTS. These performance tests comprised the major portion of the Reactor Controls Department's contribution to the Reactor Safety Program, AEC Activity No. 04-01-07-10.) The test program fulfilled two objectives: (1) to meet the requirements set forth in the BSR-II safeguard report¹ which specifies that the BSR-II core, with a complete safety system, is to be tested at SPERT-I before it is operated at ORNL with loaded excess k greater than 0.007; (2) to demonstrate, in an operating reactor, the performance of a fast safety system, that is to say, a safety system in which all time delays have been minimized and negative reactivity insertion has been accelerated.

Figure 16.1 is a photograph of the installation at the SPERT-I Project at NRTS. Reactor characteristics affecting system performance are listed below:

Size of fuel region	15 × 15 × 15 in.
Critical loading	~6 kg U ²³⁵
Neutron lifetime	~21 msec
β_{eff}	0.007 ± 10%
Average temperature coefficient of reactivity from 58 to 120°F	$5 \times 10^{-5} \delta k / ^\circ\text{F}$
Void coefficient	0.00385 $\delta k / \%$ void

The safety system (see Fig. 16.2) was originally developed by ORNL for the MTR and is in wide use in a large number of reactor installations.

¹E. G. Silver and J. Lewin, Safeguard Report for a Stainless Steel Research Reactor for the BSF (BSR-II), ORNL-2470 (July 16, 1958).

UNCLASSIFIED
PHOTO 51710



Fig. 16.1. Installation of BSR-II at SPERT-I.

References 2-10 describe the system and its components. Salient features are as follows: (1) The high rate at which magnet current decreases as reactor power and/or inverse period exceed the 100% set point. (2) Each safety channel is independent and can produce scram action, irrespective of the state of all other channels. (3) The safety rods are accelerated by springs¹ which provide additional acceleration during the first 4.5 in. of rod travel and provide an initial force of 66 lb - Fig. 16.3 shows the improvement produced by spring loading. (4) Time delays have been minimized.

Pertinent safety system data are listed below.

1. Period channels: The log N amplifier spans 6 decades below 100% power. The compensated chamber¹⁰ is located so that its output at 100% reactor power is 50×10^{-6} amp. The period amplifier produces a scram signal if the period is 1.0 sec or less.

2. Level channel: The linear channel is useful only in the region of rated reactor power. The PCP (Parallel Circular Plate) chamber output at 100% power is 30×10^{-6} amp.

²T. E. Cole, E. E. St. John, and S. H. Hanauer, The MTR Safety System and Its Components, ORNL-1139 (Apr. 25, 1952).

³H. E. Banta and S. H. Hanauer, Testing Procedures for Reactor Instrumentation, Section A, A-1 Linear Amplifier, Q-541, Feb. 8, 1954, ORNL CF-56-5-30.

⁴H. E. Banta and S. H. Hanauer, Testing Procedures for Reactor Instrumentation, Section C, Magnet Amplifier, Q-889, Feb. 8, 1954, ORNL CF-56-5-30.

⁵H. E. Banta and S. H. Hanauer, Testing Procedures for Reactor Instrumentation, Section H, Fast Servo Amplifier, Q-1095, Feb. 8, 1954, ORNL CF-56-6-30.

⁶H. E. Banta and S. H. Hanauer, Testing Procedures for Reactor Instrumentation, Section J, Compensated Chamber Field Testing, Q-1045, Feb. 8, 1954, ORNL CF-56-6-30.

⁷H. E. Banta and S. H. Hanauer, Testing Procedures for Reactor Instrumentation, Section K, ORNL Precision Pulser, Q-1066, Feb. 8, 1954, ORNL CF-56-6-30.

⁸J. B. Ruble and S. H. Hanauer, Testing Procedures for Reactor Instrumentation, Section P, Composite Safety Amplifier, Q-1565, Mar. 7, 1955, ORNL CF-56-6-30.

⁹H. E. Banta and S. H. Hanauer, Testing Procedures for Reactor Instrumentation, Section G, Period Amplifier, Q-1093, Feb. 8, 1954, ORNL CF-56-6-30.

¹⁰J. L. Kaufman, High Current Saturation Characteristics of the ORNL Compensated Ionization Chamber, Q-1045, ORNL CF-60-5-104 (May 25, 1960).

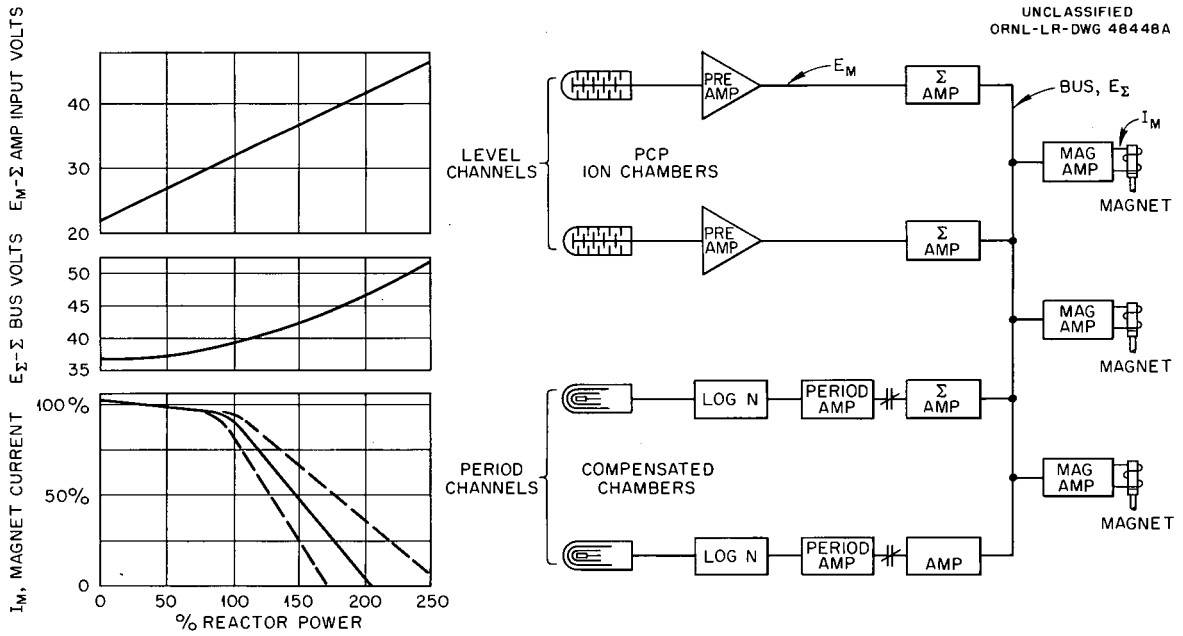


Fig. 16.2. BSR-II-SPERT-I Safety System.

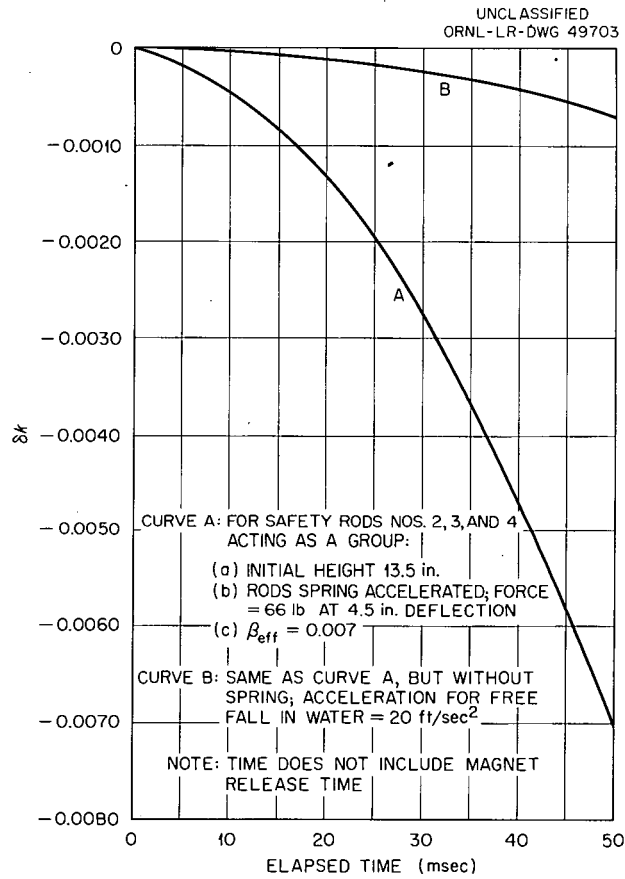


Fig. 16.3. BSR-II-SPERT-I Rod Worth vs Time.

3. Time delays: (a) In the period channel to and including the magnet amplifier the delay varies with both power and period.¹¹ (b) In the level channel to and including the magnet amplifier the delay is less than 0.001 sec. (c) Magnet release time is 0.001 to 0.005 sec.

4. Shim-safety rods: (a) A rod weighs about 11.5 lb; (b) shim-safety rod position at scram is 1.5 in. into the active portion of the core (Fig. 16.6); (c) total shim-safety rod worth (estimated by extrapolating calibration of rod 1) is \$8.00 to \$9.00.

The chambers were located so that 100% power was nominally 100 kw and, in accordance with established practice, this is at the top end of the range of the log N amplifier which supplies the signal to the period amplifier. The level safety channels were set to trip at a nominal 150% power. Since the log N amplifier is on scale 6 decades below 100% power, any short period transient initiated at low power is expected to provide the shutdown signal. Therefore, the period channels were disconnected from the sigma bus by switch contacts during level shutdown tests. Figure 16.4 is a diagram of the instrument settings and reactor levels. Because of the variable delay, the period channel is shown becoming effective in a region, not at a single value. In order to eliminate possible false

¹¹S. J. Ditto, Reactor Controls Department, Oak Ridge National Laboratory, private communication.

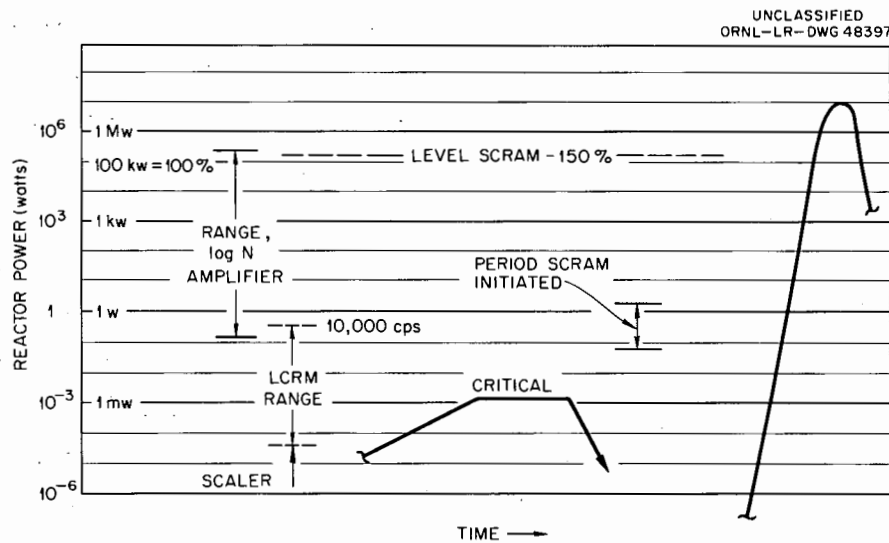


Fig. 16.4. Power vs Time During Typical Transient.

scrams produced by chamber overcompensation an auxiliary positive current, additional to chamber current, was fed to the logarithmic input diode in the log N amplifier. This ensured that the log N amplifier was barely on scale just before the transient and largely eliminated the problem of variable chamber compensation with gamma level. This device (see Fig. 16.5), suggested by S. H. Hanauer, Reactor Controls Department of this division, is being considered as a possible permanent addition to the system.

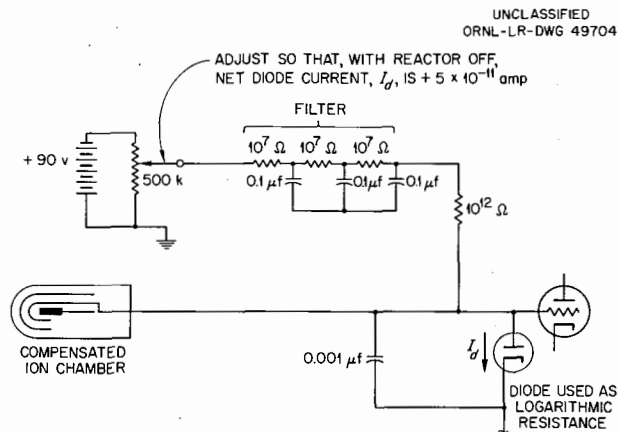


Fig. 16.5. Gamma Simulator for Compensated Chamber.

Figure 16.6 shows the step-by-step procedure used in conducting a transient. The transient rod insertion was accomplished by a fifth rod drive. Transient rod velocity was the same as for the shim-safety rods, a maximum of 76 in./sec. In early tests the reactor was operated with a source, and the initial power at the start of the transient was within the effective range of the safety system. It was not possible to attain a constant minimum transient period characteristic of a step insertion of reactivity. The period channel produced scram action before transient rod insertion was complete. Resultant power levels were too low to measure with accuracy, and periods were not constant; the operational procedure was changed. The reactor was operated without a source and at negligible initial power so that the transient period would be well established and constant at an extremely low power level. Ionization chambers positioned to read lower power levels were installed. This procedure avoided the situation in which shim-safety rod insertion was initiated by the period

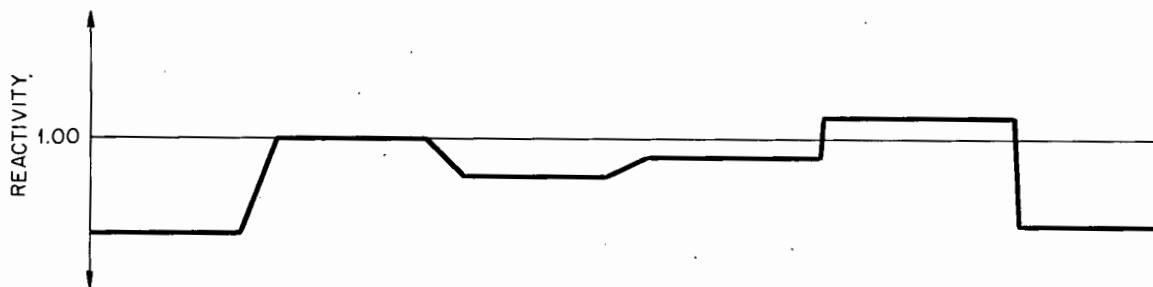
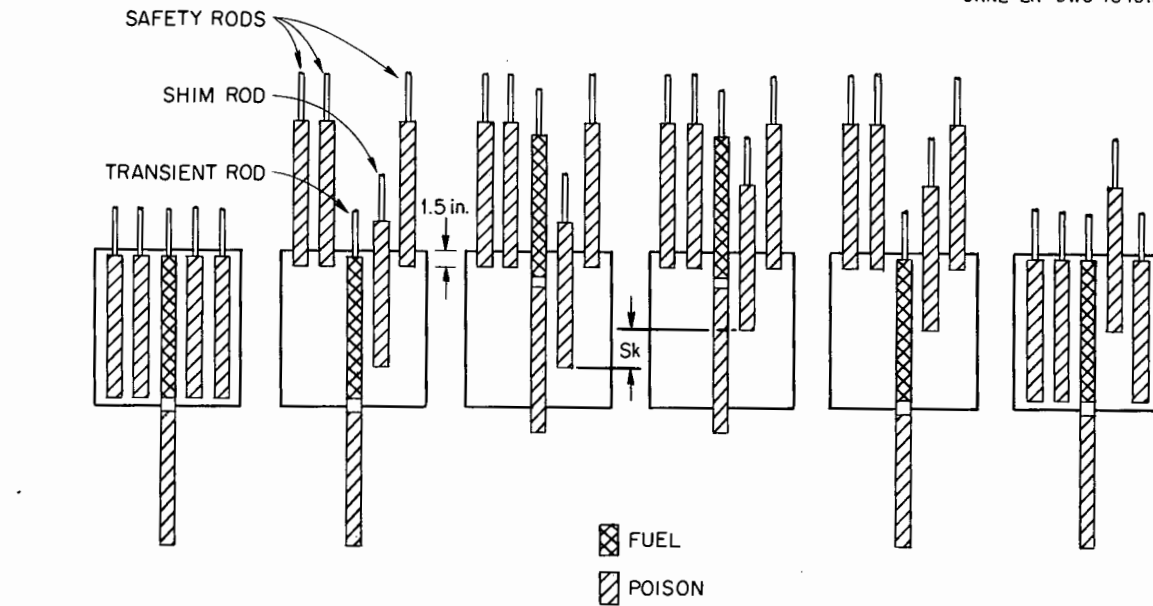


Fig. 16.6. Sequence of Rod Positions During a Transient.

channel before the transient rod was seated. Data so taken produces a conservative evaluation of the safety system and yields readily to analysis.

It is of interest that the elapsed time between transient rod seating and peak power was often in the several-hundred-millisecond region and quite variable, that is to say, in a relatively cold-clean reactor with no source, supercritical multiplication may lag the formation of supercritical configuration by several hundred milliseconds.

Tested performance exceeded expectations. An analog computation of level safety shutdown (Fig. 12 of ref 1) forecasts a three-decade rise in power with the reactor on an initial period of 0.005 to 0.006 sec.

The observed power rise was approximately two decades. The analog computation is not entirely comparable, since it assumed a longer (0.008 sec) magnet release time, and rod configurations at scram were not identical. Figure 16.7 displays observed and calculated peak powers during safety-system shutdowns.

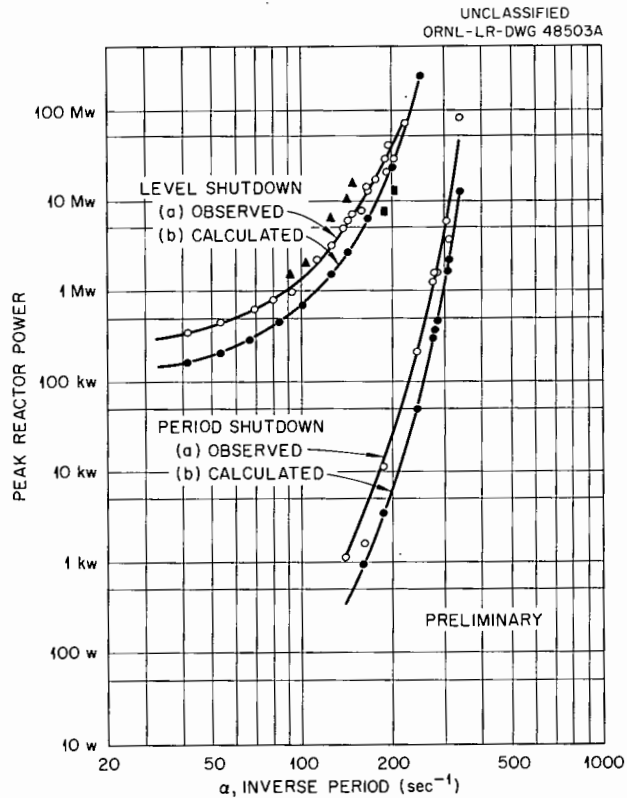


Fig. 16.7. Transient Shutdown of BSR-II at SPERT-I.

The observed data is preliminary: it is not the result of the most current calibrations, but no drastic corrections are expected.

The calculation was in accordance with Fig. 16.8, all delayed neutrons being neglected. The fixed time delays include a magnet release time of 0.002 sec. Agreement with the test results is satisfactory. The errors may be ascribed to one or more of the following causes:

1. small discrepancies in the expression used for $k(t)$, the rod-worth-vs-time curve;
2. the assumed delay, 0.002 sec, in error;
3. errors in scram-level set point.

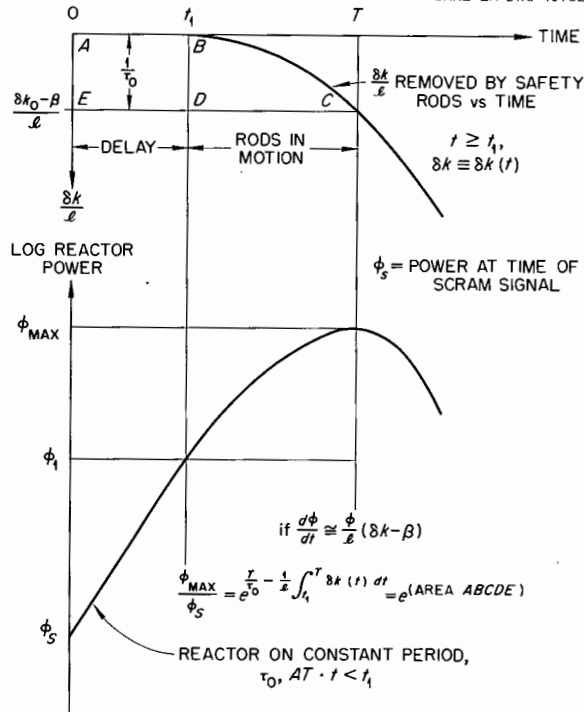


Fig. 16.8. Graphic Calculation of Reactor Shutdown.

Figure 16.9 diagrams both instrument and self-shutdown of the BSR-II. Incipient damage (fuel-plate rippling) was observed following a 0.014-sec period self-shutdown which produced a peak power of 225 Mw. The ORNL safety system, with the level channel set to trip at 100 kw, provides complete protection of the BSR-II against periods of slightly less than 0.005 sec. The period channels, becoming effective at lower powers, were even more efficient. In over 40 tests, the safety system prevented reactor damage. In a majority of these tests, the damage, without fast safety equipment, would have been substantial if not complete.

A very large majority of all credible reactor accidents must be viewed as ramp-type insertions of excess reactivity, requiring a finite time to accomplish. With a fast safety system, the slow ramp, typified by the start-up accident, is disposed of quietly and without difficulty. In fact, inexperienced operators could easily mistake such an accident, at low levels, as a false scram produced by equipment malfunction.

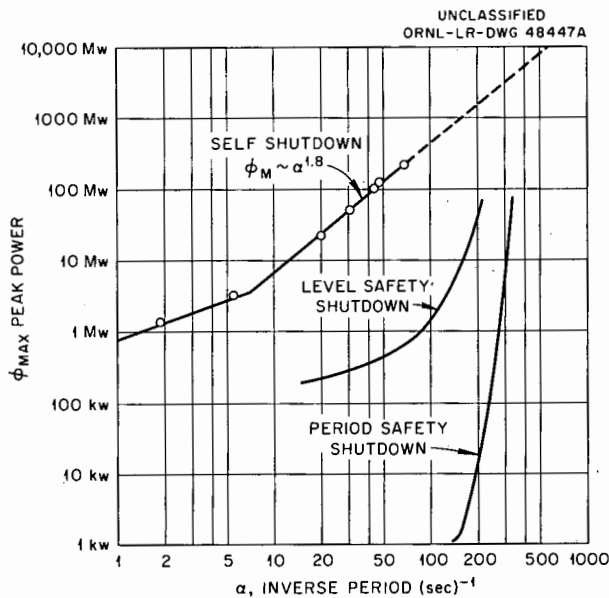


Fig. 16.9. Reactor Transient Shutdown.

A majority of fast credible ramps, a cold slug, for example, is controlled by the system. During reactor design or reactor experiment design, such accidents must be assessed from the standpoint of the following:

1. credible insertion rate of excess reactivity,
2. credible total reactivity,
3. the peak transient power limit of the reactor,
4. the known characteristics of the safety system.

It can be expected that a preponderance of such potential accidents will fall within the competence of the safety system or, by reasonable design, can be made to do so.

The preceding statements assume that the reactor is operated with an adequate source. This, of course, is usually considered a basic operational safety precaution. The long time intervals often observed between transient rod insertion and peak transient power are conclusive evidence that source-free operation is potentially disastrous. In a cold reactor, this is one possible way to achieve the effect of a true step insertion of large amounts of reactivity, even though the actual insertion rate is relatively slow. The safety system, however fast, cannot be designed to account for operational procedures which place no limits on the amount and rate of reactivity addition.

U

INTERNAL DISTRIBUTION

- | | |
|--------------------------------------|---|
| 1. C. E. Center | 155. E. E. Fairstein |
| 2. Biology Library | 156. C. W. Sheppard |
| 3. Health Physics Library | 157. W. G. Stone |
| 4-6. Central Research Library | 158. C. P. Keim |
| 7. Reactor Division Library | 159. C. D. Susano |
| 8-128. Laboratory Records Department | 160. P. M. Reyling |
| 129. Laboratory Records, ORNL R.C. | 161. G. C. Williams |
| 130. A. M. Weinberg | 162. M. J. Skinner |
| 131. L. B. Emlet (K-25) | 163. J. V. Francis |
| 132. J. P. Murray (Y-12) | 164. R. W. Johnson |
| 133. J. A. Swartout | 165. D. J. Fisher |
| 134. E. H. Taylor | 166. E. G. Struxness |
| 135. E. D. Shipley | 167. J. R. McNally, Jr. |
| 136. C. S. Harrill | 168. J. L. Gabbard |
| 137. M. L. Nelson | 169. R. A. Charpie |
| 138. W. H. Jordan | 170. T. V. Blosser |
| 139. S. C. Lind | 171. E. L. Olson |
| 140. F. L. Culler | 172. J. A. Auxier |
| 141. A. H. Snell | 173. R. K. Abele |
| 142. A. Hollaender | 174. J. R. Tallackson |
| 143. M. T. Kelley | 175. H. E. Banta |
| 144. K. Z. Morgan | 176. E. W. Burdette |
| 145. T. A. Lincoln | 177. R. S. Cockreham |
| 146. A. S. Householder | 178. C. A. Mossman |
| 147. C. E. Winters | 179. D. S. Toomb |
| 148. H. E. Seagren | 180. R. G. Affel |
| 149. D. Phillips | 181. H. J. Stripling |
| 150. C. J. Borkowski | 182. E. P. Epler |
| 151. P. R. Bell | 183. F. W. Manning |
| 152. J. L. Lovvorn | 184. ORNL - Y-12 Technical Library,
Document Reference Section |
| 153. G. S. Hurst | |
| 154. R. S. Livingston | |

EXTERNAL DISTRIBUTION

185. J. Hitch, Office of Isotope Development, AEC, Washington
186-187. Ohio State University (Professor of Naval Science)
188. R. Hofstadter, Stanford University
189. J. C. Nance, Consolidated-Vultee Aircraft Corporation
190. E. A. Rollor, ANP Project Office, Fort Worth
191. R. N. Keller, University of Colorado
192. Division of Research and Development, AEC, ORO
193-809. Given distribution as shown in TID-4500 (15th ed.) under
Instruments category (100 copies, OTS)